

Particle Identification

Warwick week 2020

Antonis Papanestis

RAL – STFC

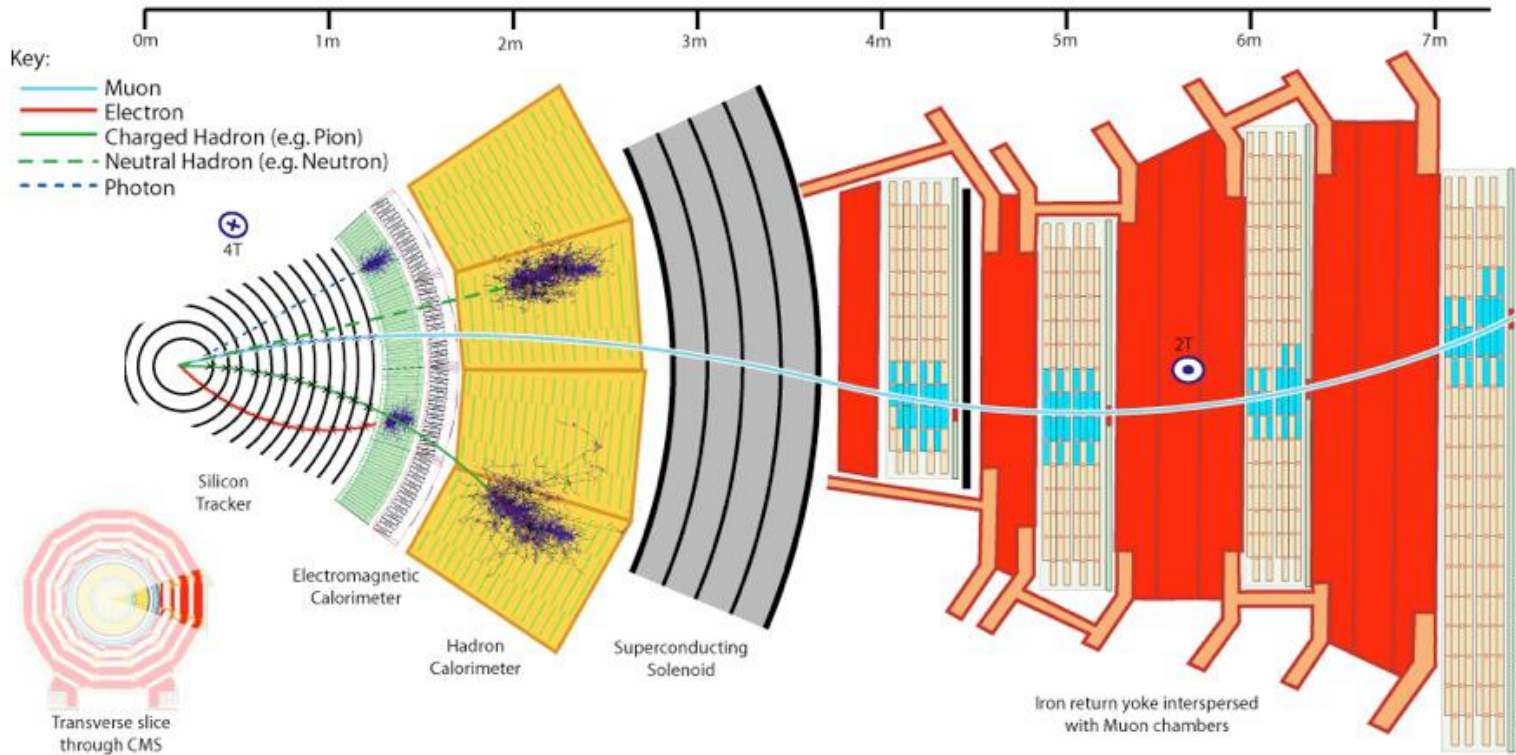
(with borrowed material from S. Easo)



Outline

- Introduction
- Particle ID techniques:
 - Time of flight
 - dE/dx
 - Transition radiation
 - Cherenkov radiation
 - RICH detectors
 - DIRC detectors
- Give examples of experiments and detectors

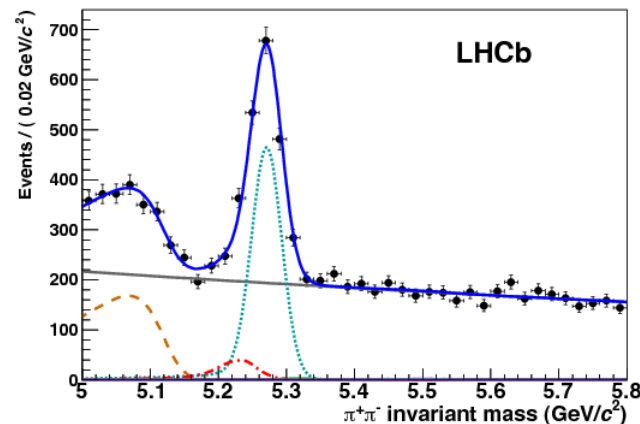
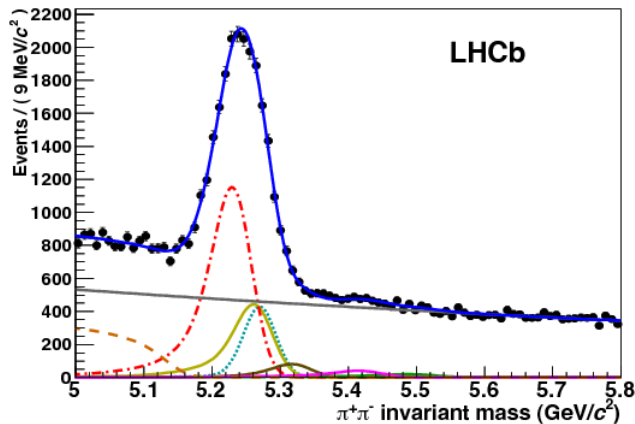
Introduction (i)



A “generic” particle physics experiment has “built-in” a lot of particle ID for:
Electrons, photons, neutrons and muons

Introduction (ii)

- Particle ID for hadrons
 - Distinguish between kaons, pions, protons, deuterons
 - Required for flavour physics
- Specific experiment requirements
 - Distinguish between electrons and charged pions
 - Distinguish between electrons and muons
 - For neutrino experiments
 - For rare decay searches



$B \rightarrow \pi^+\pi^- (h^+h^-)$ before and after RICH PID

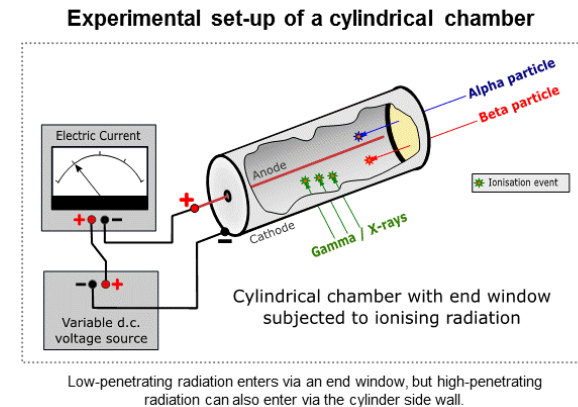
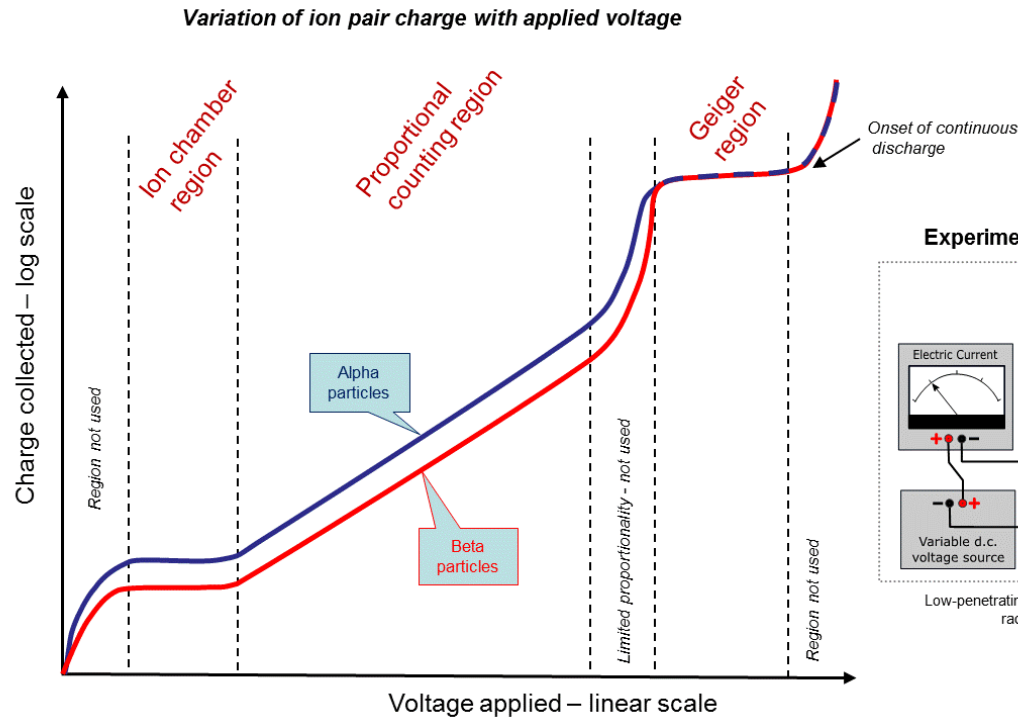


Detector technologies

Practical Gaseous Ionisation Detection Regions

This diagram shows the relationship of the gaseous detection regions, using an experimental concept of applying a varying voltage to a cylindrical chamber which is subjected to ionising radiation. Alpha and beta particles are plotted to demonstrate the effect of different ionising energies, but the same principle extends to all forms of ionising radiation.

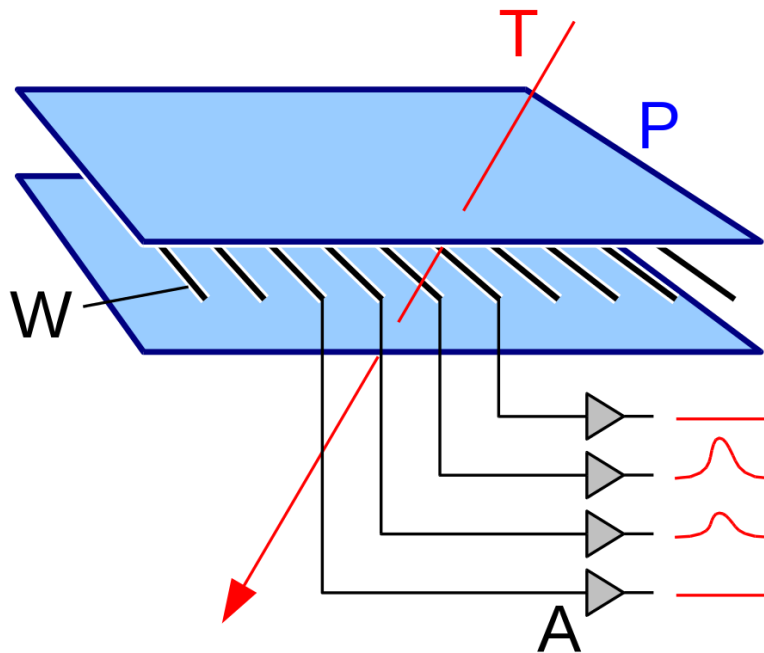
The ion chamber and proportional regions can operate at atmospheric pressure, and their output varies with radiation energy. However, in practice the Geiger region is operated at a reduced pressure (about $1/10^{\text{th}}$ of an atmosphere) to allow operation at much lower voltages; otherwise impractically high voltages would be required. The Geiger region output does not differentiate between radiation energies.



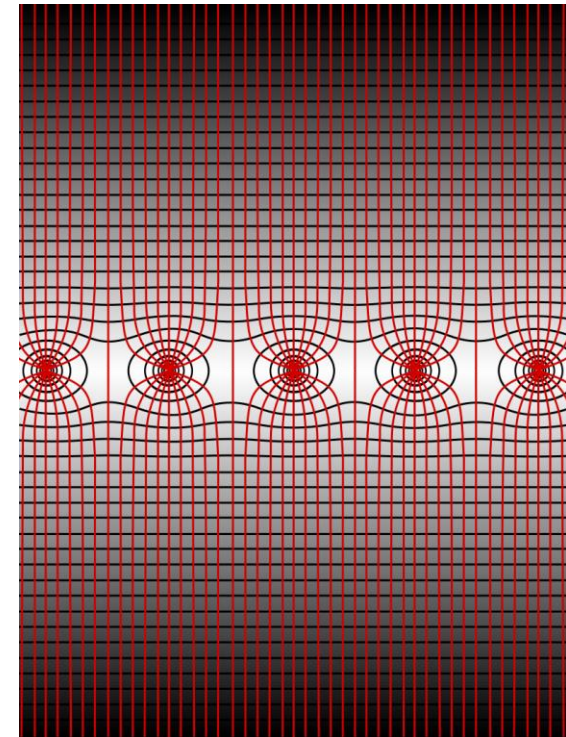
From Wikipedia



Multiwire proportional chamber

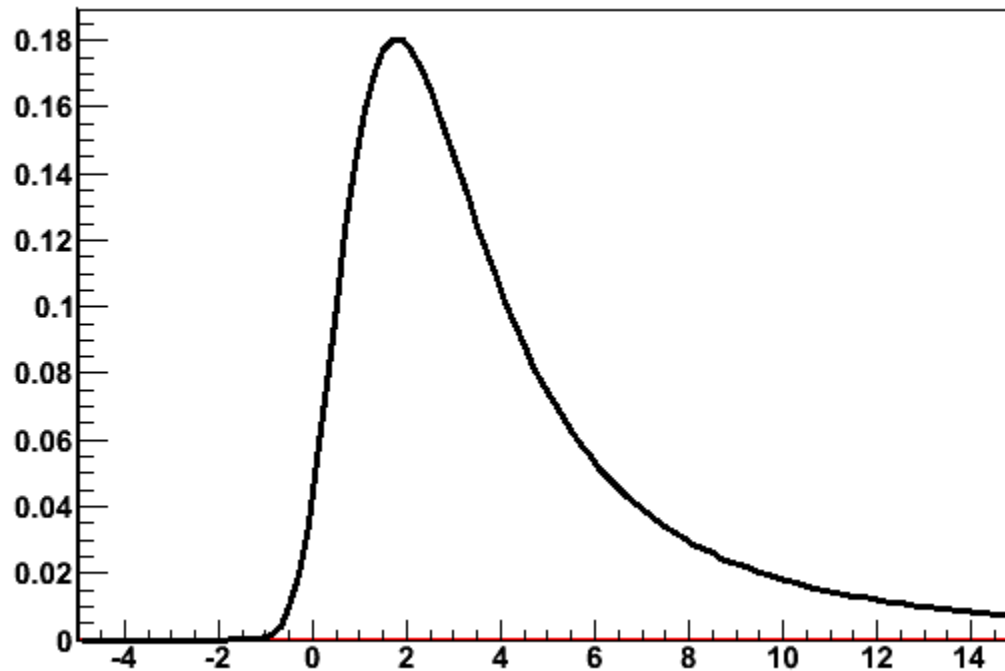


By Michael Schmid - CC BY-SA 3.0,
<https://commons.wikimedia.org/w/index.php?curid=442715>



By Wiso - CC BY-SA 3.0,
<https://commons.wikimedia.org/w/index.php?curid=2934457>

Landau distribution



Time of flight

Time difference for two particles with masses m_1 and m_2 for length L

$$\Delta t = \frac{L}{\beta_1 c} - \frac{L}{\beta_2 c} = \frac{L}{c} \left[\sqrt{\left(1 + \frac{m_1^2 c^2}{P^2}\right)} - \sqrt{\left(1 + \frac{m_2^2 c^2}{P^2}\right)} \right]$$

$$P^2 \gg m^2 c^2$$

$$\Delta t \sim \frac{Lc(m_1^2 - m_2^2)}{2P^2}$$

Mass resolution depends on time resolution of detectors and distance L
Typical values: $L=3.5$ m, $\Delta t=100$ ps, for 3σ separation, $P_{\max}=2.1$ GeV/c

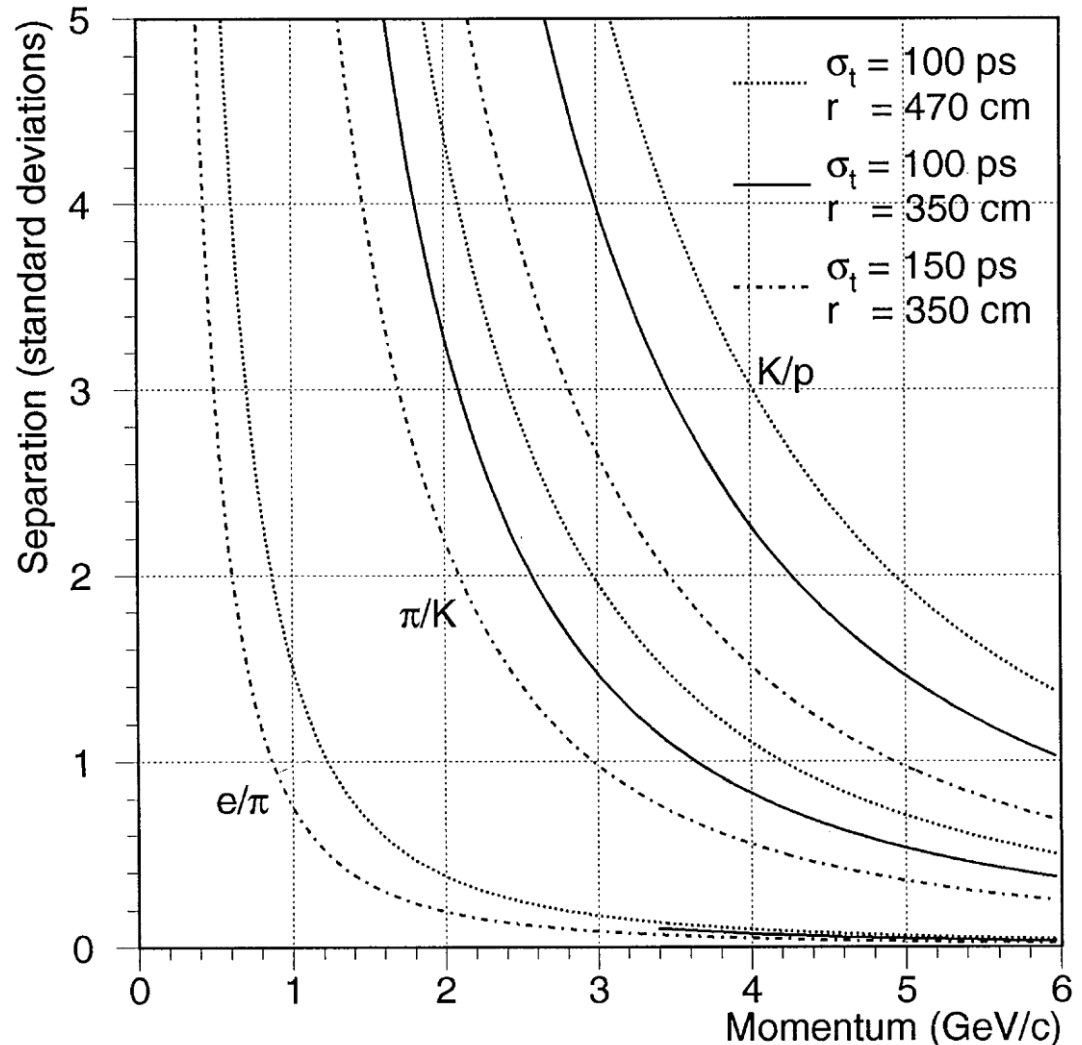
Requires fast detectors: scintillation, Cherenkov, fast collection of ionisation



PID with TOF

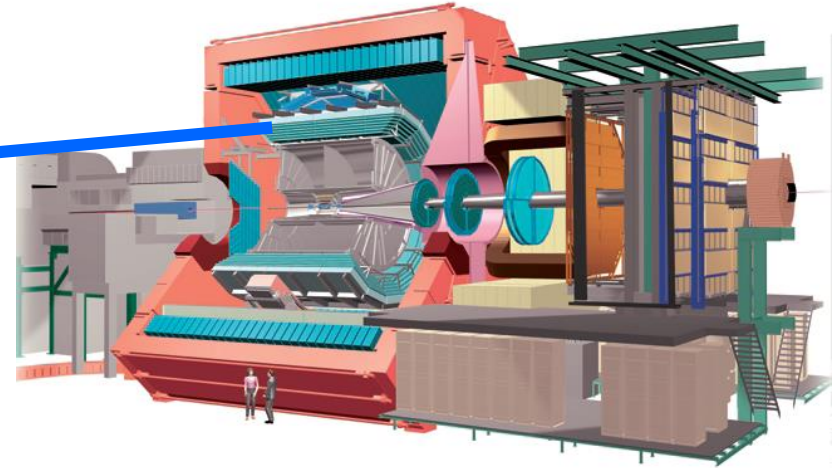
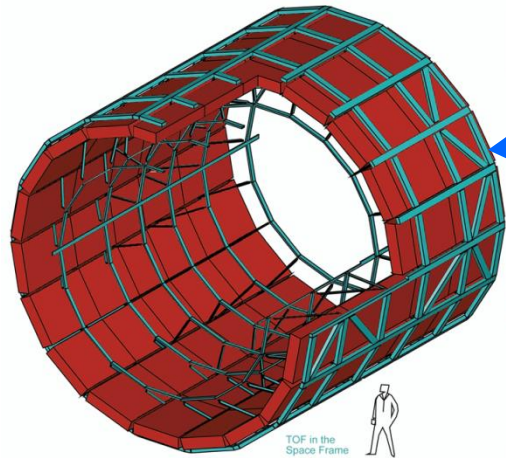
Expected PID performance for various path lengths and time resolutions

TORCH, a proposed future detector, can push π/K separation to 9 GeV/c with $L \sim 10$ m and time resolution per track ~ 20 ps

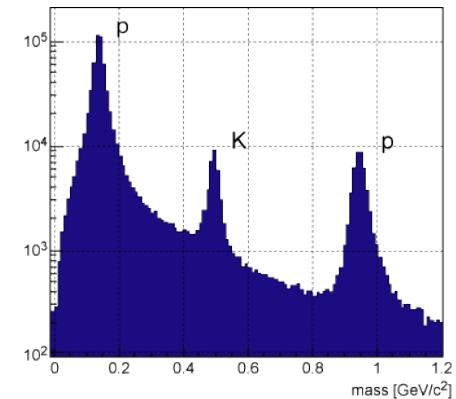
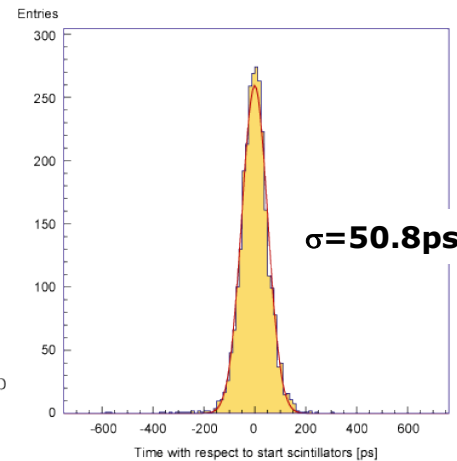
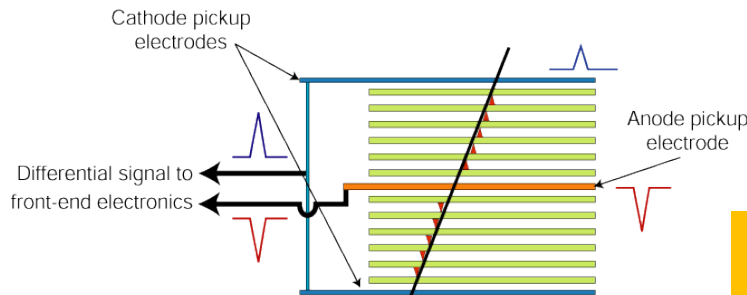


TOF: ALICE experiment

http://aliceinfo.cern.ch/Public/en/Chapter2/Chap2_TOF.html



Resistive plates made of glass.
2 X5 gaps : 250 mm
Readout by HPTDC chip (High Performance Time to Digital Converter)



3σ π/K separation up to 2.2 GeV/c
and K/p separation up to 4 GeV/c.



Ionisation Measurement (dE/dx)

$$-\frac{dE}{dx} (\text{eVcm}^2\text{g}^{-1}) = Kq^2 \frac{Z}{A\beta^2} \left[\frac{1}{2} \ln \frac{2m_e c^2 \beta^2 \gamma^2 T_{\max}}{I^2} - \beta^2 \frac{\delta(\beta\gamma)}{2} \right]$$

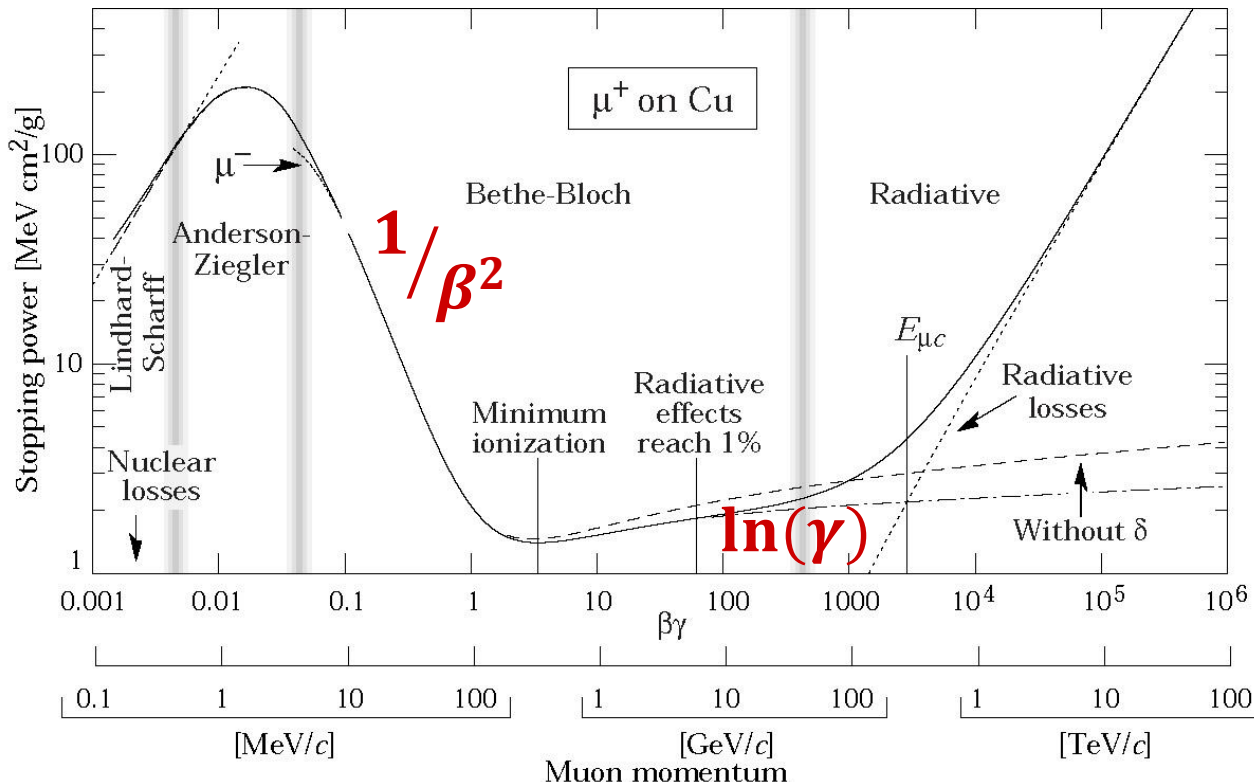
Ionisation Constant for material

Density correction

$$T_{\max} \approx 2m_e c^2 \beta^2 \gamma^2$$

Max energy in single collision

$$K = 4\pi N r_e^2 m_e c^2$$



dE/dx in silicon

Bethe-Block formula (for $2\gamma m/M \ll 1$)

$$\frac{dE}{dx} = \frac{4\pi N e^4}{m c^2 \beta^2} Z^2 \left(\ln \frac{2 m c^2 \beta^2 \gamma^2}{I} - \beta^2 \right)$$

For $0.2 < \beta < 0.9$, $dE/dx \sim (M/p)^2$

M,p= mass, momentum of the traversing particle

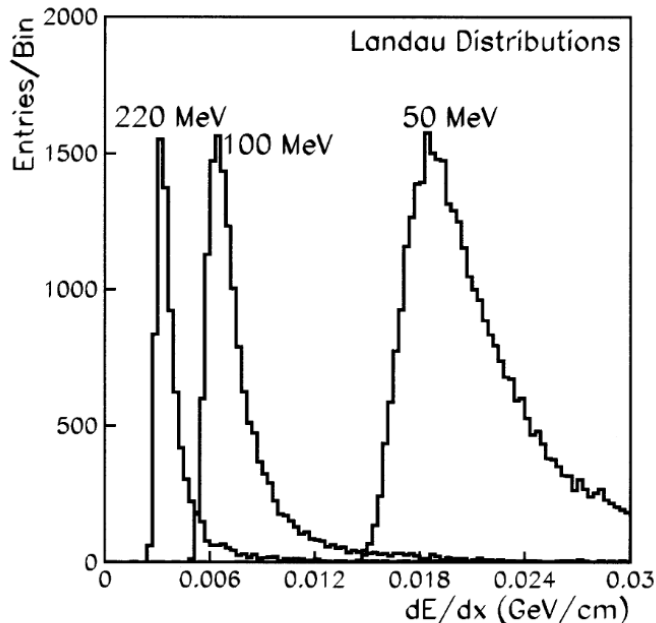


Fig. 1. Landau $\langle dE/dx \rangle$ distributions for pions of momenta 220, 100 and 50 MeV going through 300 μm of silicon.

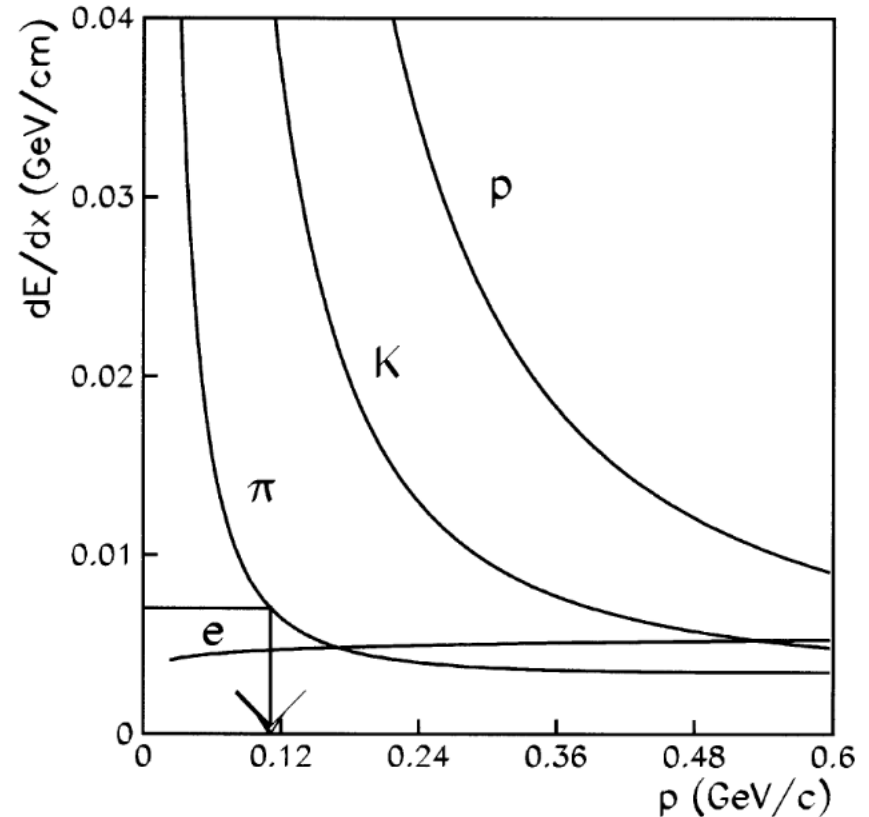


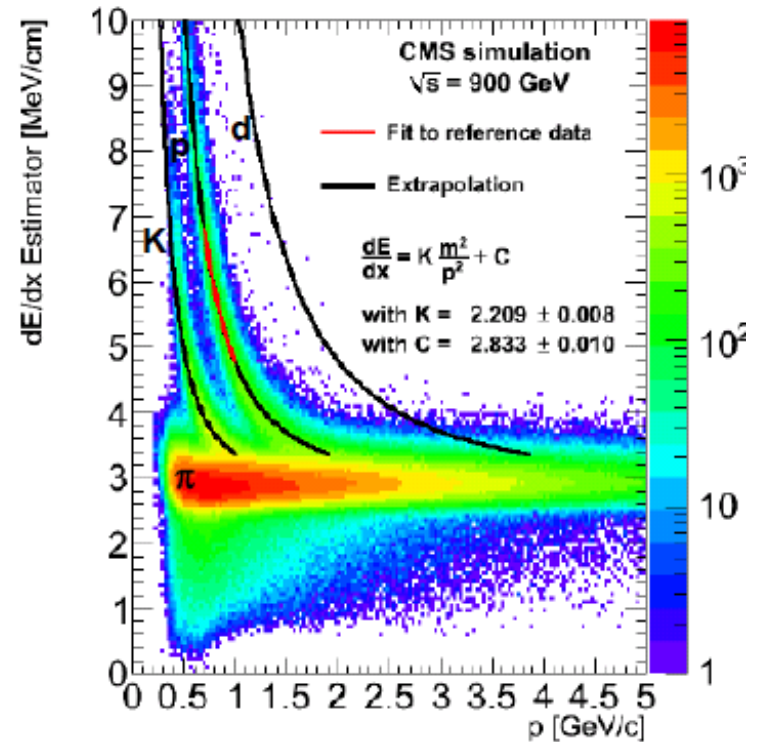
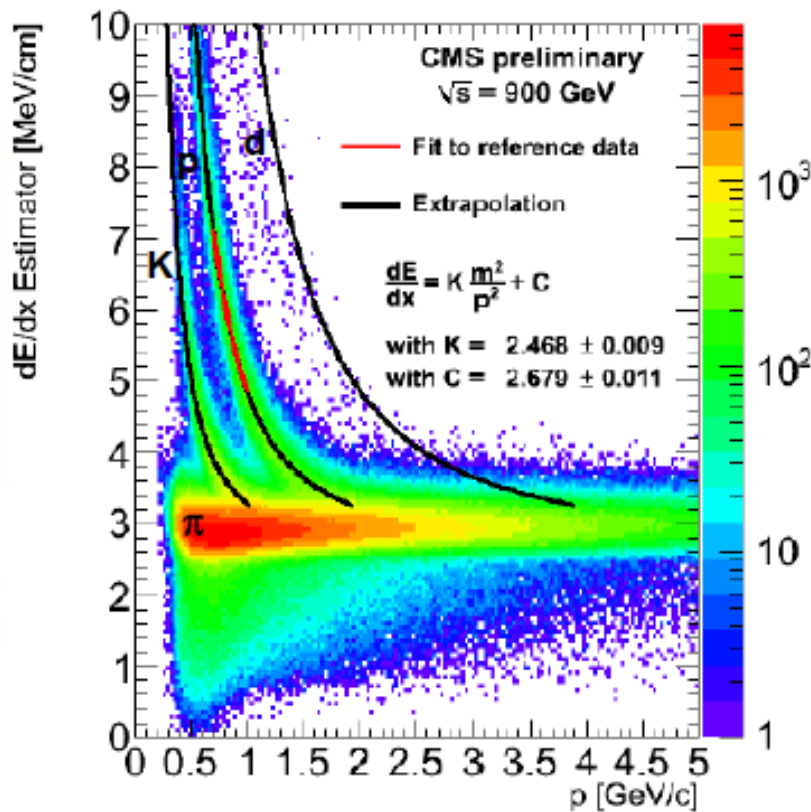
Fig. 3. $\langle dE/dx \rangle$ as a function of momentum in STAR-SVT. For low momentum pions one can use the pion curve to extract the momentum from the measured dE/dx as shown.

Ref: NIMA 469(2001) 311-315

Warwick week 2020 - A Papanestis

dE/dx: CMS Si tracker

- Each Silicon sensor gives a dE/dx measurement.
- Estimate the Most Probable Value from several (10-25) measurements (Truncated Mean: Ignore upper 40%)



Data

Warwick week 2020 - A Papanestis

MC

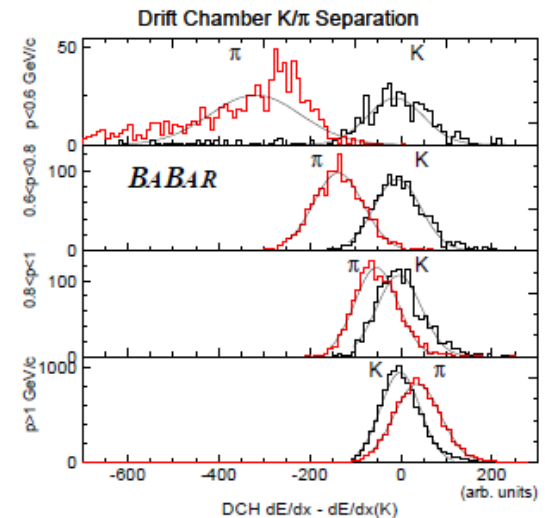
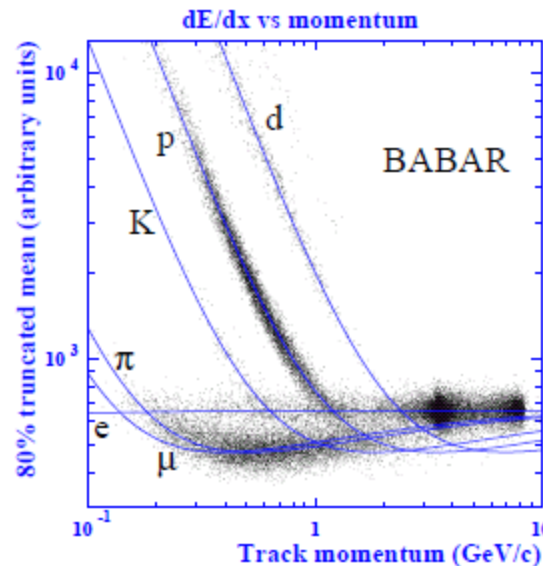
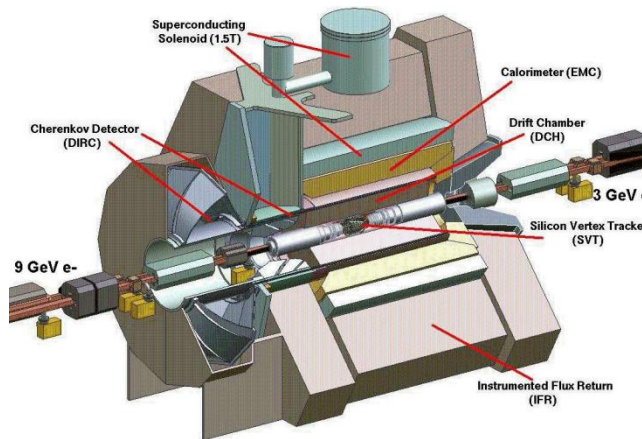
dE/dx : Drift Chambers

Larger Landau fluctuations compared to those from Silicon detectors.
 So many measurements needed to get the average.

Ref: IEEE-TNS VOL:47 , NO:6, Dec2000.

BABAR Drift Chamber:

Gas mixture 80% helium, 20% isobutane,
 3500–4000 ppm water vapor, ~ 80 ppm O_2



Good π/K separation up to ~ 700 MeV/c. dE/dx resolution $\sim 7.5\%$

Combined TOF and dE/dx

NA 49: Heavy ion experiment,

TOF: Scintillator thickness=2.3 cm, time resolutions= 59 ps, 95 ps

TPC for dE/dx.

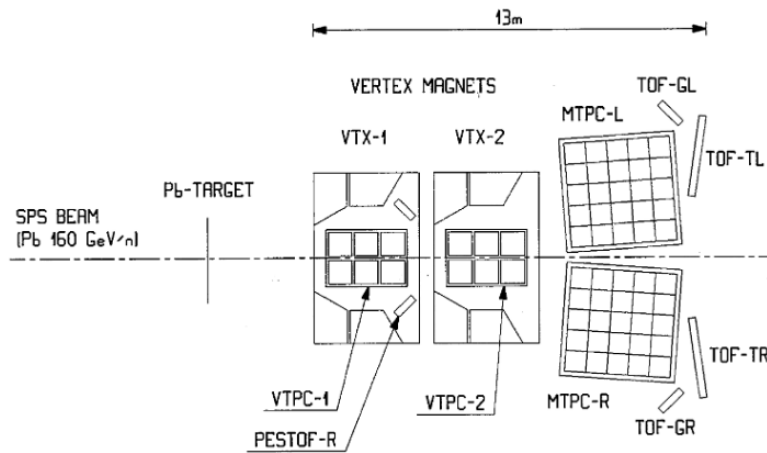


Fig. 2. Central part of the NA49 experimental setup.

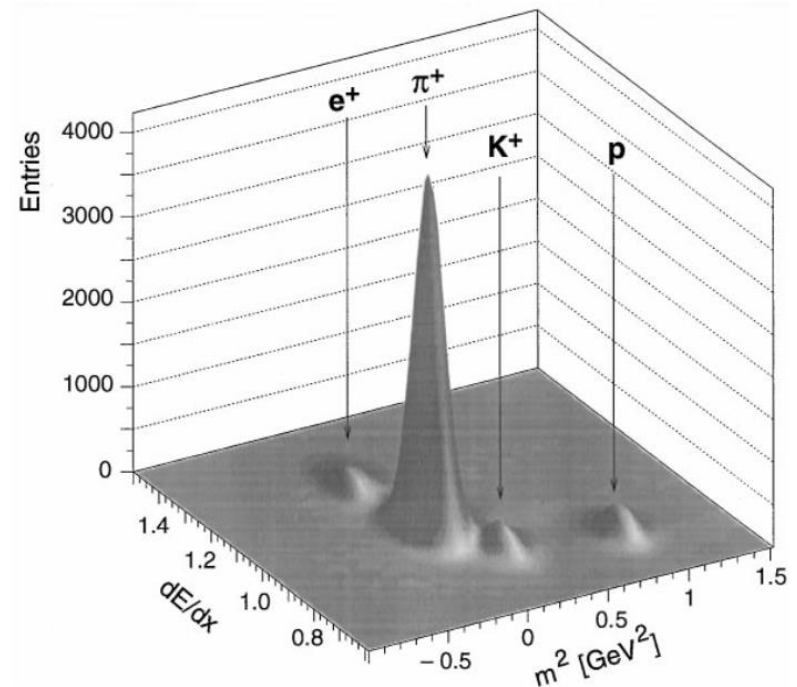


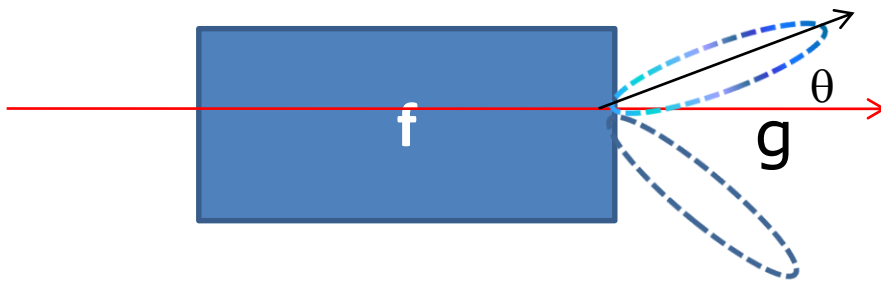
Fig. 5. Particle separation in NA49 with combined dE/dx and TOF information.

Transition Radiation (TR)

- Transition Radiation: Radiation in the x-ray region when ultra relativistic particles cross the boundary between 2 media with different dielectric constants.
- Mainly for e^- separation in 0.5 GeV/c \rightarrow 200 GeV/c.

Full explanations and the derivations from Maxwell's equations:

NIMA 326 (1993) 434-469 and references there in.



The radiation is peaked at a small angle:

$$\theta = 1/\gamma$$

$$\frac{dW}{d\omega d\theta} = \frac{2\alpha}{\pi} f_0(\theta)$$

$$f_0(\theta) = \theta^3 \left(\frac{1}{\gamma^{-2} + \theta^2 + \xi_g^2} - \frac{1}{\gamma^{-2} + \theta^2 + \xi_f^2} \right)$$

$$\xi_i = \omega_i/\omega \quad \omega_i = \text{plasma freq of medium } i$$

TR Detection

Integrating the previous equation, one can get , for $\xi_g=0$,

$$W_{TR} = 2.43 \times 10^{-3} \omega_f \gamma$$

- $\gamma = E/m$ of the particle. This makes PID possible by measuring W.
- Lighter particle give larger signal
- $\omega_f =$ plasma frequency = $28.8 (\rho Z/A)^{0.5}$ eV
 ρ =density, Z=atomic weight, A=atomic number

For example, for $\omega_f = 0.02$ keV and $\gamma = 5000$, most of the photon energy is in the range $10 \text{ keV} < \omega < 100 \text{ keV}$ (ie. $0.1 \omega_c < \omega < \omega_c$ where $\omega_c =$ cut-off frequency).

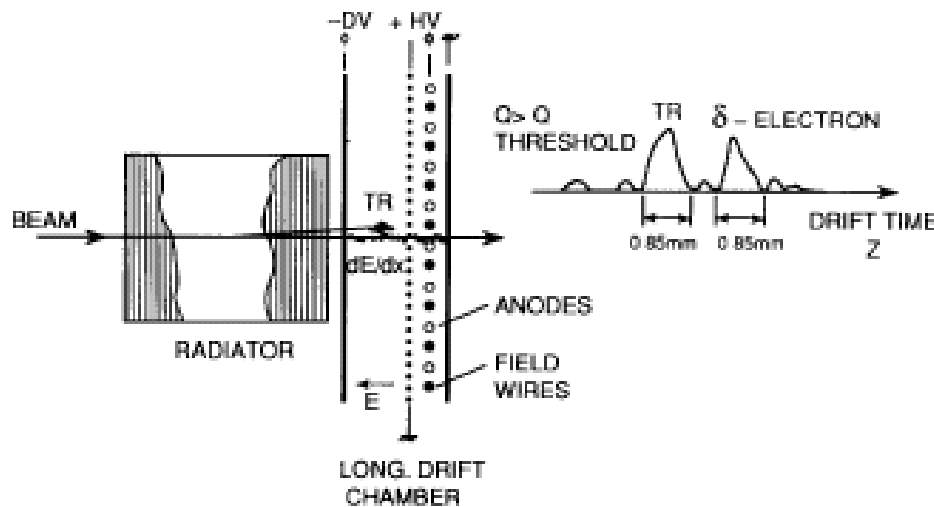
$$\text{Number of photons produced} = N(> \omega) = \frac{\alpha}{\pi} \left\{ \ln \frac{\omega_c}{\omega} \left(\ln \frac{\omega_c}{\omega} - 2 \right) + \frac{\pi^2}{12} + 1 \right\}$$

For $\omega_c=100$ keV and $\omega=1$ keV, $N= 0.03$ for a single surface.

Hence to get sufficient number of photons , large number of interfaces are used: a stack of many foils with gaps in between.

TRD Example 1: HELIOS experiment (NA34)

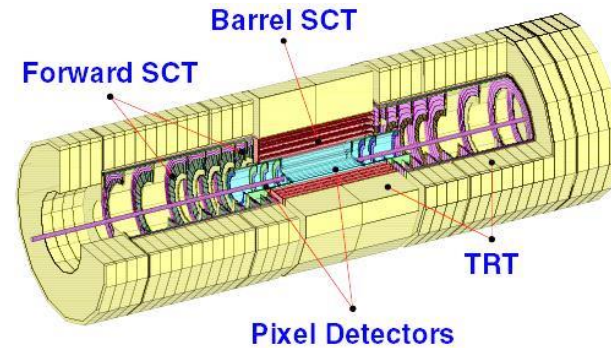
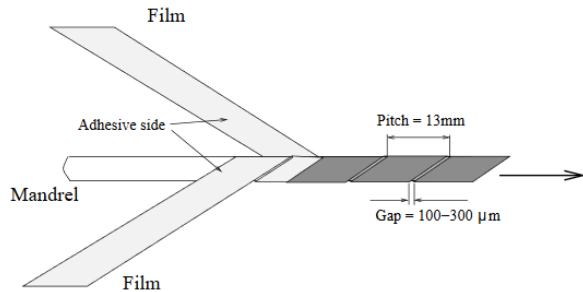
- The minimum thickness of the foils and air gaps are determined by the size of the 'formation zone' and the interference effects.
(typically foils can be 10-20 μm thick and are made of polypropelene)
- Behind a TRD foil stack there is a MWPC or drift chamber where the TRD signal is detected along with the signal from the charged track.



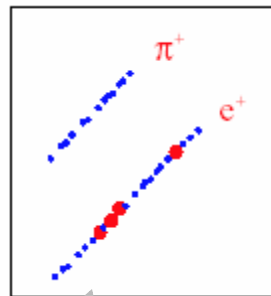
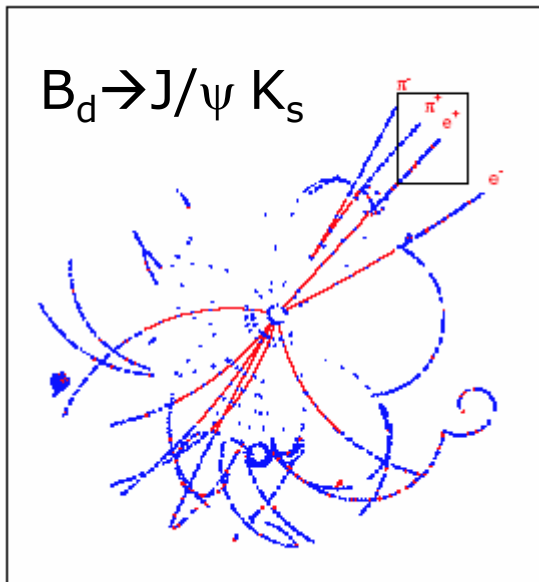
Drift space = 10 mm,
Anode space = 6 mm
Drift time = 0.5 \rightarrow 1 μs
May use FADC or
discriminators

TRD Example 2: ATLAS TRT

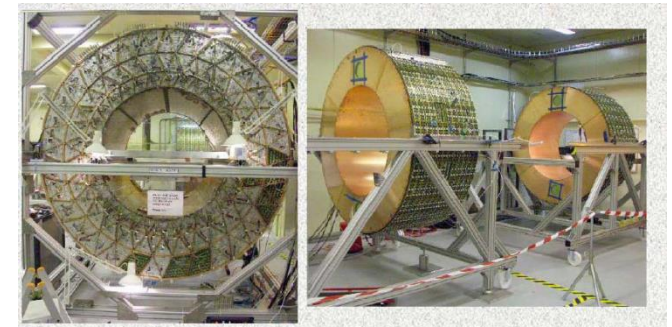
TRT straw wall design



Barrel and endcap TRT

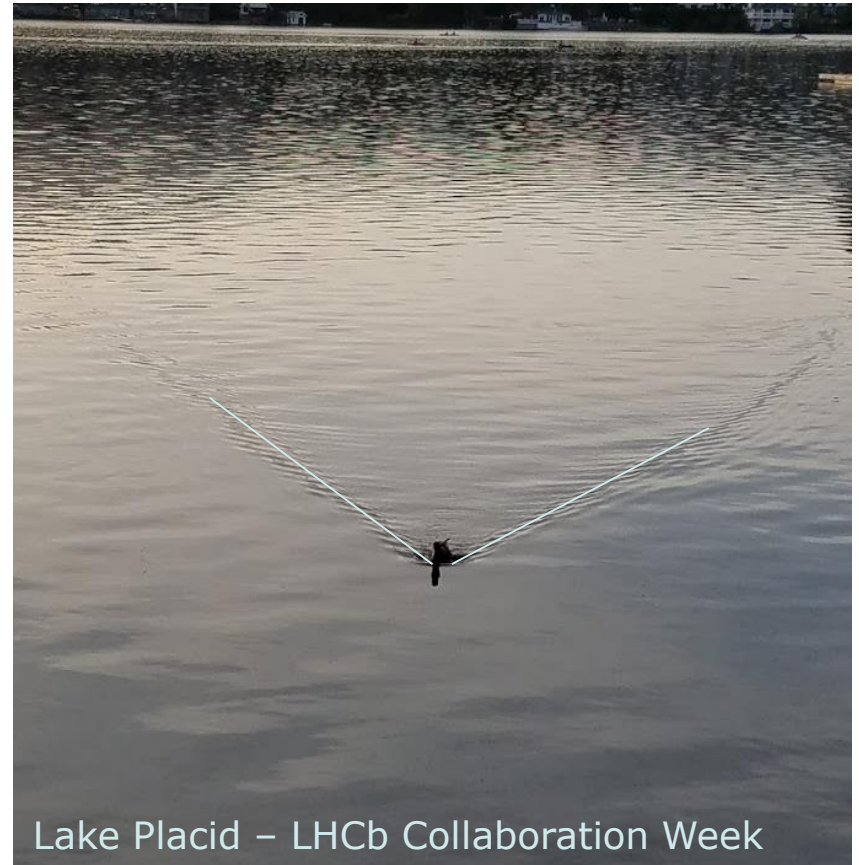


Blue dots: ionizing hits
Red dots : TR hits



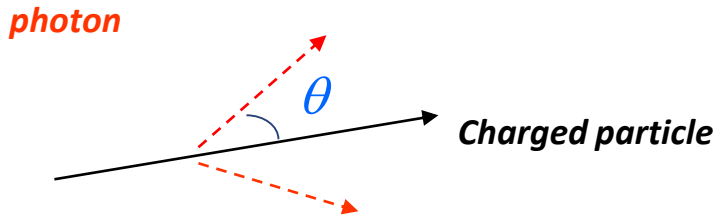
*In an average event, energy deposit from:
Ionization loss of charged particles ~ 2.5 keV
TR photon > 5 keV.
(Photon emission spectrum peaks at 10-30keV)*

Cherenkov radiation



Lake Placid – LHCb Collaboration Week

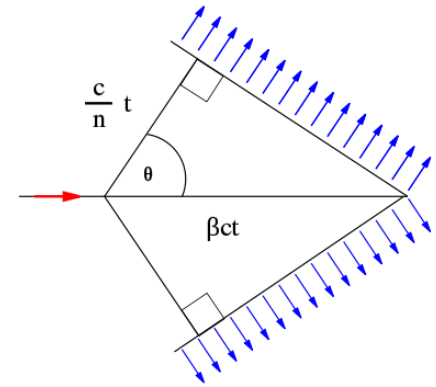
Basics of Cherenkov radiation



$$\cos(\theta) = \frac{1}{n(\lambda)\beta}$$

$$n(E_{ph}) = c/c_M \quad \text{Refractive index}$$

$$\beta = v/c = P/E = P/\sqrt{P^2 + m^2} = \frac{1}{\sqrt{1 + (m/p)^2}}$$



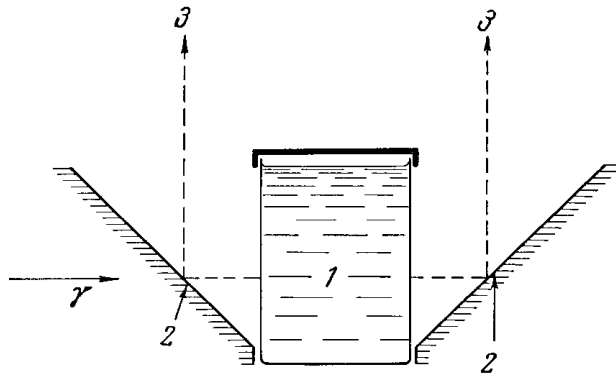
β = velocity of the charged particle in units of speed of light (c) vacuum
 P, E, m = momentum, energy, mass of the charged particle
 c_M = speed of light in the medium (phase velocity)
 E_{ph} = photon energy
 λ = Photon wavelength

Theory of Cherenkov Radiation: Classical Electrodynamics by J. D. Jackson (Section 13.5)

History of Cherenkov radiation

- The formula $\cos(\theta) = 1/(n\beta)$ was already predicted by Heaviside in 1888
- ~1900: 'Blue glow' seen in fluids containing concentrated Radium (Marie & Pierre Curie)
- Pavel Alexeevich Cherenkov (1904-1990): Lebedev Physical Institute of the Russian Academy of Sciences.
- Discovery and Validation of Cherenkov Effect : 1934-37
- Full Explanation using Maxwell's equations: I.M. Frank and I.E. Tamm in 1937
- Nobel Prize in 1958: Cherenkov, Frank and Tamm.

First experiments



- 1: vessel with liquid
- 2: mirror
- 3: Cherenkov photons towards the photographic plate

Typical Apparatus used by Cherenkov to study the angular distribution of Cherenkov photons. (Incident γ ray produces electrons by Compton scattering in the liquid).

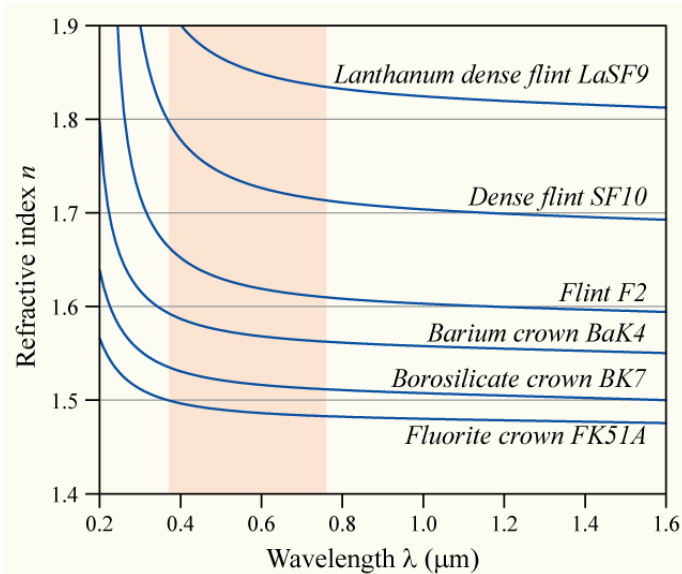
P. Cherenkov established that:

- Light Intensity is proportional to the electron path length in the medium.
- Light comes only from the 'fast' electrons above a velocity threshold, in his Apparatus.
- Light emission is prompt and the light is polarized.
- The wavelength spectrum of the light produced is continuous. No special spectral lines.
- The angular distribution of the radiation, its intensity, wavelength spectrum and its dependence on the refractive index agree with the theory proposed by his colleagues Frank and Tamm.

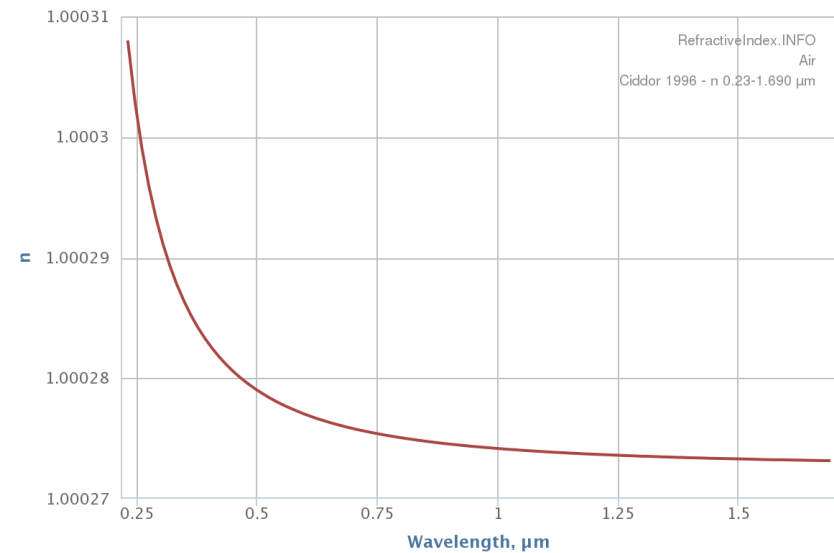


Refractive index

Glass



Air



- Dependence of the refractive index on photon frequency means the Cherenkov angle is not constant
- The spread of angles is referred to as **Chromatic Error**

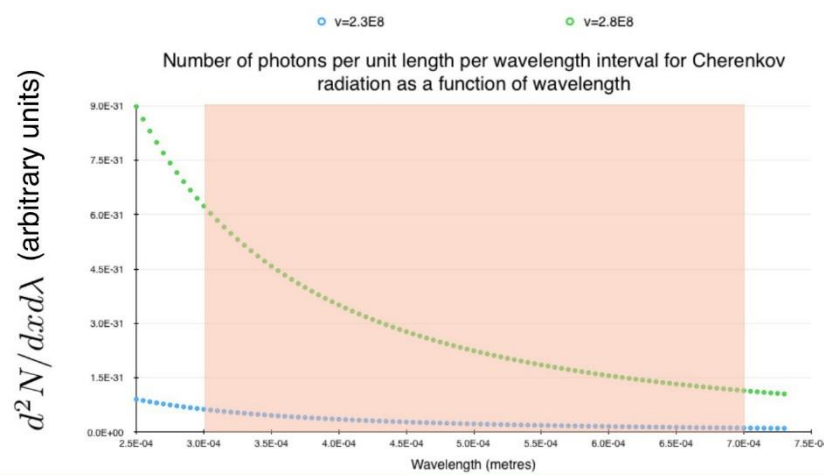


Number of photons

Number of emitted photons: $\frac{\partial^2 N}{\partial x \partial \lambda} = 2\pi a \left(1 - \frac{1}{\beta^2 n^2}\right) \frac{1}{\lambda^2}$

Between two wavelengths: $\frac{\partial N}{\partial x} = 2\pi a \left(1 - \frac{1}{\beta^2 n^2}\right) \left(\frac{1}{\lambda_L} - \frac{1}{\lambda_H}\right)$

The number of photons increases with energy



Using frequency instead of wavelength

$$\frac{dE}{dx} = \frac{q^2}{4\pi} \int_{v > \frac{c}{n(\omega)}} \mu(\omega) \omega \left(1 - \frac{c^2}{v^2 n^2(\omega)}\right) d\omega$$

Typical example: Charged particle with momentum of few GeV/c or more emitting Cherenkov photons with few eV of energy



Detected photons

$$\frac{\partial N}{\partial x} = 2\pi a \left(1 - \frac{1}{\beta^2 n^2}\right) \left(\frac{1}{\lambda_L} - \frac{1}{\lambda_H}\right) \quad \text{For } \lambda_L=400 \text{ nm and } \lambda_H=700 \text{ nm}$$

$$\frac{N}{L} = 490 \sin^2 \theta$$

If the photons are reflected by a mirror with reflectivity $R(\lambda)$, and detected by a photon detector with quantum efficiency $QE(\lambda)$ through a window with transmission $T(\lambda)$

$$N = 490 L R Q T \sin^2 \theta$$

$$= N_0 L \sin^2 \theta \quad \text{And if we assume the mean angle } \theta_c$$

$$N = N_0 L \sin^2 \theta_c$$

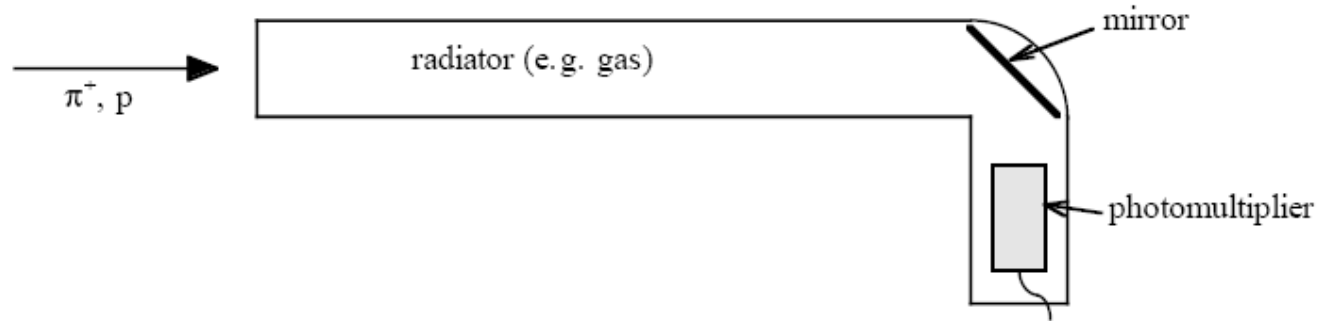
N_0 is a figure of merit for a Cherenkov detector; e.g. $N_0=200/\text{cm}$ is a good value



A variety of Cherenkov detectors

- Detector design:
 - Threshold Counters
 - Imaging detectors
 - Differential Cherenkov detectors
 - Ring Imaging Cherenkov detectors (RICH)
 - Detector for Internally Reflected light (DIRC)
- Types of photon detectors:
 - Gas based
 - Vacuum
 - Solid state
- Applications:
 - Accelerator HEP detectors
 - Astroparticle Physics detectors
 - Neutrino detectors

Threshold Cherenkov Counters



- Signal produced from only those particles which are above Cherenkov Threshold.
Basic version: Yes/No decision on the existence of the particle type.
- One counts the number of photoelectrons detected.
- Improved version: Use the number of observed photoelectrons or a calibrated pulse height to discriminate between particle types.
- For typical detectors: $N_o = 90 \text{ cm}^{-1}$,

$$N_{\text{ph}} \text{ per unit length of the radiator} = N_o * (m_1^2 - m_2^2)/(p^2 + m_1^2)$$

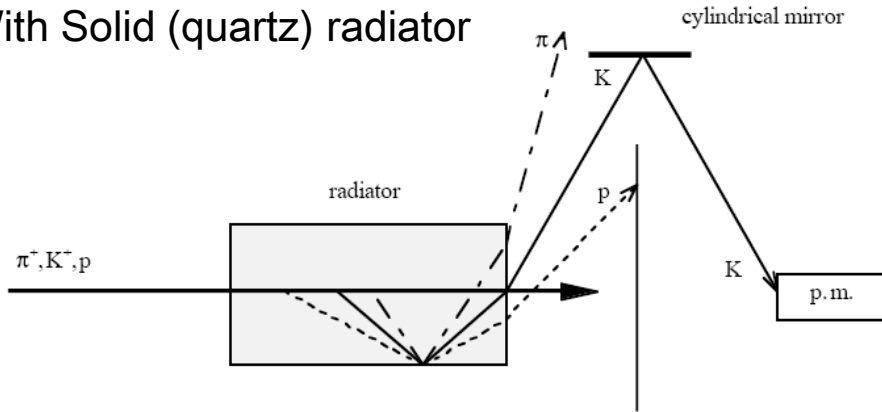
At $p = 1 \text{ GeV}/c$, N_{ph} per unit length = 16 /cm for Pions and 0 for Kaons.

At $p = 5 \text{ GeV}/c$, N_{ph} per unit length = 0.8 /cm for Pions and 0 for Kaons.

- $\Delta \beta / \beta = \tan^2 \theta / (2 * \text{sqrt} (N_{\text{ph}}))$

Differential Cherenkov Detectors

With Solid (quartz) radiator

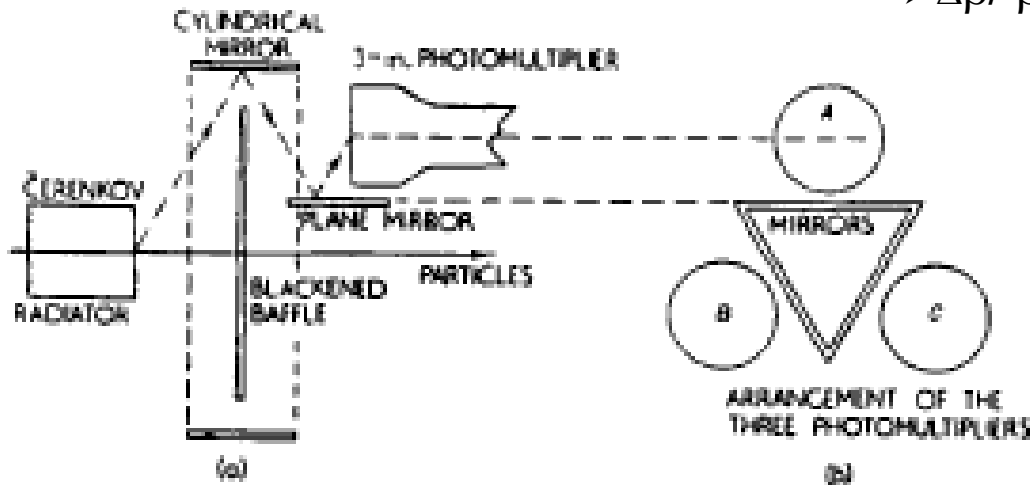


- Very small acceptance in β and direction of the charged particle. (Narrow range in velocity and direction intervals).
- Mostly used for identifying particles in the beam lines.

$$\Delta \beta / \beta = (m_1^2 - m_2^2) / 2 p^2 = \tan \theta \quad \Delta \theta$$

m_1, m_2 (particle masses) $\ll p$ (momentum)

- $\Delta \beta / \beta$ from 0.011 to $4 \cdot 10^{-6}$ achieved.



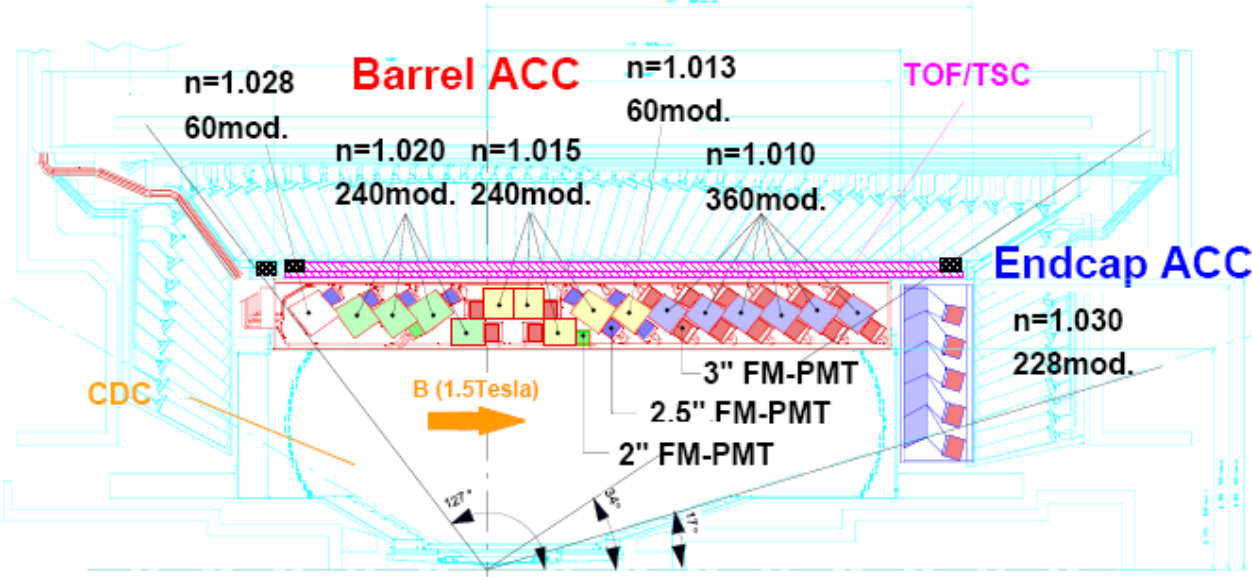
- Discovery of anti-proton in 1955 by Chamberlain, Segre et. al. at Berkeley.

Fig. 2. The differential Cherenkov counter used in the anti-proton discovery experiment: (a) side view; (b) end view.

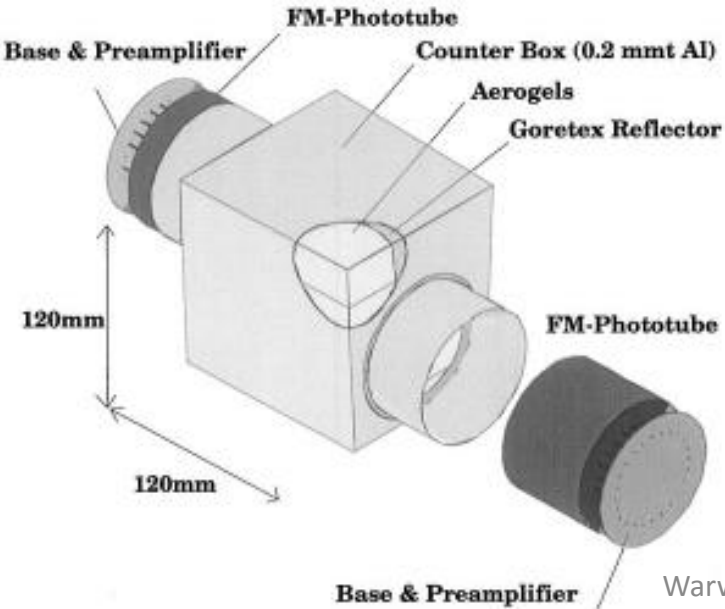
- Nobel Prize in 1959

Threshold Counters

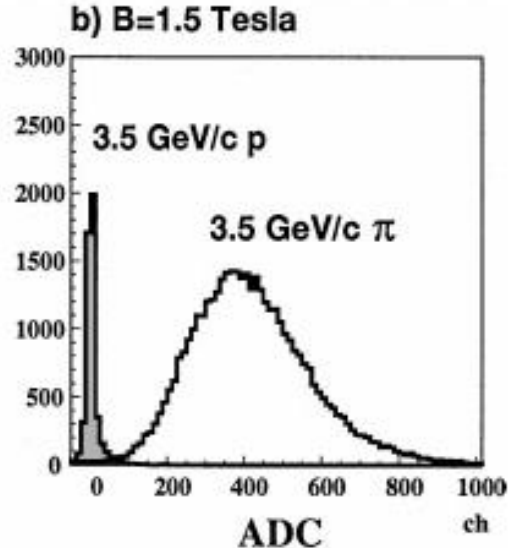
BELLE: Threshold Cherenkov Detector



- Five aerogel tiles inside an aluminum box lined with a white reflector (Goretex reflector)
- Performance from test-beam



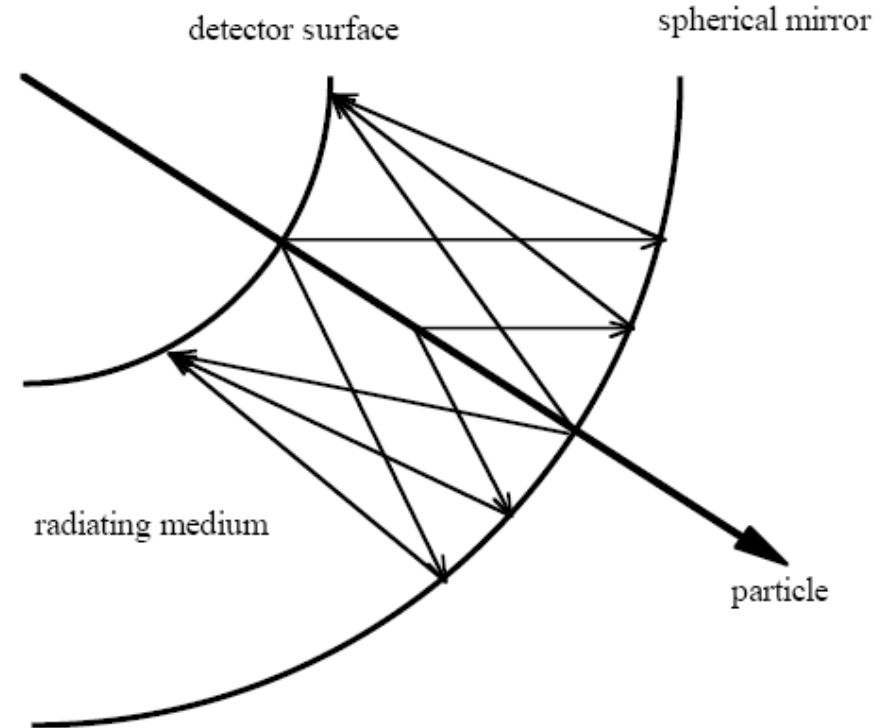
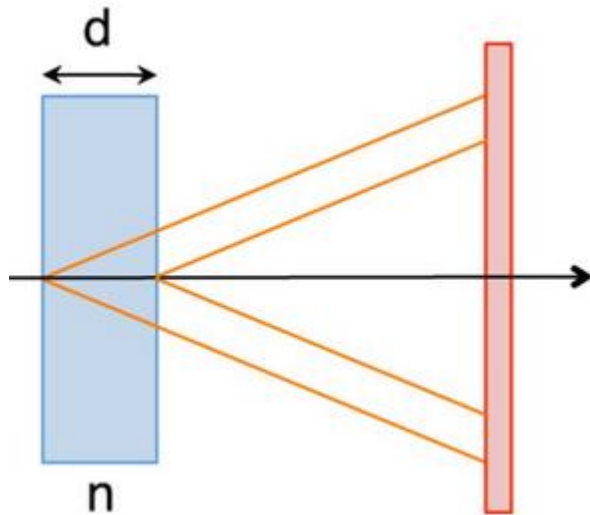
- Approx . 20 photoelectrons per Pion detected at 3.5 GeV/c
- More than 3σ separation



p below and π above Threshold

RICH Detectors

Proximity focusing geometry



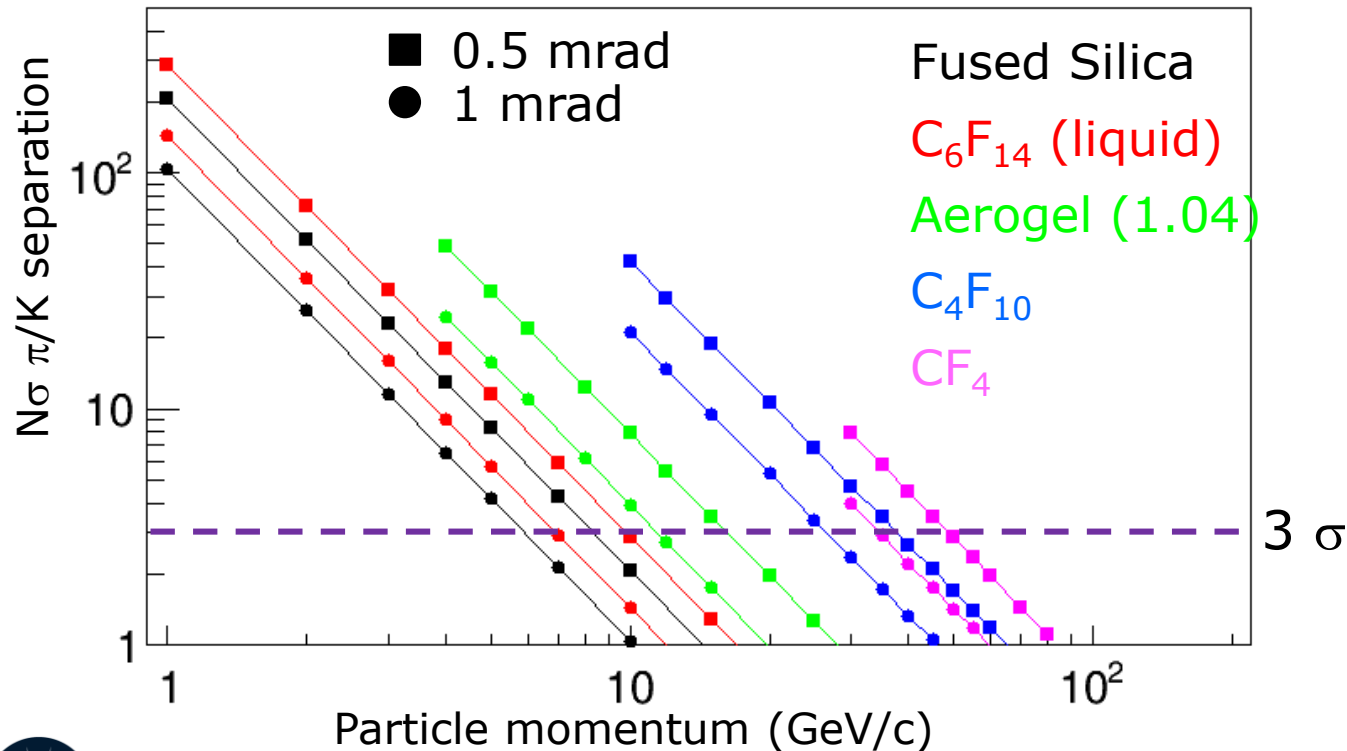
- Measures both the Cherenkov angle and the number of photoelectrons detected.
- Can be used over particle identification over large surfaces.
- Requires photodetectors with single photon identification capability.

RICH performance

$$N_\sigma \approx \frac{|m_1^2 - m_2^2|}{2P^2 \sigma[\theta_c(\text{tot})] \sqrt{n^2 - 1}}$$

For particles well above threshold

B. N. Ratcliff, NIMA 502 (2003) 211-221



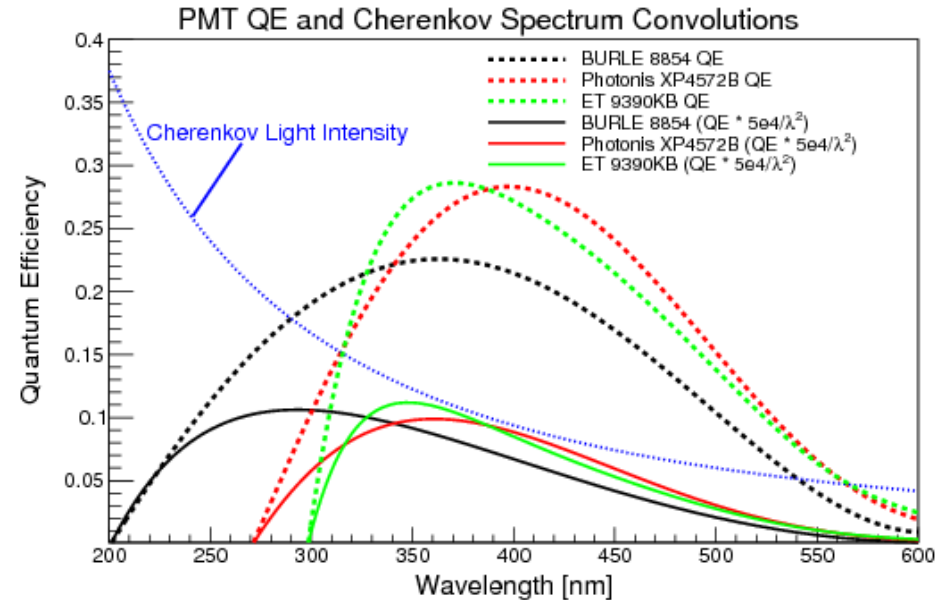
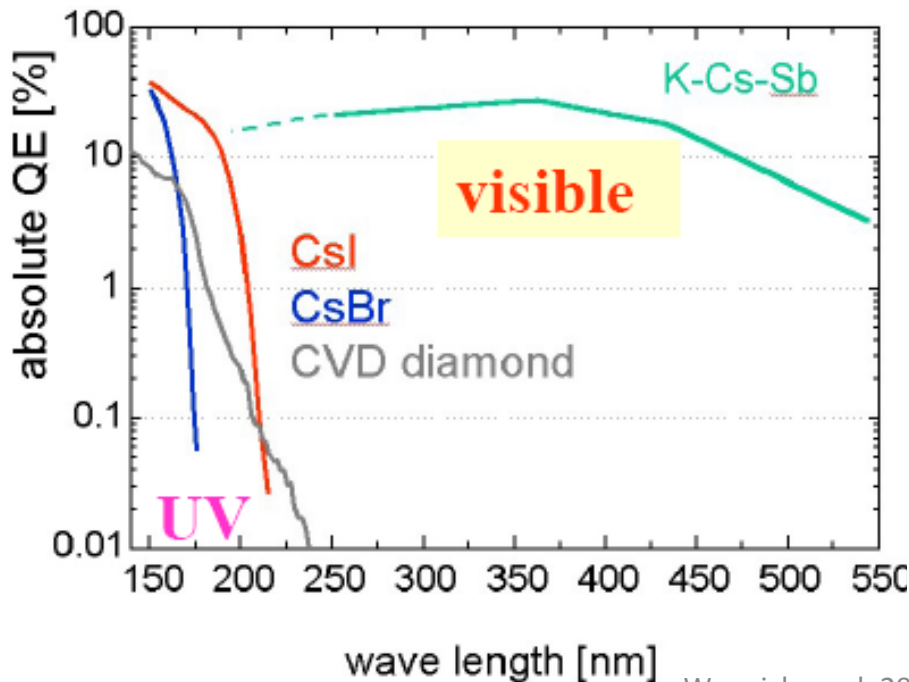
Detection of Photoelectrons

- Principle:
 - Convert Photons → Photoelectrons using a photocathode
 - Detect these photoelectrons using 'charged track detectors'.
 - Measure the position and (/or) time of photoelectrons in the tracking detector.
- General introduction to tracking detectors and silicon detectors is not covered in this lecture.
- In this lecture, we focus on some of the aspects related to the detection of photoelectrons in Cherenkov Detectors.
- Gas based detectors:
 - MWPC (Multi Wire Proportional Chambers)
 - GEM (Gas Electron Multiplier)
- Vacuum based detectors: **PMT (Photomultiplier tubes)**
HPD (Hybrid Photodiodes)
- Solid state detectors: **Silicon photomultipliers**

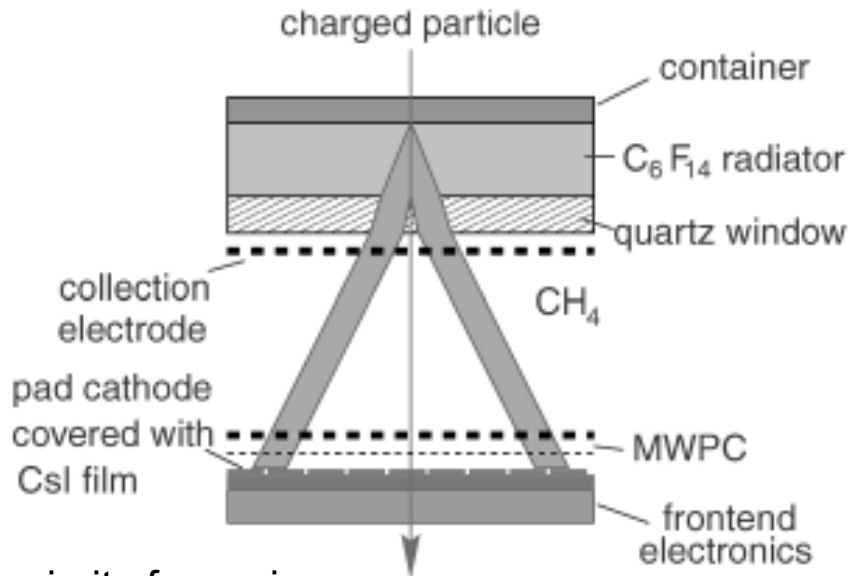
Photodetectors

➤ Photon Conversion:

- Photoelectric Effect : Photon energy to be above the 'work function' (Einstein : Nobel Prize in 1921).
- Commercial alkaline Photocathodes: Alkali , Trialkali (S20) , CsI etc.
- Alkali metals have relatively low 'work function'.
- There are also gases where the photon conversion takes place.
- Different photocathodes are efficient at different wavelength ranges.
- Quantum Efficiency (QE) : Fraction of photons converted to electrons



Photodetector with CsI photocathode



➤ Used in ALICE experiment at CERN

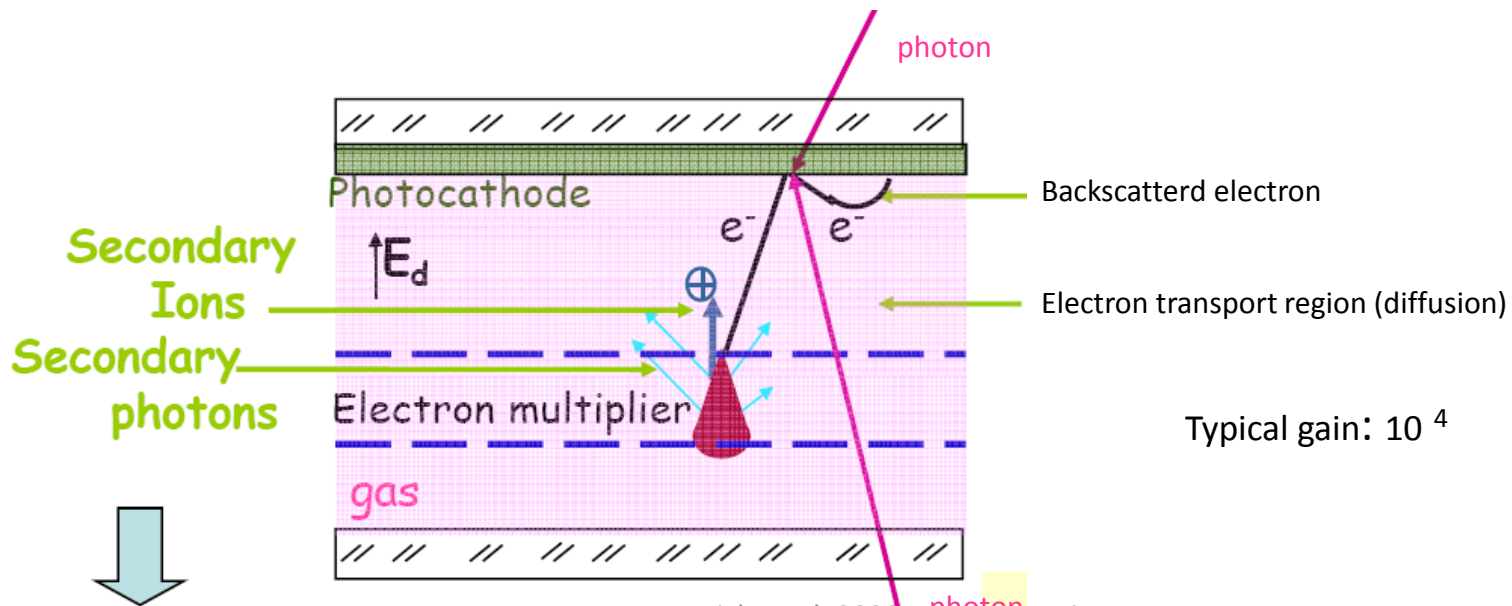
➤ Thickness of :

- radiator = 10mm
- quartz window= 5mm
- MWPC gaps= 2 mm
- Wire cathode pitch=2 mm
- Anode pitch= 4 mm
- anode diameter= 20 micron
- pad size = 8*8 mm²

➤ Total detector area: 12 m²

➤ Open geometry: using MWPC

Proximity focussing

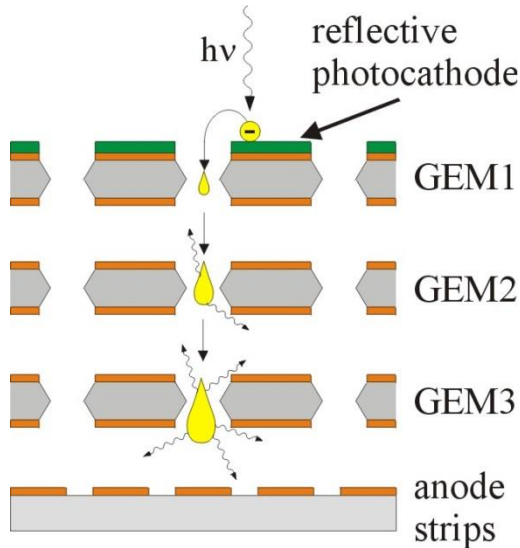


Typical gain: 10⁴

cause feedback: leading to loss of original signal info.

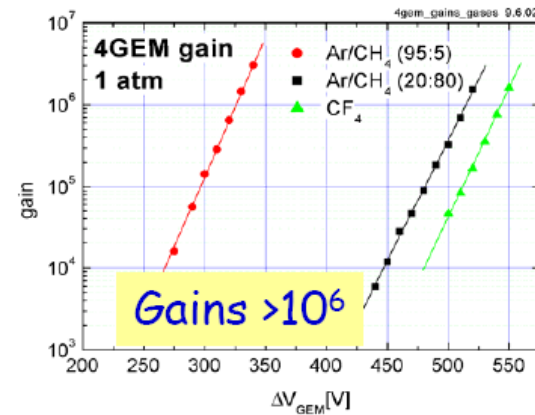
Recent Developments: Gas Based Photodetectors

GEM: Gas Electron Multiplier

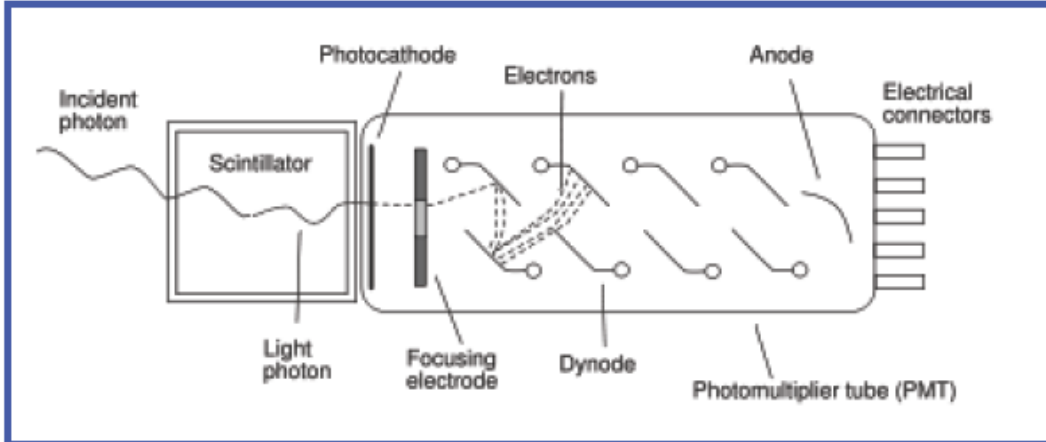


GEM with semi-transparent Photocathode (K-Cs-Sb)

- Photon and ion feed back reduced.
- Gated operation to reduce noise.
(no readout outside a 'time window of signal')
- For now only closed geometry (in sealed tubes):
Reduced fraction of useful area for photon detection (Active Area Fraction) compared to open geometry.



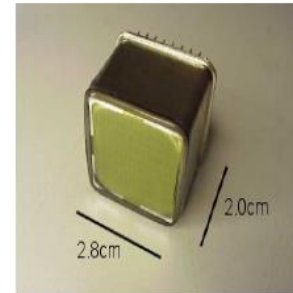
Vacuum Based Photodetectors



Schematic of a photomultiplier tube coupled to a [scintillator](#).

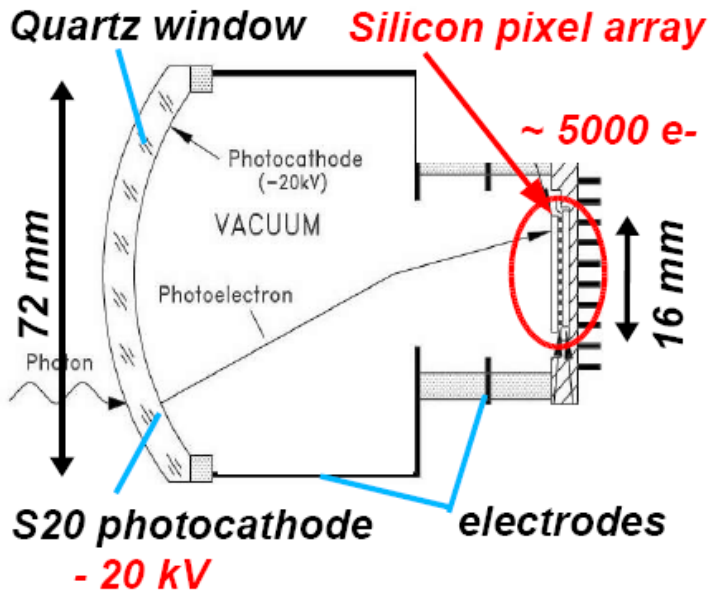


PMTs

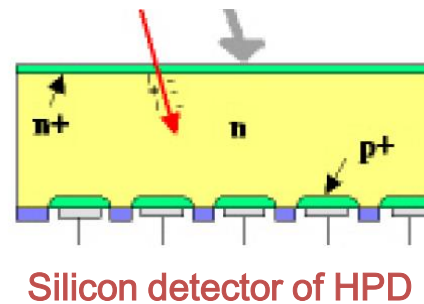


MAPMT

Schematic view of HPD



- PMTs Commercially produced: more info in www.sales.hamamatsu.com

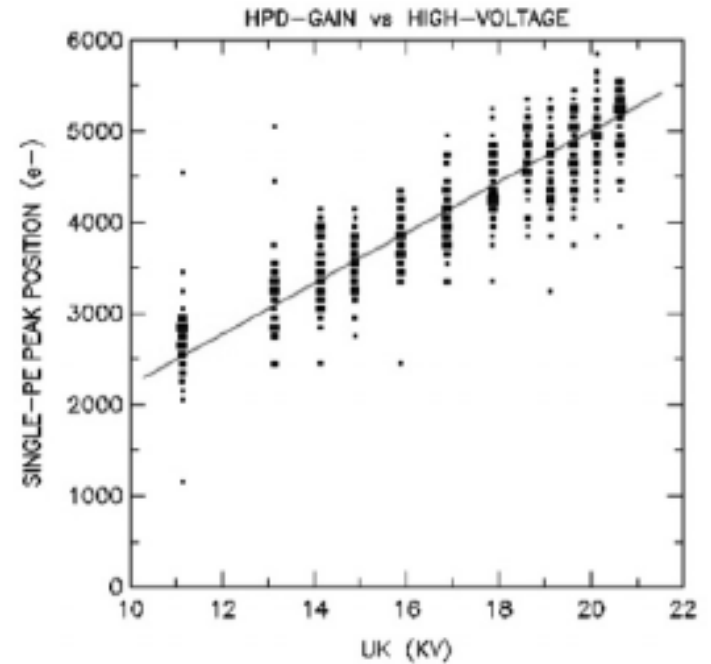
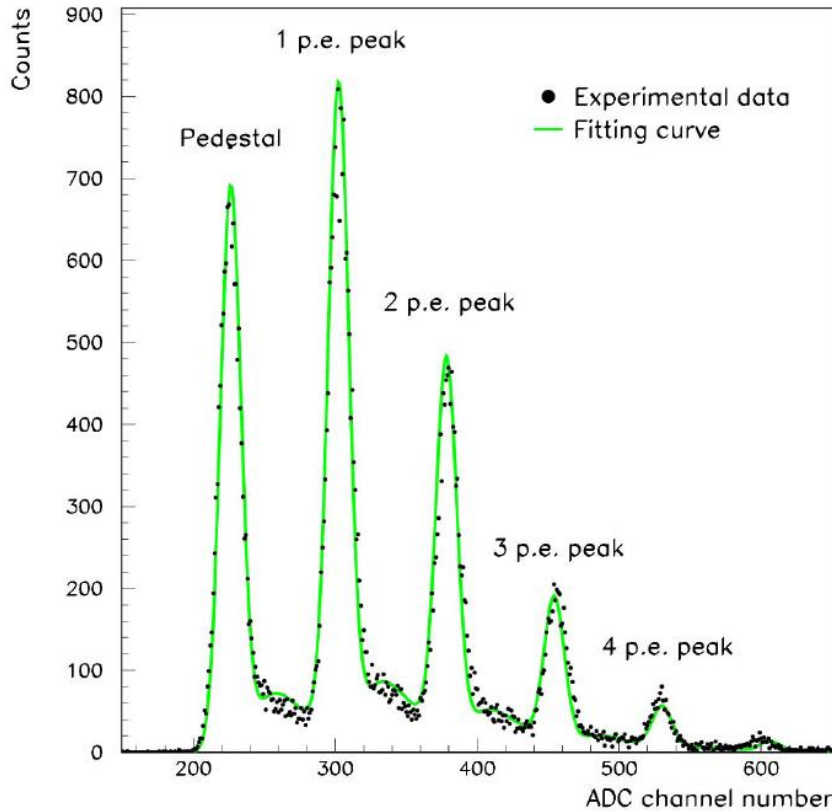


Silicon detector of HPD



HPD

Features of HPD



Signal pulse height spectrum of a 61-pixel HPD
Illuminated with Cherenkov photons

- Band gap in Silicon = 3.16eV; Typical Max Gain = $20 \text{ keV} / 3.16 \text{ eV} = 5000$ (approx)

Features of the PMTs and HPDs

- PMT:
 - Typical Gain of MAPMT 300 K.
 - Excellent time resolution: 125 ps for example (Ex: used in underwater Cherenkov detectors).
 - Active area fraction: 40 % : Fraction of effective detection area. This can be Improved with a lens, but then one may loose some photons at the lens surface.
 - Recent developments: Flat panel pmts with 89 % active area fraction. New photocathodes with >45% QE at 400 nm

- HPD:
 - Typical gain 5K, but quite uniform across different channels.
 - Excellent Single photon identification capability.
 - Active area fraction: 35→ 76 %

Comparison of photodetectors

- Choice of photodetector depends on the design of the Cherenkov detectors and constraints on cost etc.

- Gaseous:

Issues:

- Related to photon and ion feed back and high gains at high rate.
- Detection in visible wavelength range (for better resolution)

Advantages:

- Can operate in high magnetic field
- Lower cost for large size detectors compared to vacuum based

- Vacuum based:

Issues:

- Sensitivity to magnetic field
- Active Area Fraction

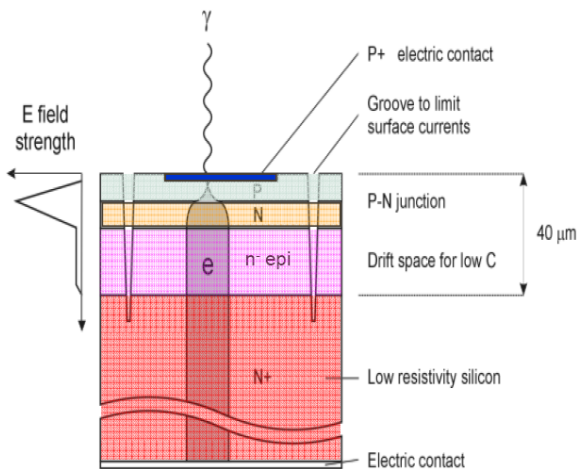
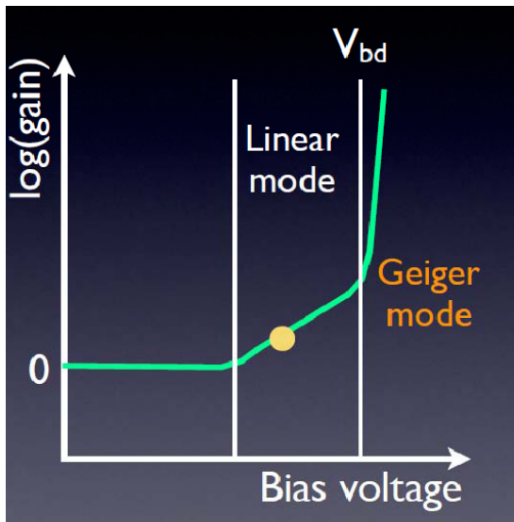
Advantages:

- Can easily operate at high rate (eg. LHC rates and higher).
- Operates also in visible wavelengths.
- Ease of operation at remote locations: underwater, in space etc.
- HPD: uniform gain over large number of tubes and small noise.

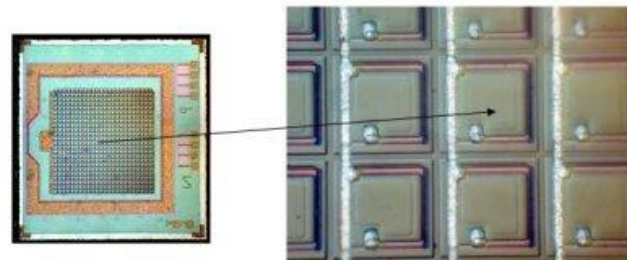
- Other Types and new developments: **APD, Silicon photomultiplier, HAPD, MCP etc.**

Recent Developments: Silicon Photomultipliers

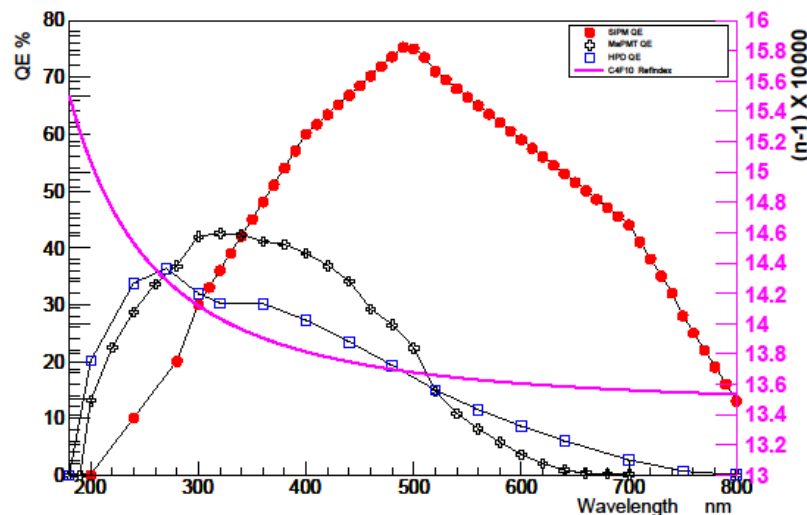
- Primary building block, GM-APD.



Array of APDs

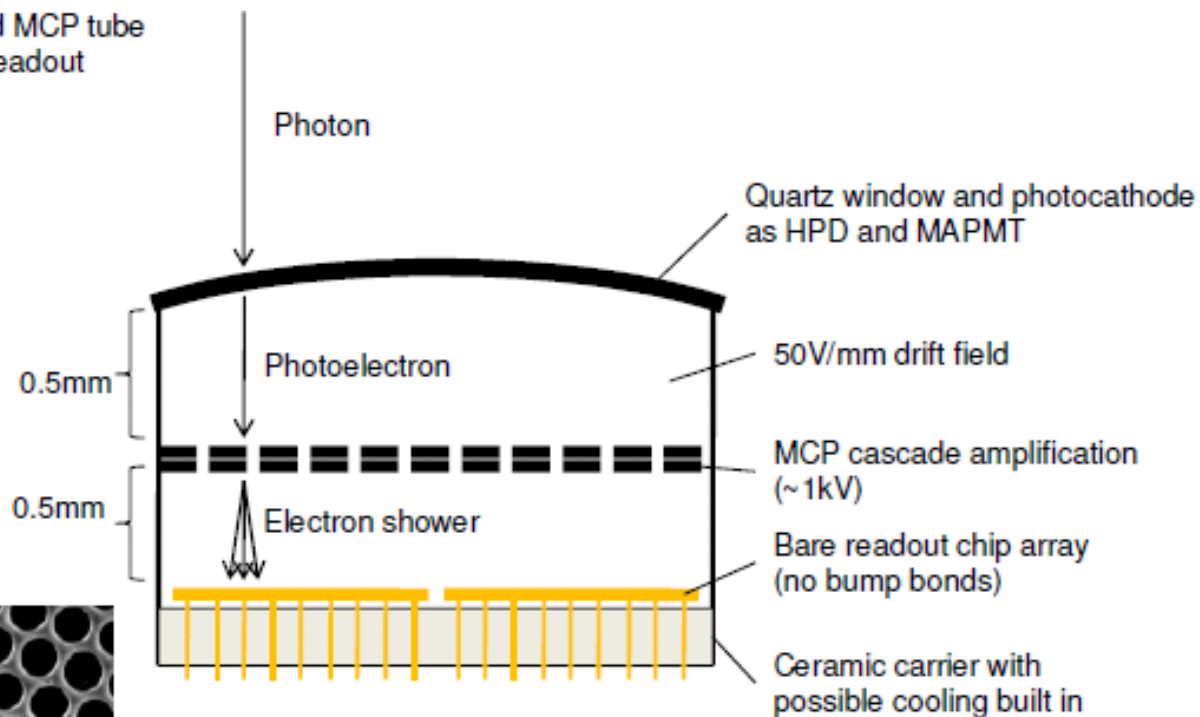


- Photon Detection Efficiency (PDE) for SiPM is better than that of ordinary PMT.
- Time resolution = ~ 100 ps.
- Works in magnetic field
- gain = $\sim 10^6$
- Reducing noise levels for single photon detection is still an issue and is being worked upon.



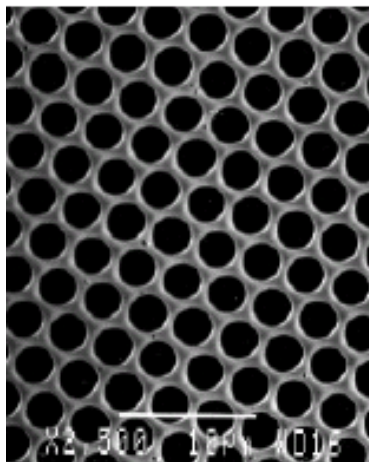
New Developments: Micro Channel Plate (MCP) Photon Detectors

Proximity focused MCP tube with 55um pixel readout



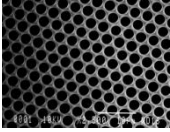
Tuning the lower drift field allows the electron shower profile to be well controlled

Cascade amplification similar in principle to a PMT



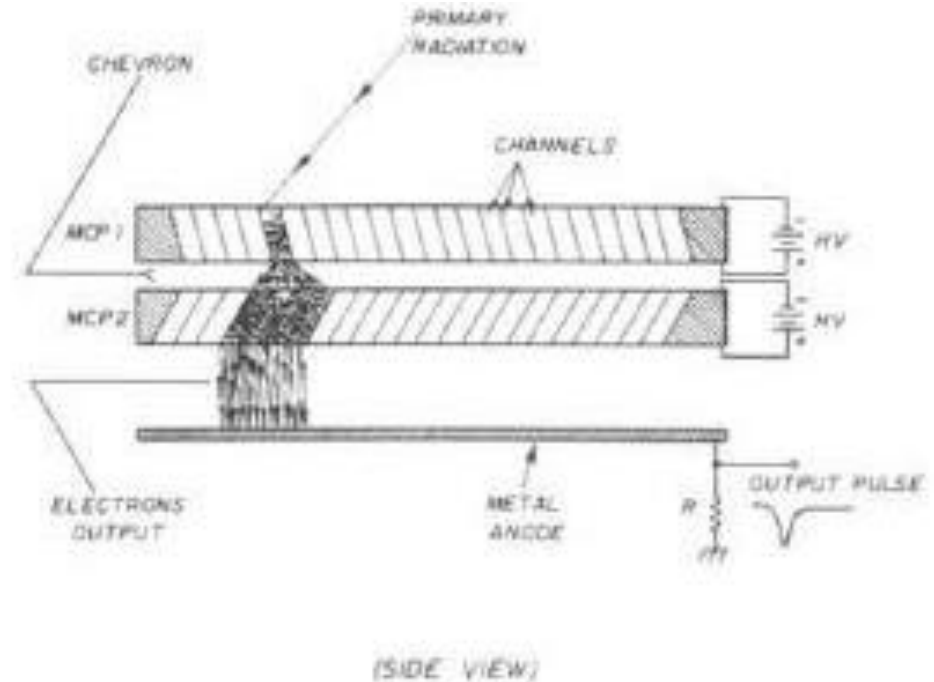
10um pores in an MCP

New Developments: Micro Channel Plates (MCP)



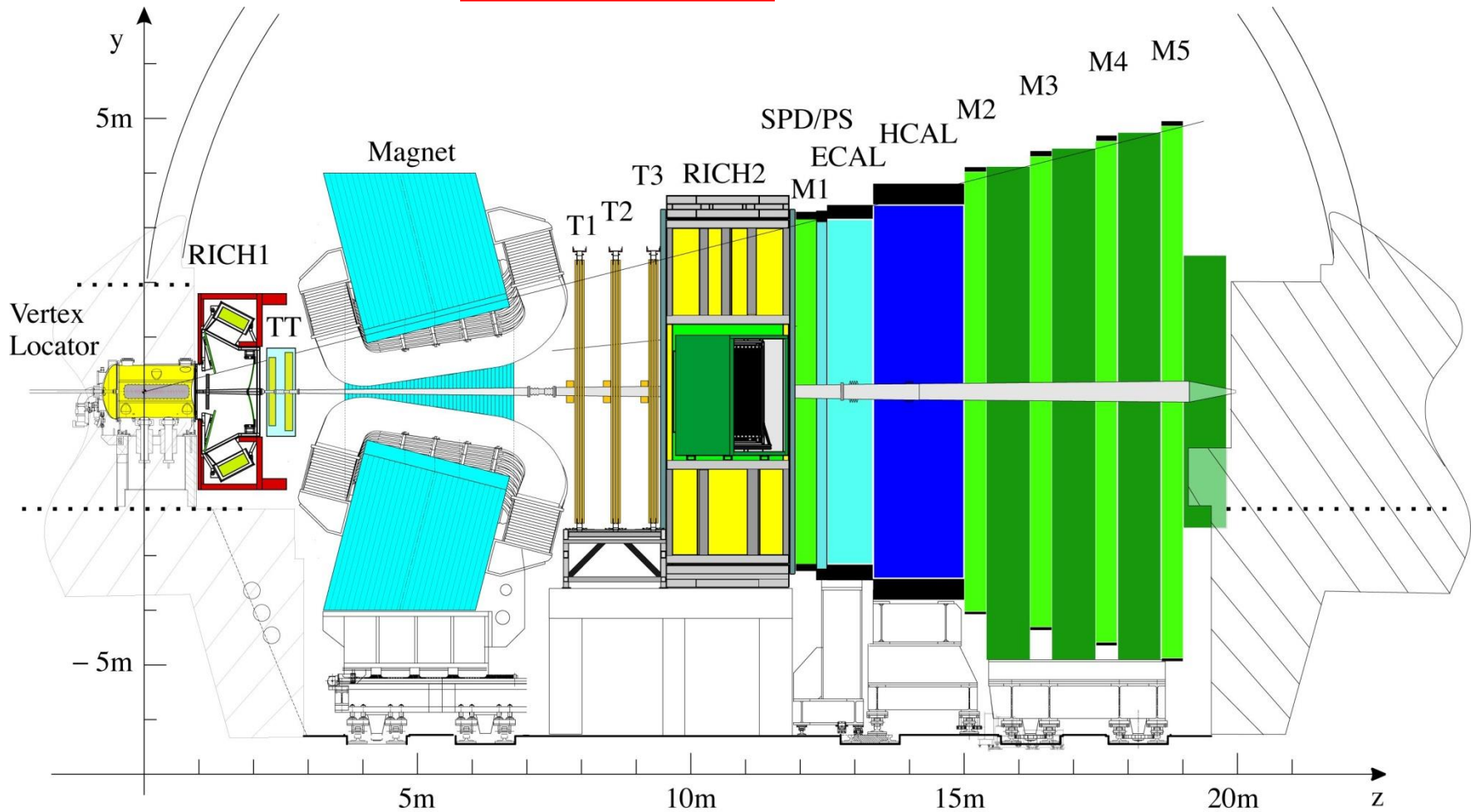
Typical Size:

- 2 mm thickness, 51 mm X 51 mm active area.
- 10 micron pores separated by 15 microns
- Chevron: 8 degree tilt : To increase th gain and reduce ion-feed back
- Gain: $\sim 5 * 10^5$
- Typically ~ 1000 channels per MCP.



- Measure Space and time of the hits.
- Manufactured by industry (Photonics for example).
- Resolutions: Space: ~ 100 microns, Time: $\sim 50 - 100$ psec.
- Short flight path of photoelectrons: Resistant to magnetic fields up to 0.8 Tesla.
- Can work at 40 MHz readout rate.
- Can detect single photons (No noise from 'first dynode' as in MAPMT).
- Fast 'ageing' at large luminosity (eg: LHC) is an issue, but there are some solutions.

LHCb Experiment



- Precision measurement of B-Decays and search for signals beyond standard model.
- Two RICH detectors covering the particle momentum range $1 \rightarrow 100$ GeV/c using aerogel, C_4F_{10} and CF_4 gas radiators.

LHCb-RICH Specifications

RICH1: Aerogel $2 \rightarrow 10 \text{ GeV}/c$

C_4F_{10} $< 70 \text{ GeV}/c$

RICH2: CF_4 $< 100 \text{ GeV}/c$

Aerogel C_4F_{10} CF_4

L 5 86 196 cm

θ_c^{\max} 242 53 32 mrad

π_{Th} 0.6 2.6 4.4 GeV/c

K_{Th} 2.0 9.3 15.6 GeV/c

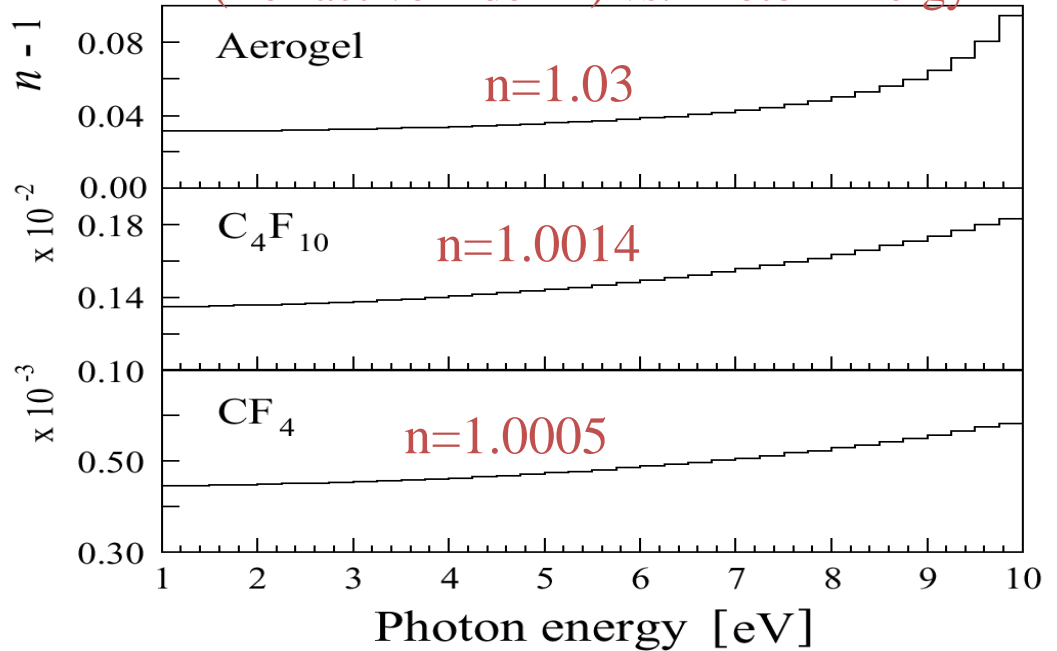
Aerogel: Rayleigh Scattering

Not used from 2015 onwards

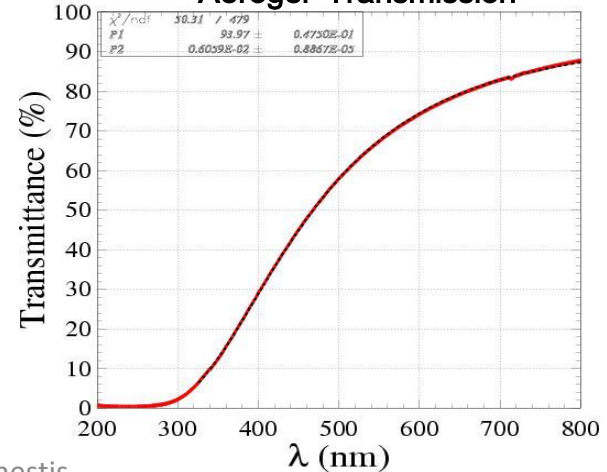
$$T = A e^{-C t / \lambda^4}$$

Typically: $A = 0.94$, $C = 0.0059 \mu\text{m}^4/\text{cm}$

(Refractive Index-1) vs. Photon Energy

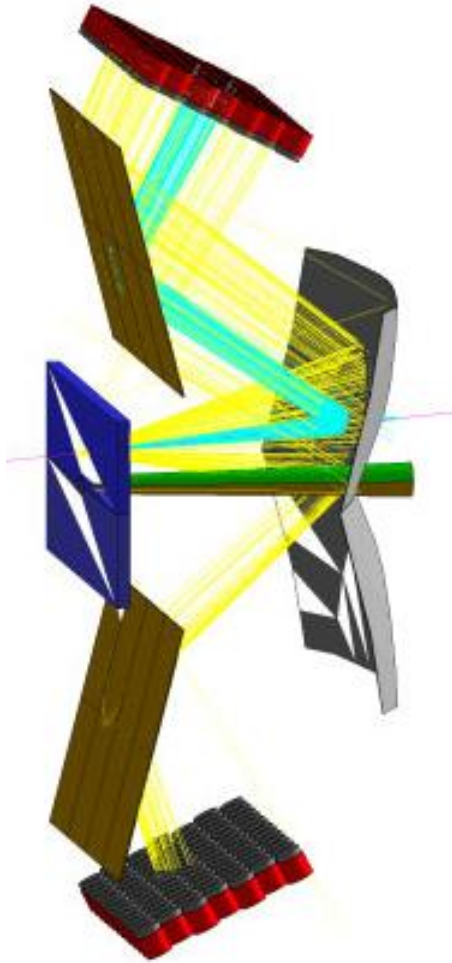


Aerogel Transmission



LHCb- RICH1 SCHEMATIC

RICH1 OPTICS



Magnetic Shield

Gas Enclosure

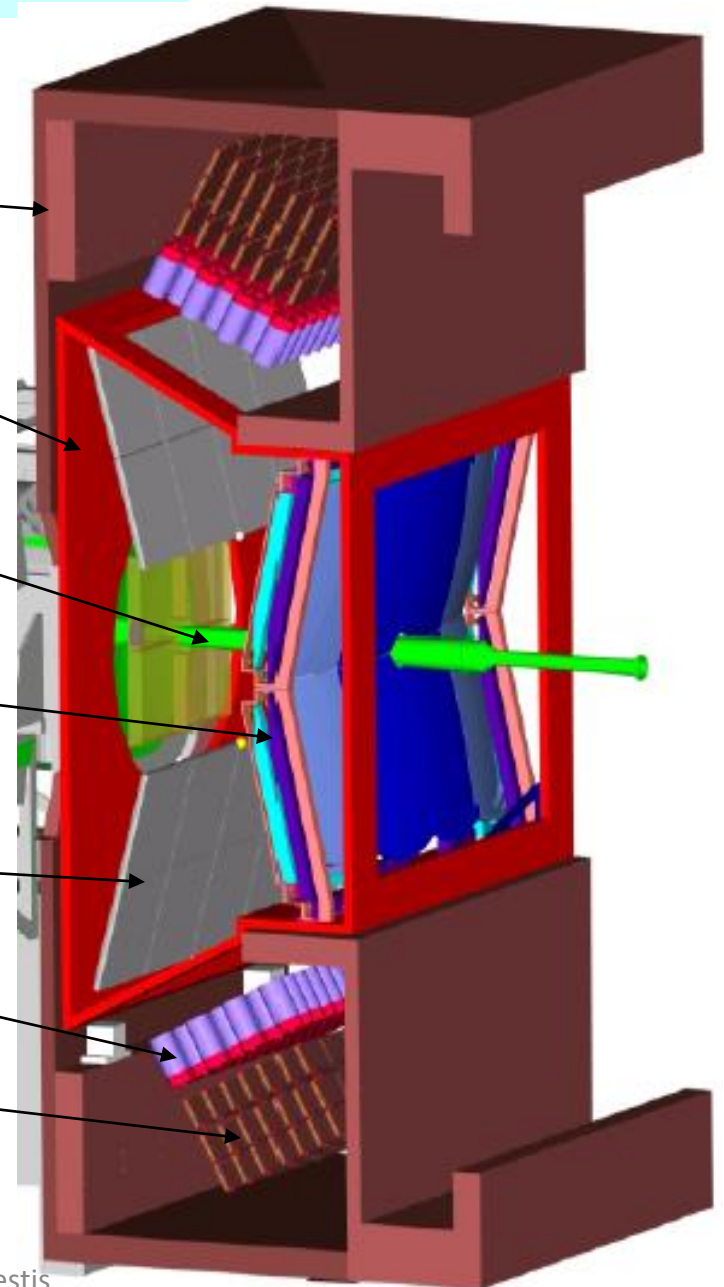
Beam Pipe

Spherical Mirror

Flat Mirror

Photodetectors

Readout Electronics



- Spherical Mirror tilted to keep photodetectors outside acceptance (tilt ~ 0.3 rad)

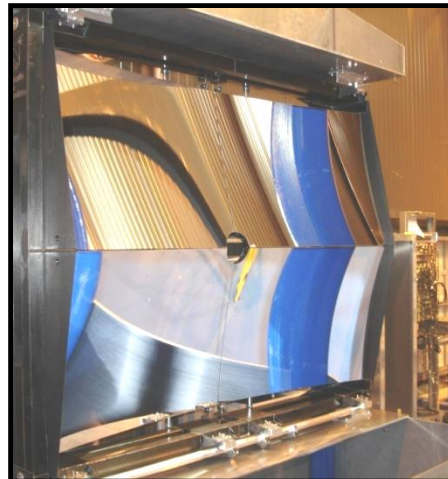
RICH1 Photos



RICH1-HPDs

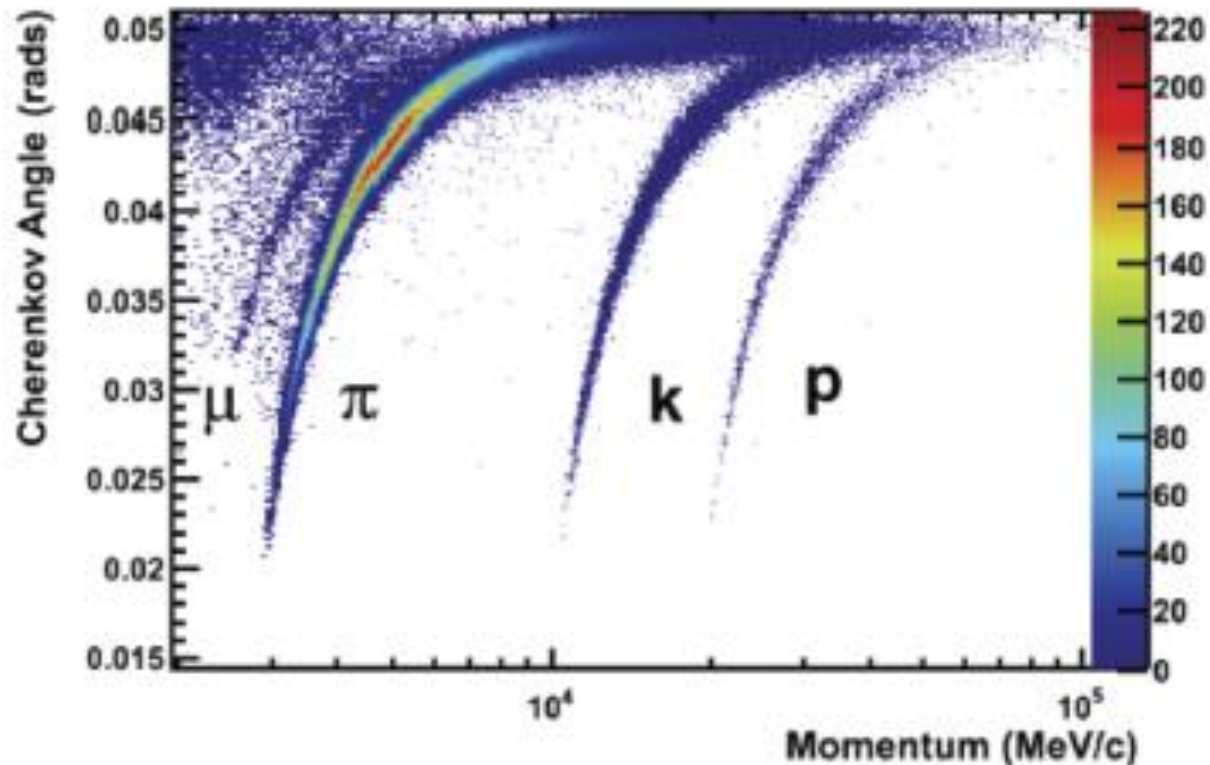


RICH1 mirrors



Performance of LHCb RICH

- From isolated Cherenkov rings from RICH1 in Real Data

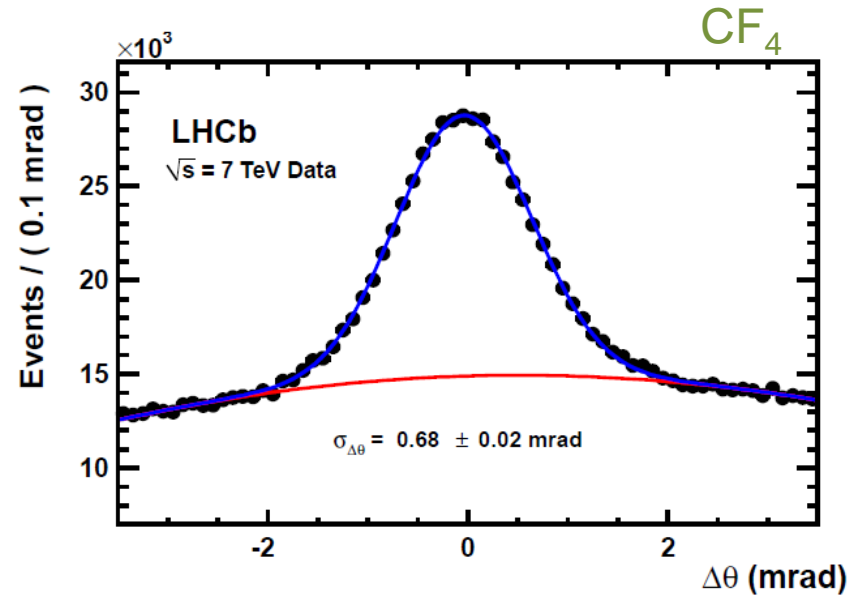
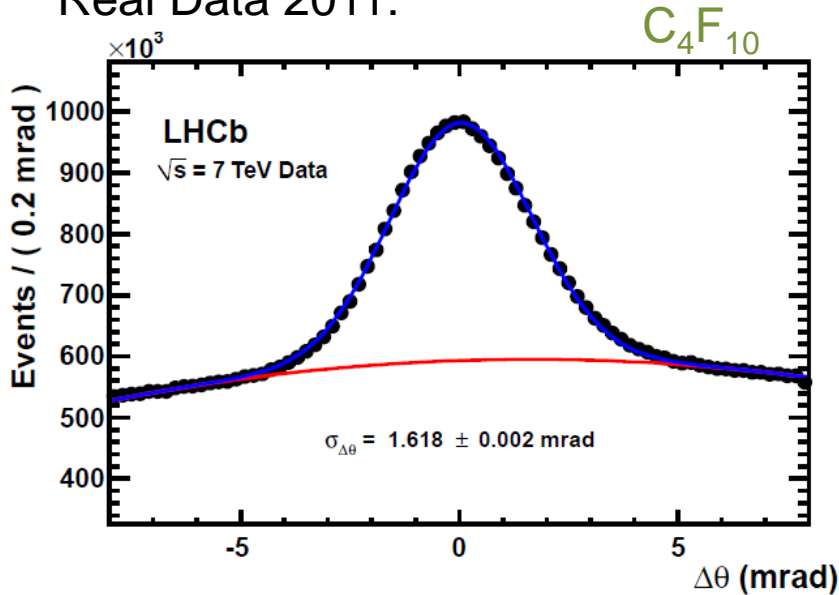


Compare with the expectations plotted in page 9.

LHCb-RICH resolution

Single photon resolutions

Real Data 2011:



From simulation in 2011:

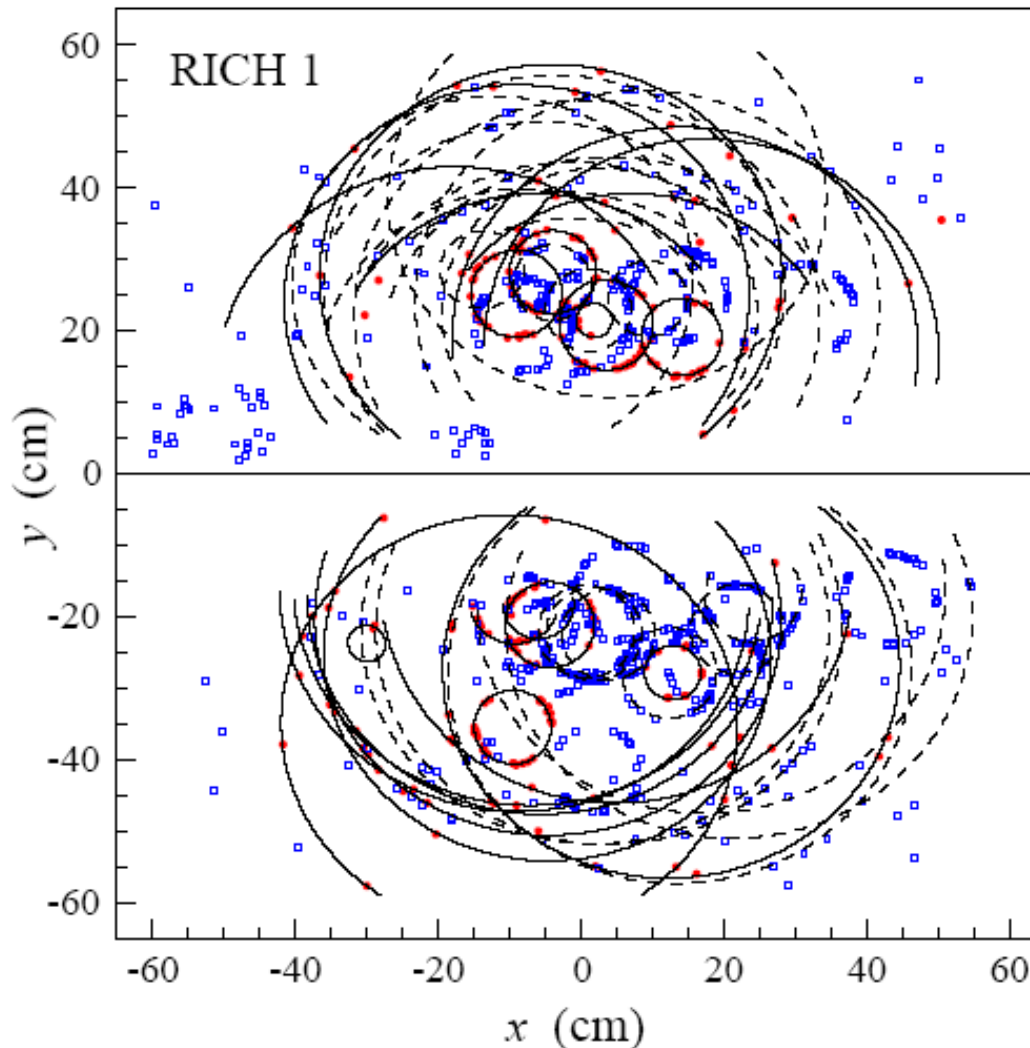
$$\sigma_{\Delta\theta} = 1.53 \text{ mrad}$$

From simulation in 2011:

$$\sigma_{\Delta\theta} = 0.68 \text{ mrad}$$

- Resolution components:
- Chromatic : ref. index variation
 - Emission Point: tilt of the mirror
 - Pixel size: granularity of the pixel
 - PSF: spread of photo electron direction inside HPD

LHCb: Hits on the RICH from Simulation



Red: From particles from Primary and Secondary Vertex

Blue: From secondaries and background processes (sometimes with no reconstructed track)

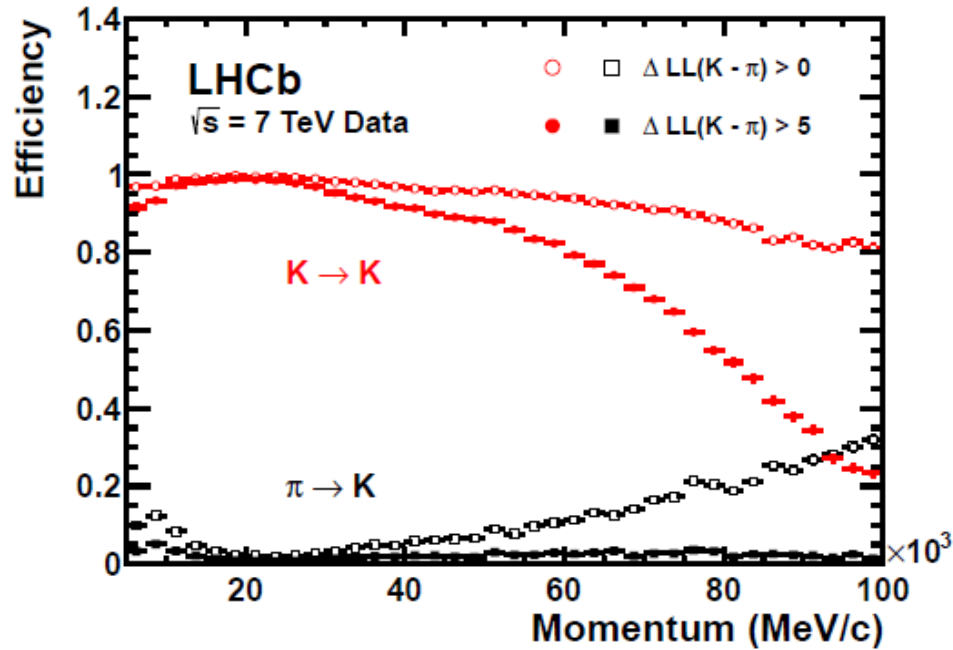
Pattern Recognition in Accelerator based Cherenkov Detector

- Events with large number of charged tracks giving rise to several overlapping Cherenkov Rings on the Photo detector plane.
Problem: To identify which tracks correspond to which hits and then identify the type (e, π , p etc.) of the particle which created the tracks.
- Hough Transform:
 - Project the particle direction on to the detector plane
 - Accumulate the distance of each hit from these projection points in case of circular rings.
 - Collect the peaks in the accumulated set and associate the corresponding hits to the tracks.

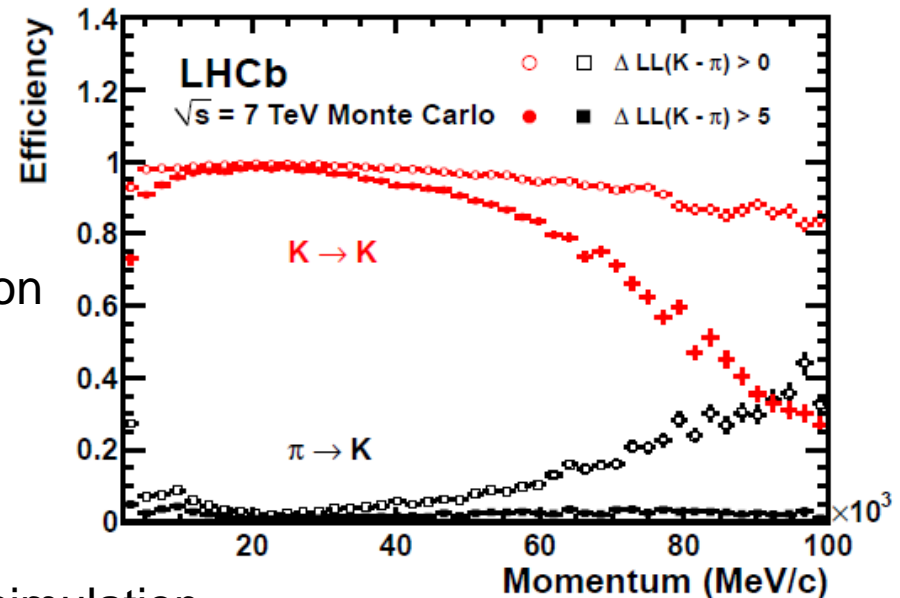
(used by ALICE at CERN)
- Likelihood Method:
 - For each of the track in the event, for a given mass hypothesis, create photons and project them to the detector plane using the knowledge of the geometry of the detector and its optical properties. Repeat this for all the other tracks.
 - From this calculate the probability that a signal would be seen in each pixel of the detector from all tracks.
 - Compare this with the observed set of photoelectron signal on the pixels, by creating a likelihood.
 - Repeat all the above after changing the set of mass hypothesis of the tracks. Find the set of mass hypothesis, which maximize the likelihood.

(used by LHCb at CERN)

LHCb-RICH PID performance



Real data



Simulation

Red: Kaon identification efficiency

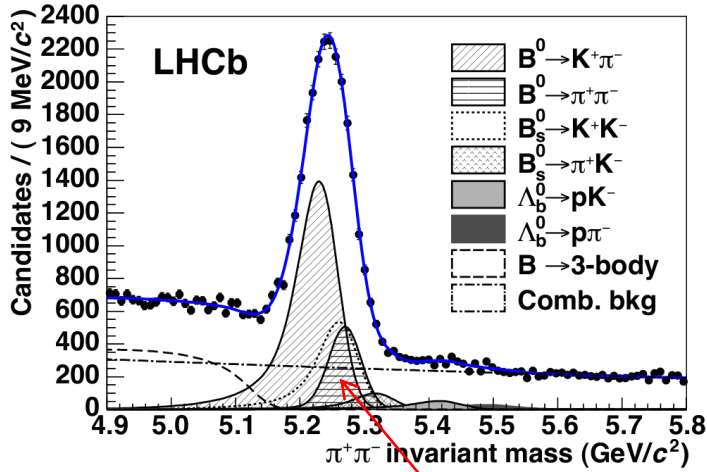
Black: Pion mis-identification probability

PID performance in D^ events (calibration channel)*

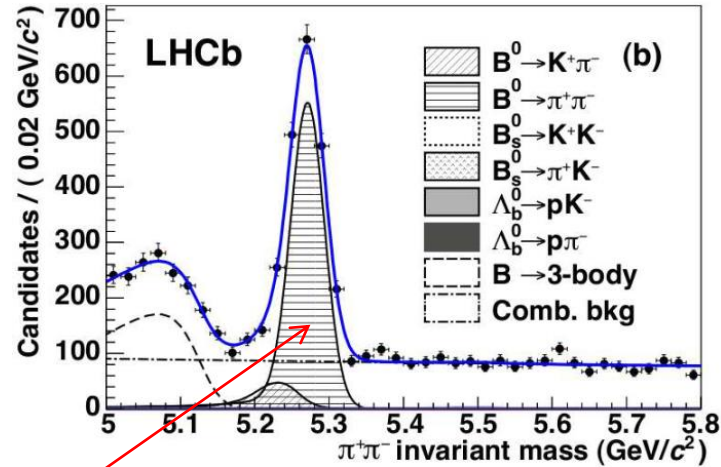
General agreement between real data and simulation

RICH Detectors in LHCb

Real data from 2011



Before RICH PID



After RICH PID

Without RICH PID, the $B^0 \rightarrow \pi^+ \pi^-$ is completely dominated by $B^0 \rightarrow K^+ \pi^-$

RICH PID useful for physics analysis

JHEP 10 (2012) 037

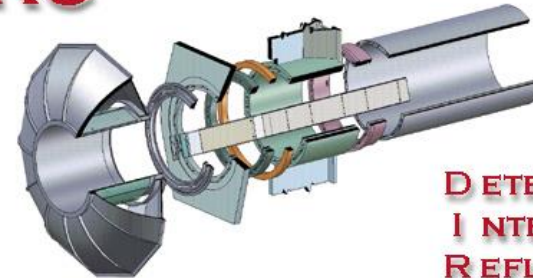
How to make a better RICH detector

- Increase the number of photons
 - Better photon detectors (photo-cathodes)
 - Better area coverage by photon detectors
 - Better optical coupling of components
- Improve Cherenkov angle resolution
 - Smaller pixels
 - Lower chromatic error
 - Detectors sensitive to green rather than blue
 - Improve aberrations
 - Light weight mirrors in the acceptance

DIRC

- Direct Internally Reflected Cherenkov light
- Detectors outside the “acceptance”
- Can fit in a narrow space

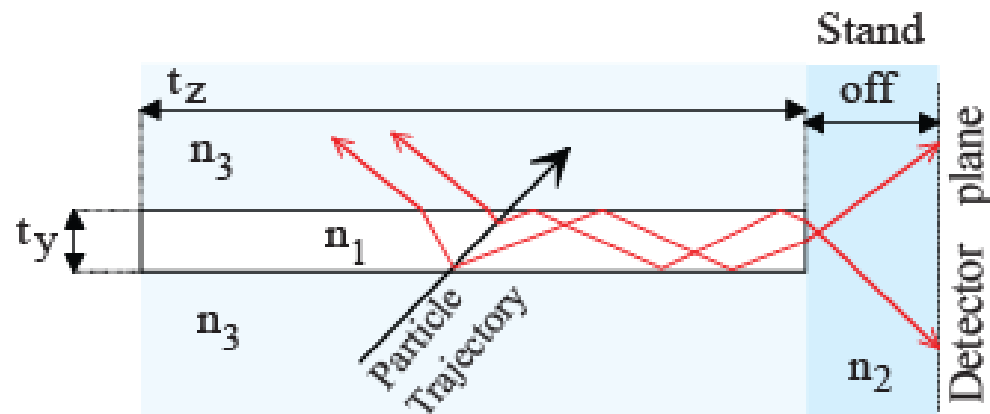
DIRC



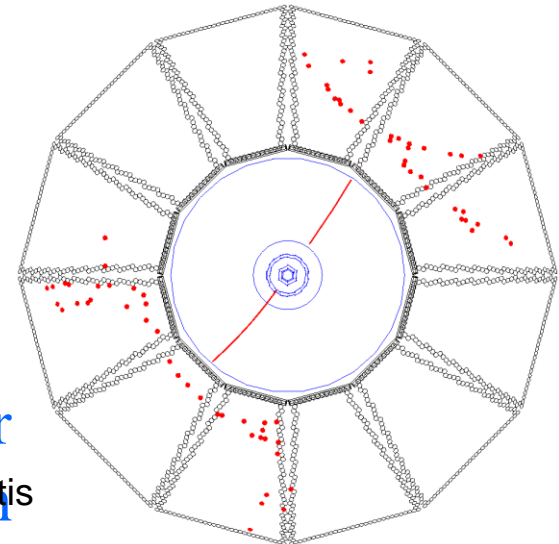
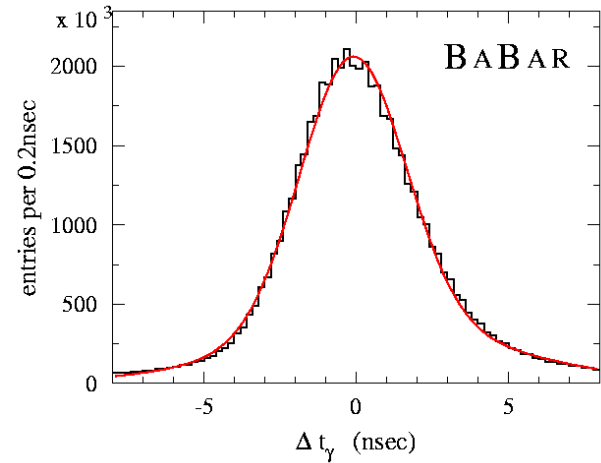
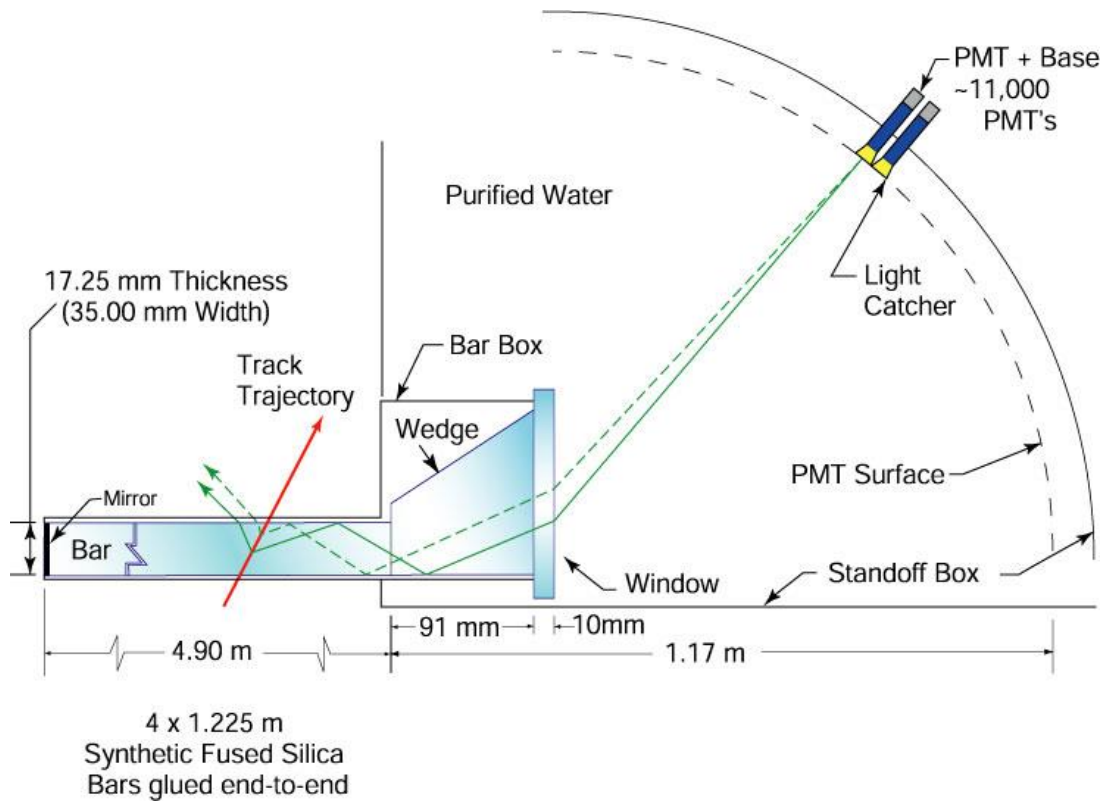
**DETECTION OF
I NTERNALLY
R E F L E C T E D
C H E R E N K O V L I G H T**

The standoff region is designed to maximize the transfer efficiency between the radiator and the detector.

If this region has the same index of refraction as the radiator, $n_1 \cong n_2$, the transfer efficiency is maximized and the image will emerge without reflection or refraction at the end surface.



Babar DIRC



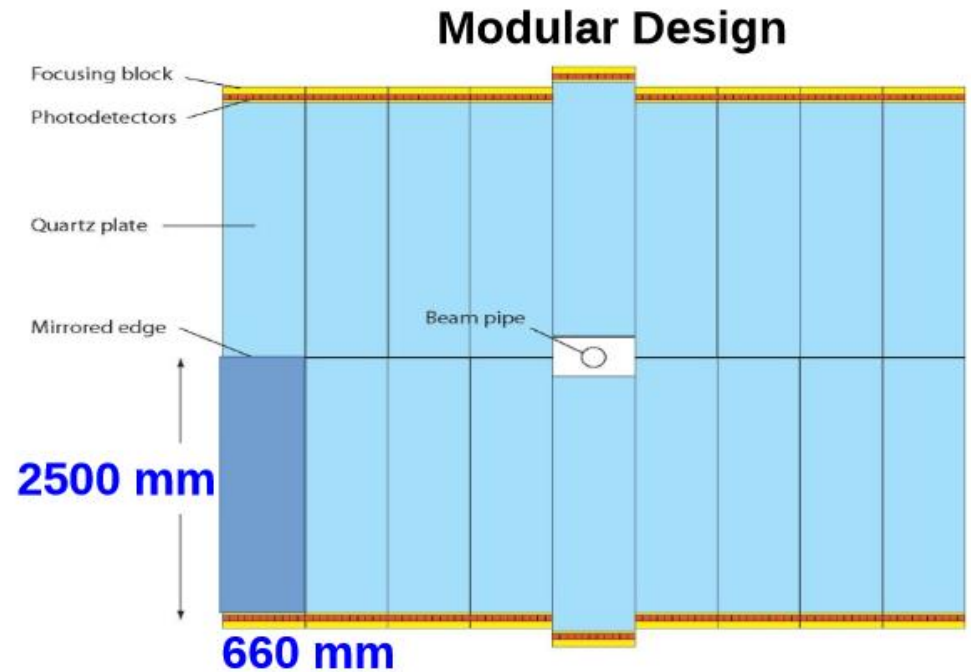
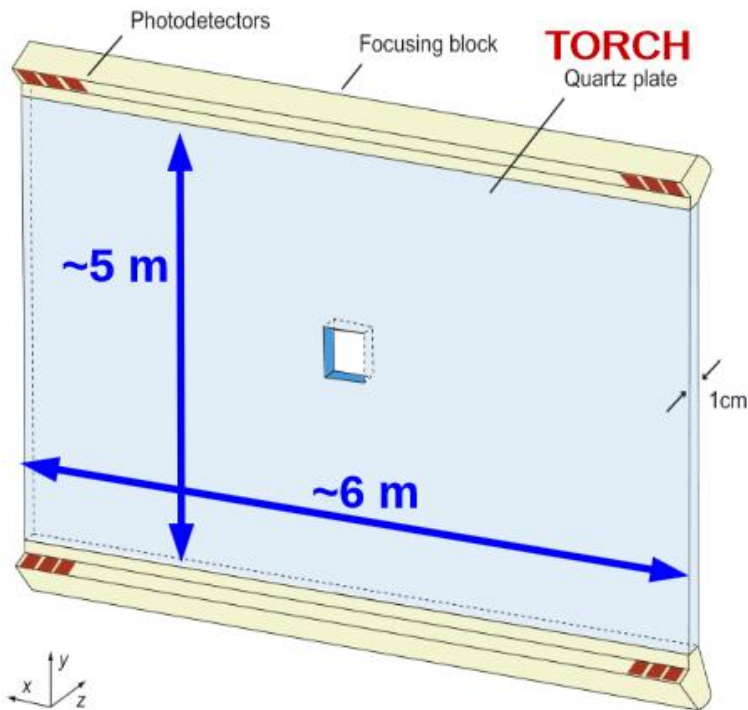
± 8 ns Δt window for
background rejection

Warwick week 2020 - A Papanestis



TORCH (i)

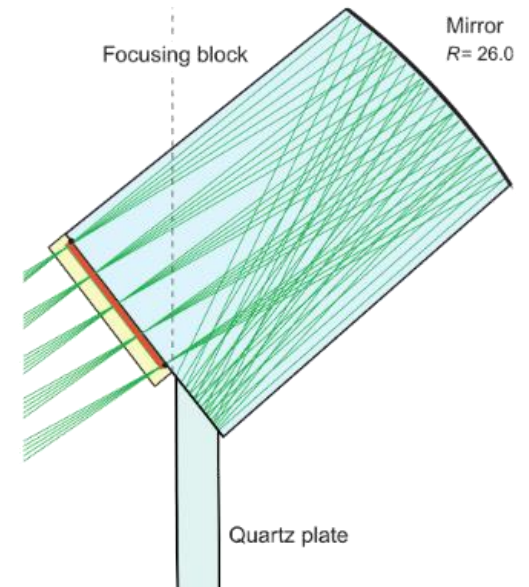
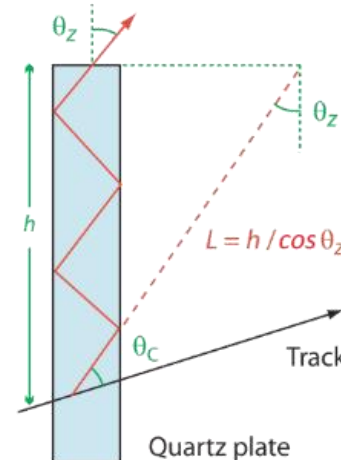
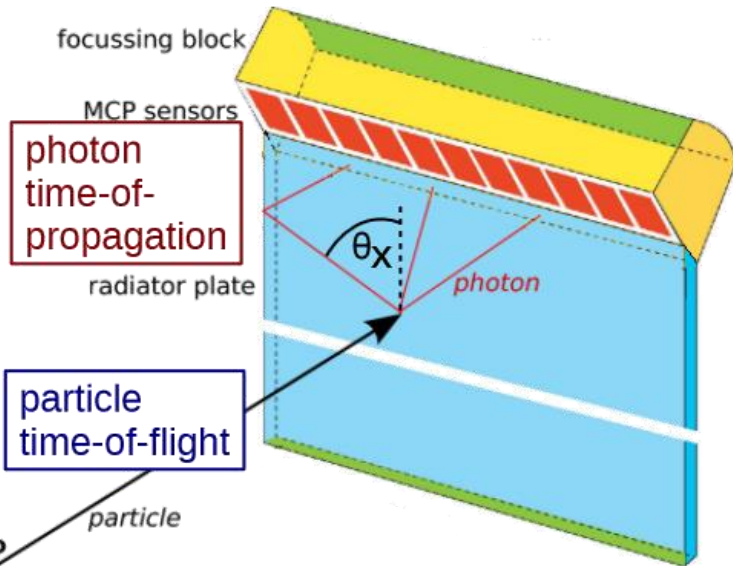
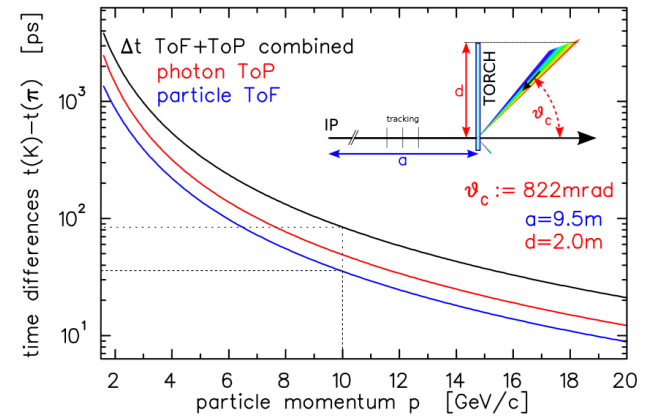
A time of flight detector based on Cherenkov radiation



TORCH (ii)

The focusing unit converts angles to positions allowing the measurement of propagation time

Multiple photons from the same track can improve the time accuracy



Summary

- The field of Particle Identification Detectors is an evolving field.
- They have contributed to some of the important discoveries in High Energy Physics in the last 50 years and they continue to be a crucial part of some of the recent experiments.
- The RICH detectors offer excellent Particle Identification capability for the hadrons since they can be designed to have very good single photon Cherenkov Angle resolution and large Photoelectron yield. Recent advances in photodetectors enhance the capability of these detectors.
- The particle ID using dE/dx , time-of-flight and Transition Radiation detectors continue to provide Particle Identification in different experiments.
- Particle identification is a crucial part of some of the Astroparticle physics experiments and long base line neutrino experiments

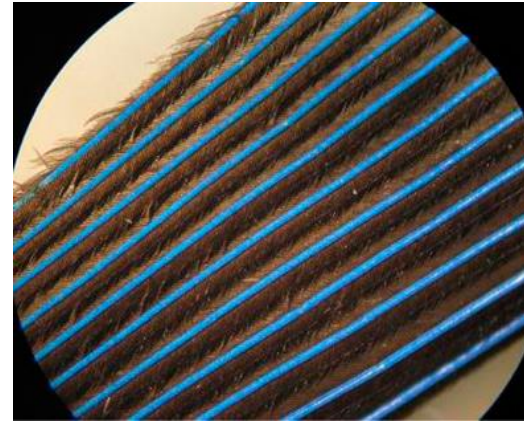
The end

Thank you for
your attention

Any (more) questions?



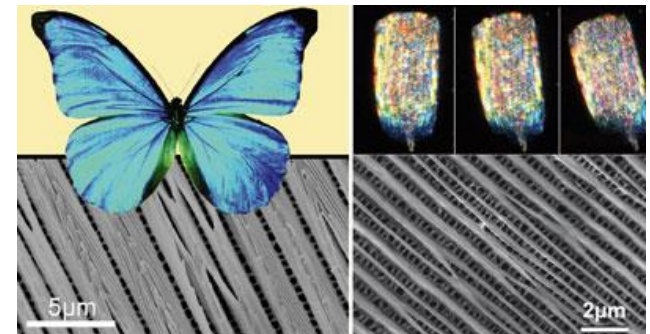
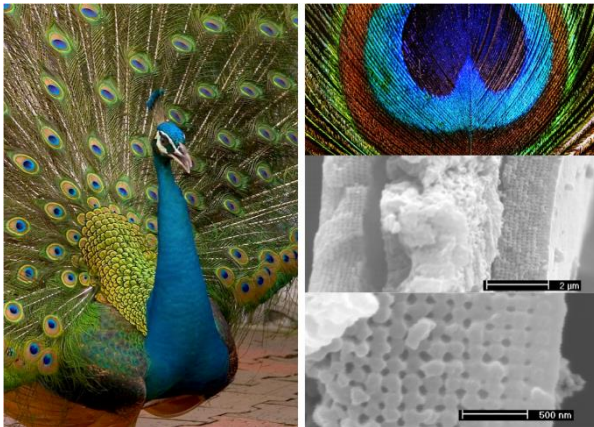
Photonic Crystals



Optical micrograph of blue feather barbs

www.pnas.org/cgi/doi/10.1073/pnas.1204383109

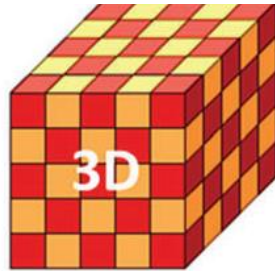
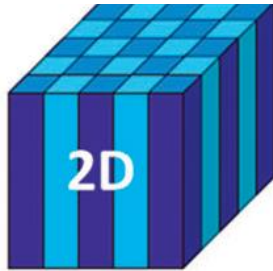
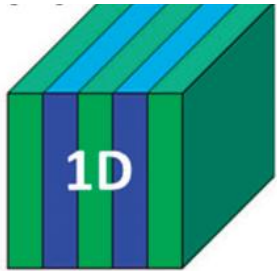
Parrot (scarlet macaw) in a tropical forest



CERN Courier Aug23, 2005

Phys. Rev. E **72**, 016902 (2005)

Photonic Crystals



- Periodic arrangement of objects with two different refractive indices.
- Lattice constants comparable to the wavelength of light in the material
- electrons in pure semi-conductor : similar features to photons in photonic crystal

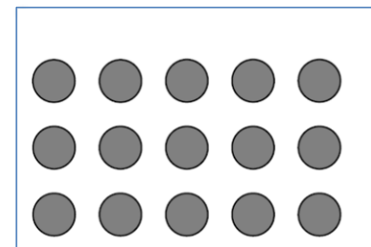
▪ Cherenkov radiation:

- Physical origin is a mixture of conventional Cherenkov radiation and Transition radiation
- Photon propagation in the crystal in the form of Bloch waves
- All the properties can be derived from solving Maxwell's equations for periodic lattice
- There is no Cherenkov Threshold
- Cherenkov cone can be forward or backward

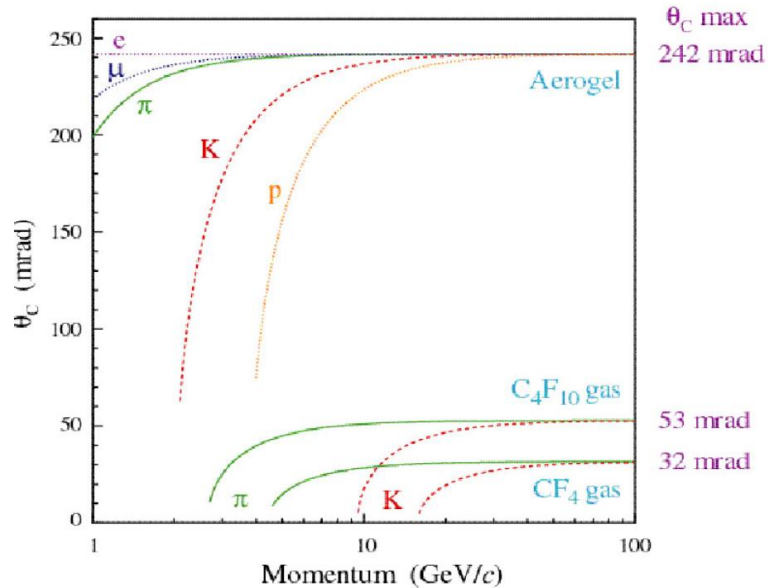
[arXiv:0808:3519](https://arxiv.org/abs/0808.3519)

- Starting from two media with refractive indices n_1 and n_2 , create a new effective refractive index n_3 .

r =cylinder radius
 a = lattice constant



Possibility of particle identification with periodic media

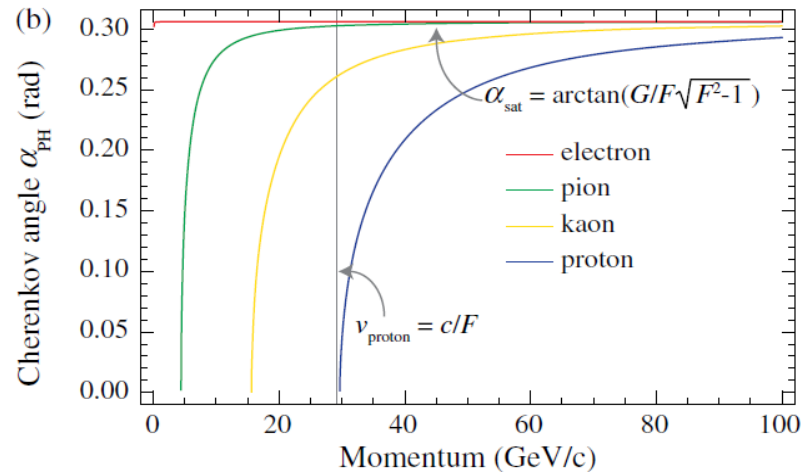
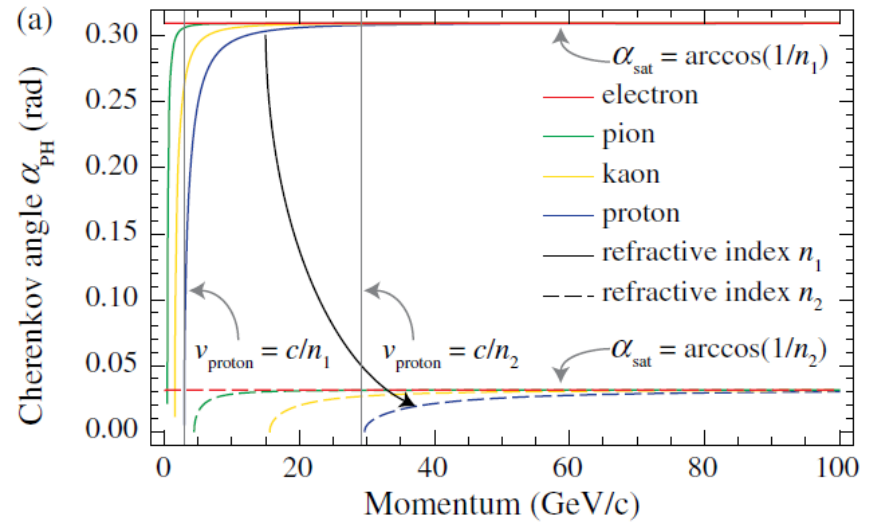


$$\text{Sensitivity} = \theta_{\text{electron}} - \theta_{\text{proton}}$$

Transformation optics:

- Longitudinal stretching = $F=1.005$: Shift curves to right
- Transverse stretching = $G=10$: Increase θ

PRL 113, 167402 (2014)



Cherenkov Detectors in Astro Particle Physics

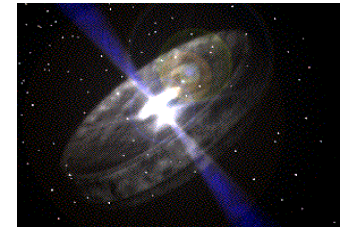
Goal: Contribute to the understanding of our Universe.

- ❖ Understanding production mechanism ('cosmic accelerators') of HE cosmic rays ;
- ❖ Study very energetic galactic / extragalactic objects : SN remnants, microquasars, GRB, AGN,....;
- ❖ Search for Dark matter (wimps)
- ❖ . . .

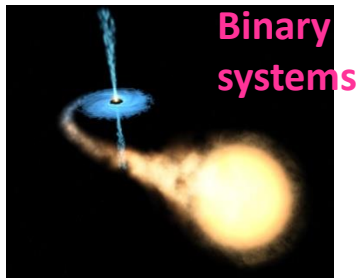
SNR



AGN

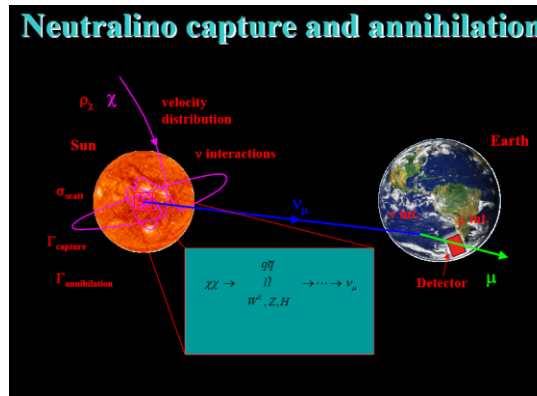


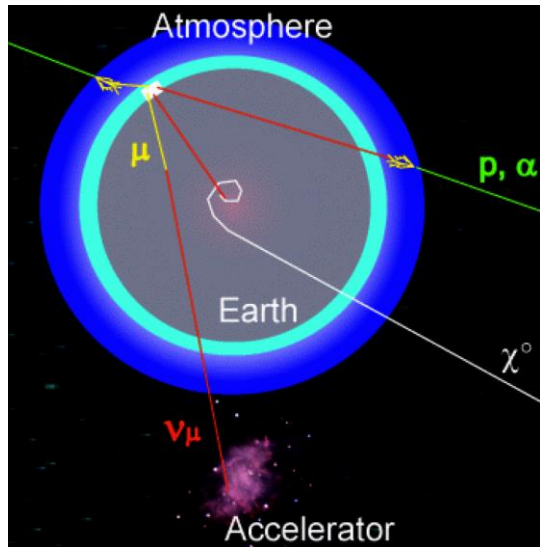
GRB



Binary systems

Micro-quasars





Search for :

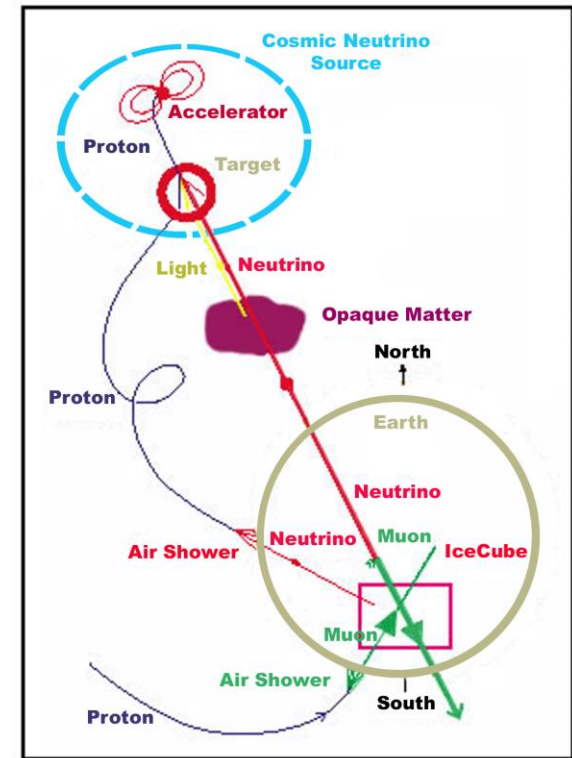
- Neutrinos → muons
- High energy Gamma and other Cosmic rays → Air showers
- Ultra high energy Gamma ($> 10^{19}$ eV) → Air showers

Neutrinos: Advantages:

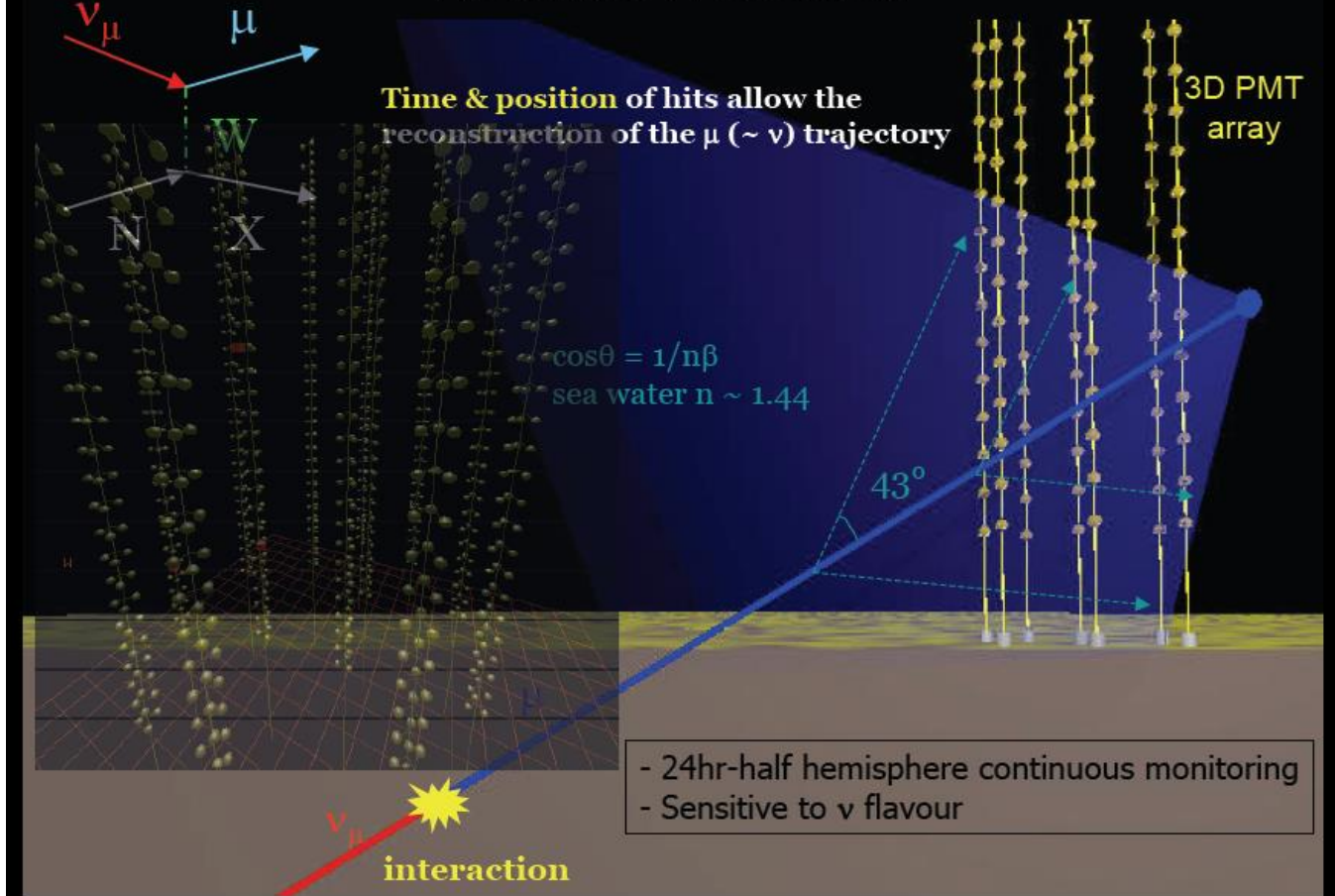
- Neutral : Hence Weak interaction only
- Neutrinos point back to the astrophysical production source
 - Unlike photons which interact with CMB and matter...
 - or protons: which also undergo deflection by magnetic fields

Disadvantages:

- Rate of arrival very low. Hence need very large detectors.
- Using the Ocean , ice in Antartica etc.



Neutrino Detection



• Typically 1γ / PMT
40 m from μ axis

• Measure position and time of the hits.

Angle between the μ and ν direction=

$$\theta \leq \frac{1.5 \text{ deg.}}{\sqrt{E_\nu [\text{TeV}]}}$$

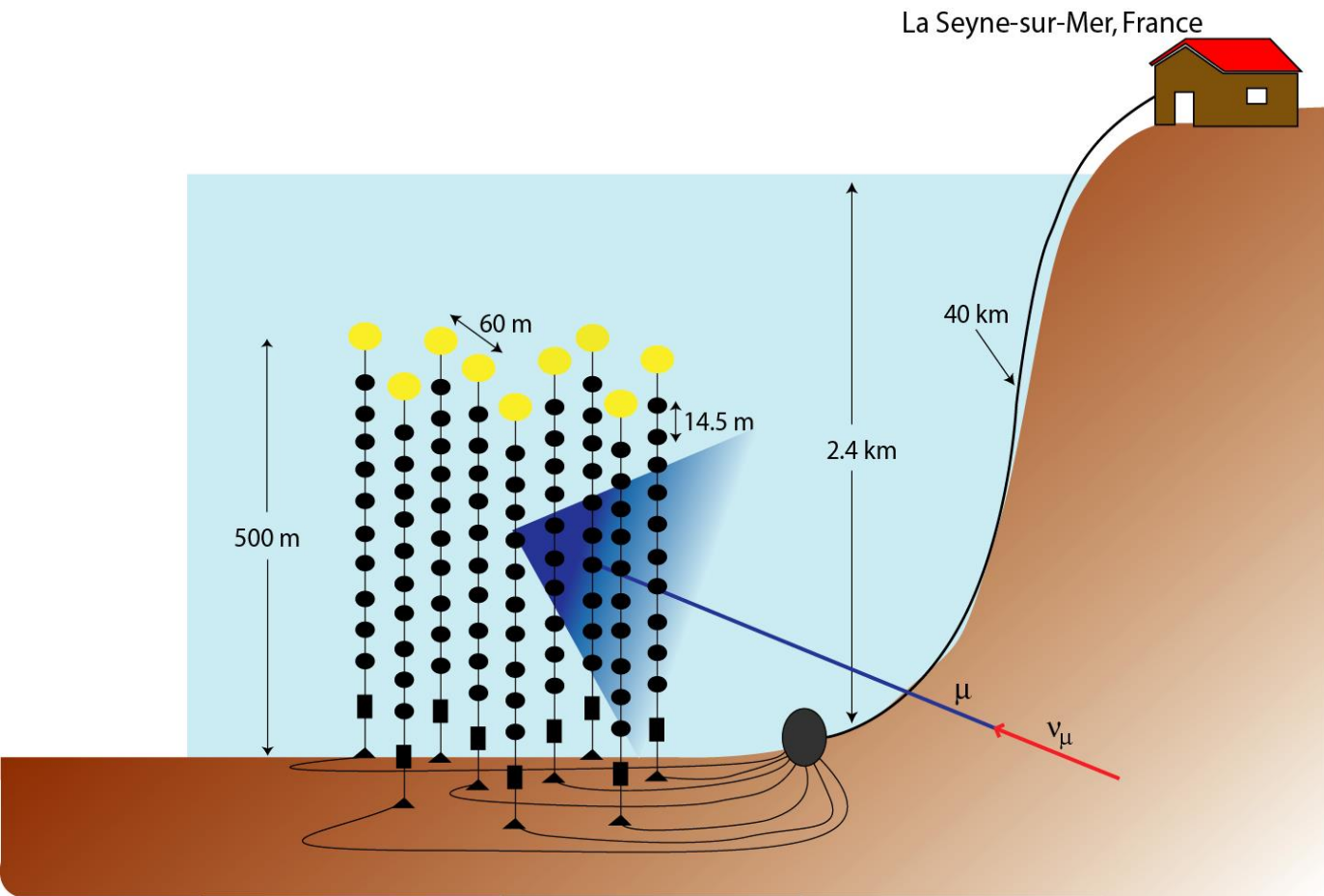
Importance of Timing Resolution

c in water ~ 20 cm/ns

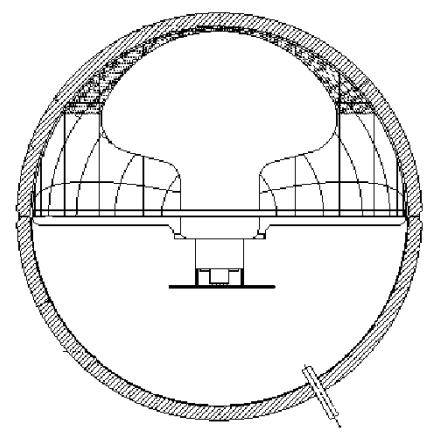
Chromatic dispersion ~ 2 ns (40 m typ. Path)

(PMT TTS $s \sim 1.3$ ns) so detector not dominant source of error

ANTARES Experiment in the sea.



Optical Module

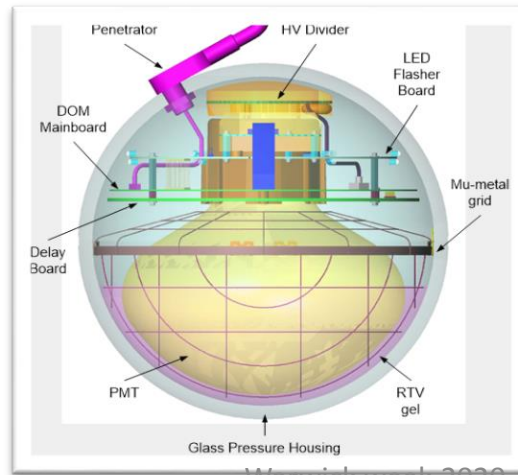
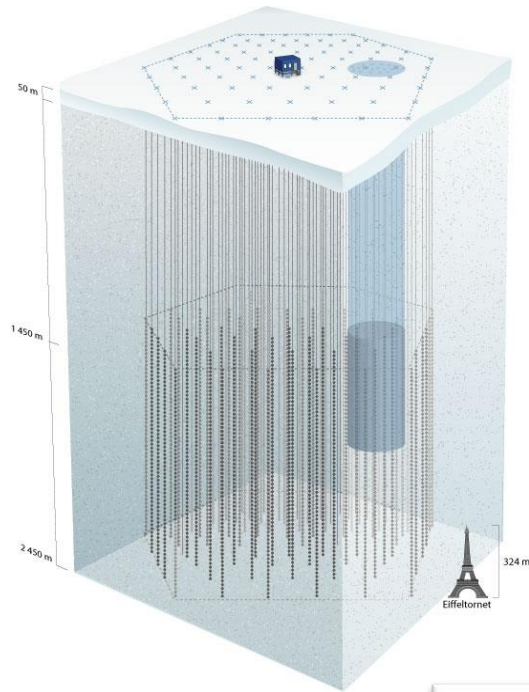


Hamamatsu PMT :
Size :10 inch



Warwick work 2009. A. Paoletti
Glass pressure sphere.

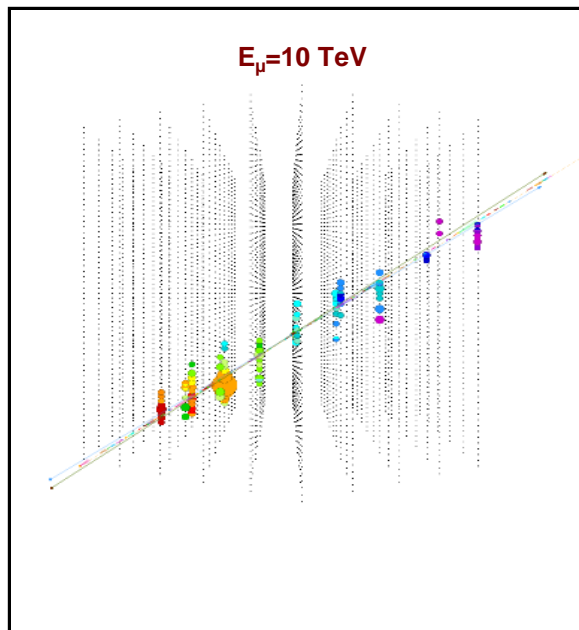
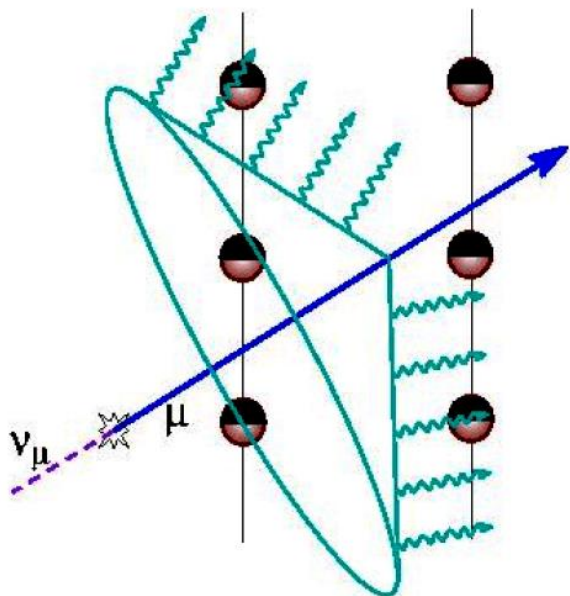
IceCube Experiment in Antarctica



Design Specifications

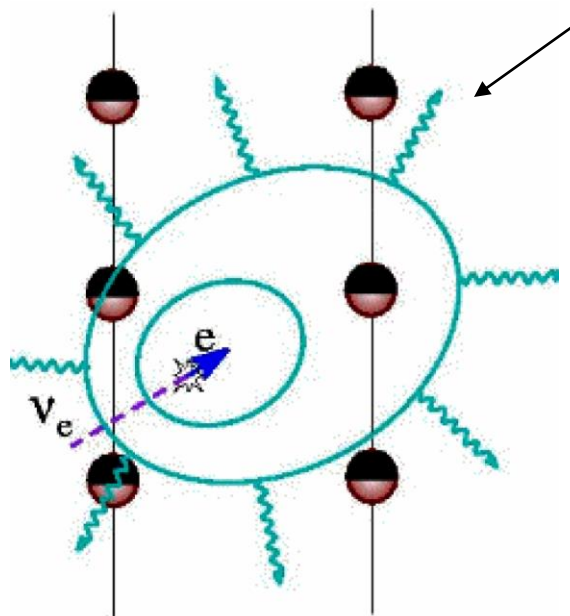
- Fully digital detector concept.
 - Number of strings – 75
 - Number of surface tanks – 160
 - Number of DOMs – 4820
 - Instrumented volume – 1 km³
 - Angular resolution of in-ice array < 1.0°
-
- Fast timing: resolution < 5 ns DOM-to-DOM
 - Pulse resolution < 10 ns
 - Optical sens. 330 nm to 500 nm
 - Dynamic range
 - 1000 pe / 10 ns
 - 10,000 pe / 1 us.
 - Low noise: < 500 Hz background
 - High gain: O(10⁷) PMT
 - Charge resolution: P/V > 2
 - Low power: 3.75 W
 - Ability to self-calibrate
 - Field-programmable HV generated internal to unit.
 - 10000 psi external

Ice Cube/AMANDA Event signatures

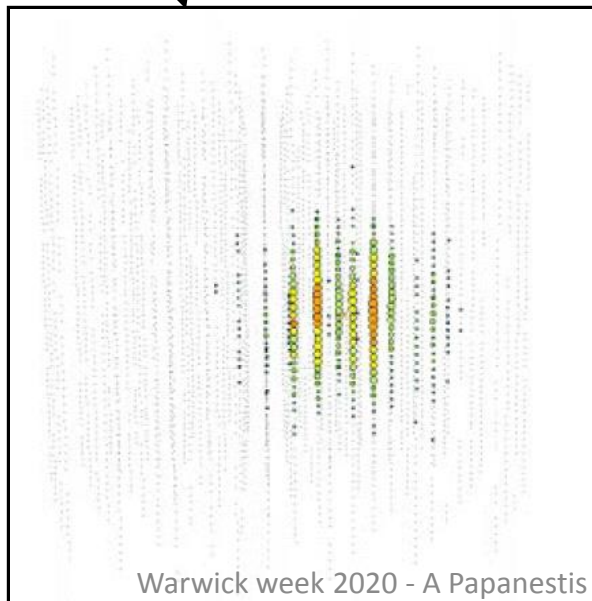


ν_μ from CC interactions

All signals from Cherenkov Radiation.

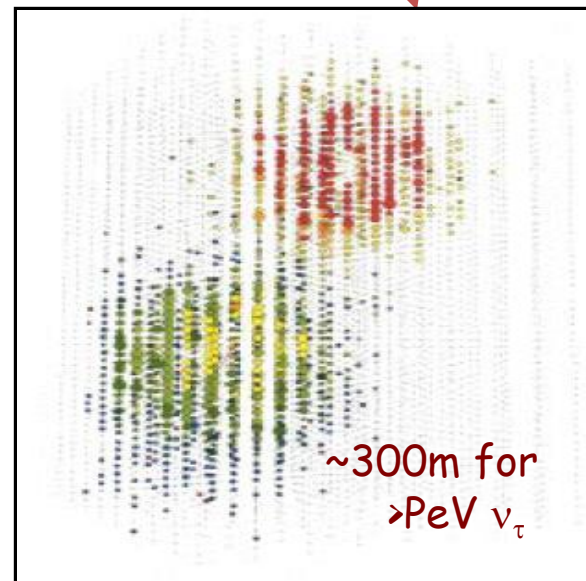


ν_e from CC or ν_x from NC interactions

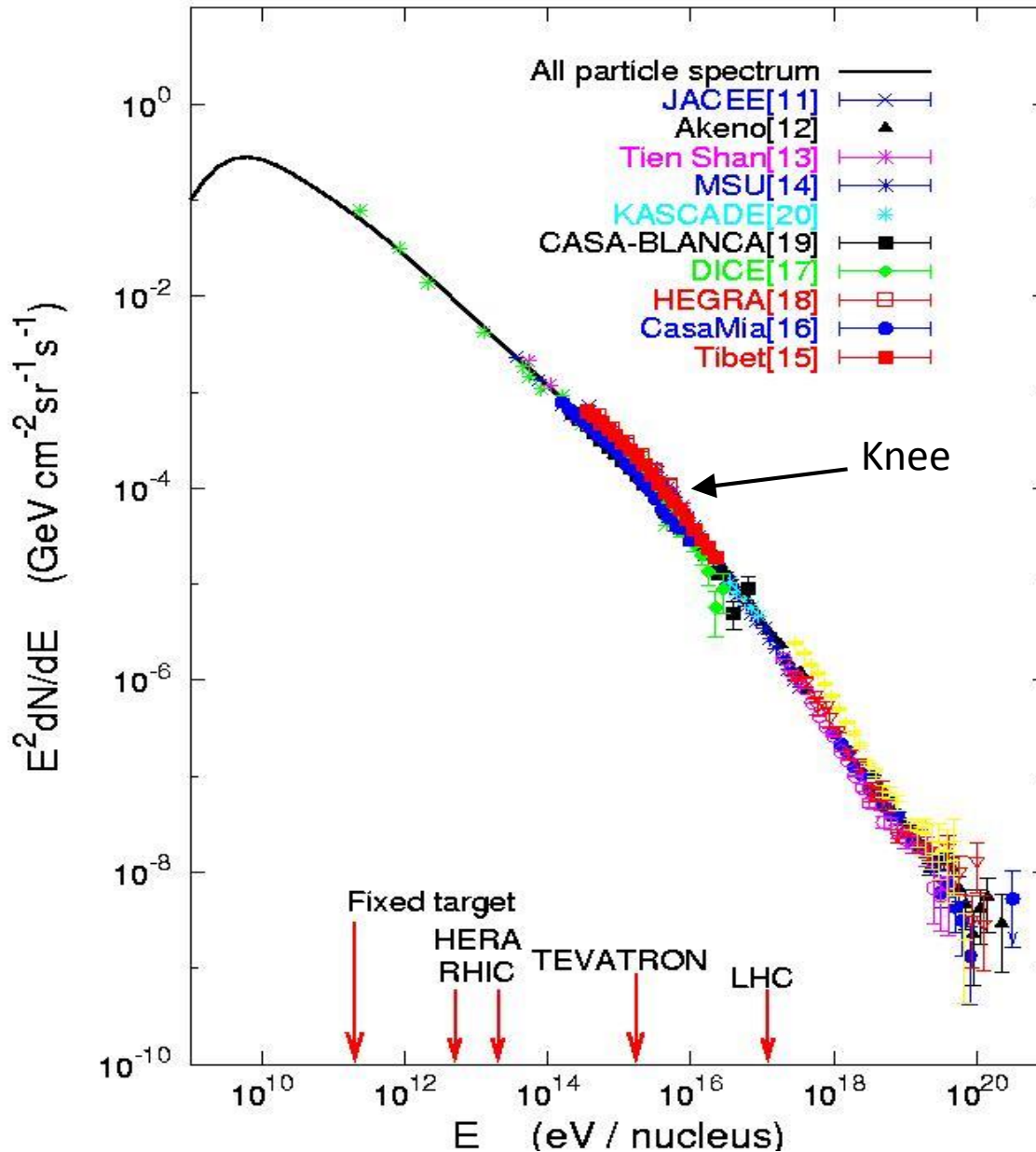


Warwick week 2020 - A Papanestis

$\nu_\tau \rightarrow \tau \rightarrow \mu$



High Energy Cosmic Ray Spectrum.



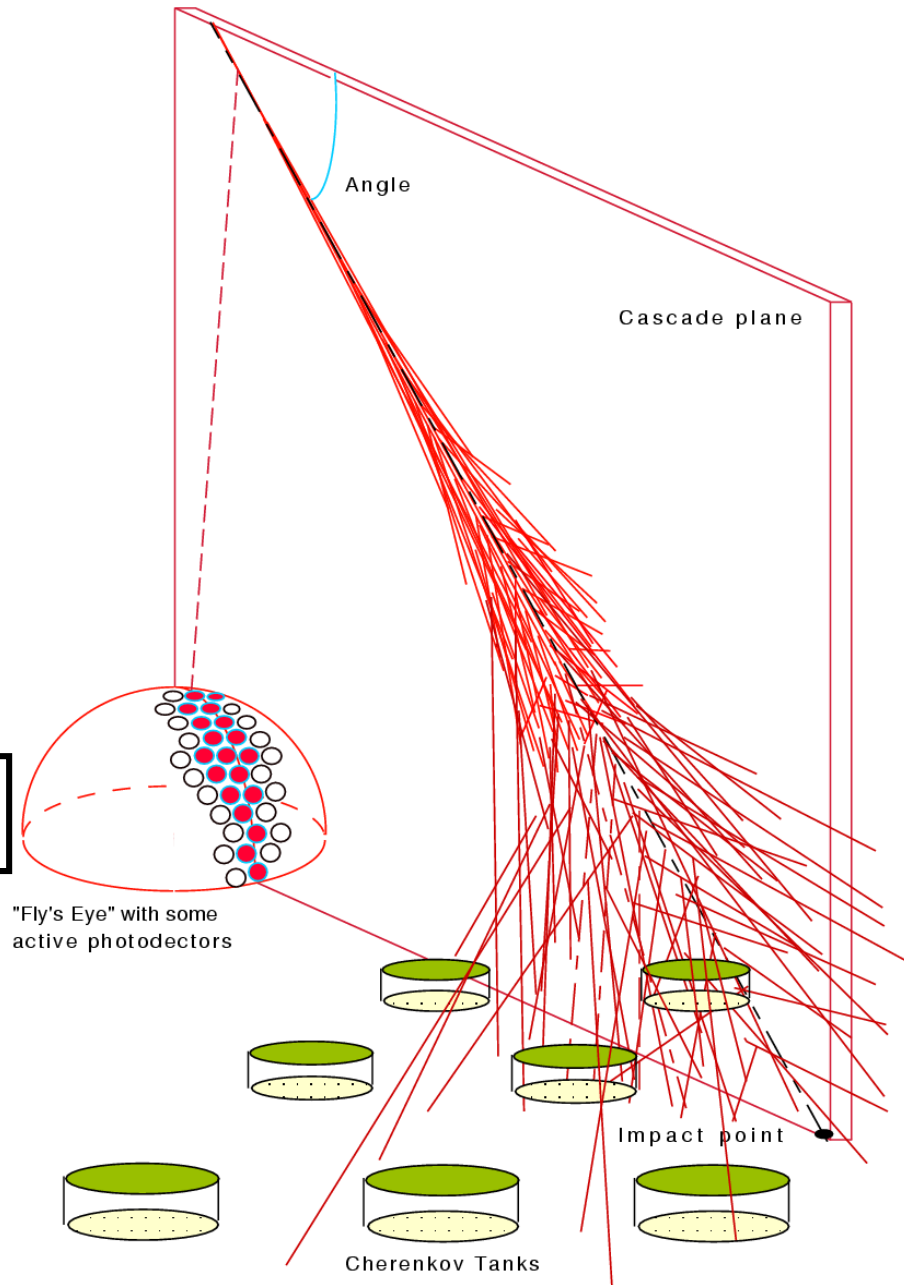
- Measure the Energy Spectrum
- Determine the Arrival Direction distribution etc.
- Composed of Baryons, photons, neutrinos etc.

$>10^{19}$ eV
 $1 \text{ km}^{-2} \text{ year}^{-1} \text{ sr}^{-1}$

Principle of Auger Project

Fluorescence →

Array of water
Cherenkov detectors →



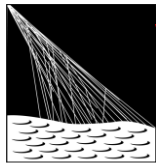
The Pierre Auger Observatory

38° South, Argentina, Mendoza,
Malargue 1.4 km altitude, 850

Argentina
Australia
Bolivia*
Brasil
Czech Republic
France
Germany
Italy
Poland
Mexico
Slovenia
Spain
United Kingdom
USA
Vietnam*

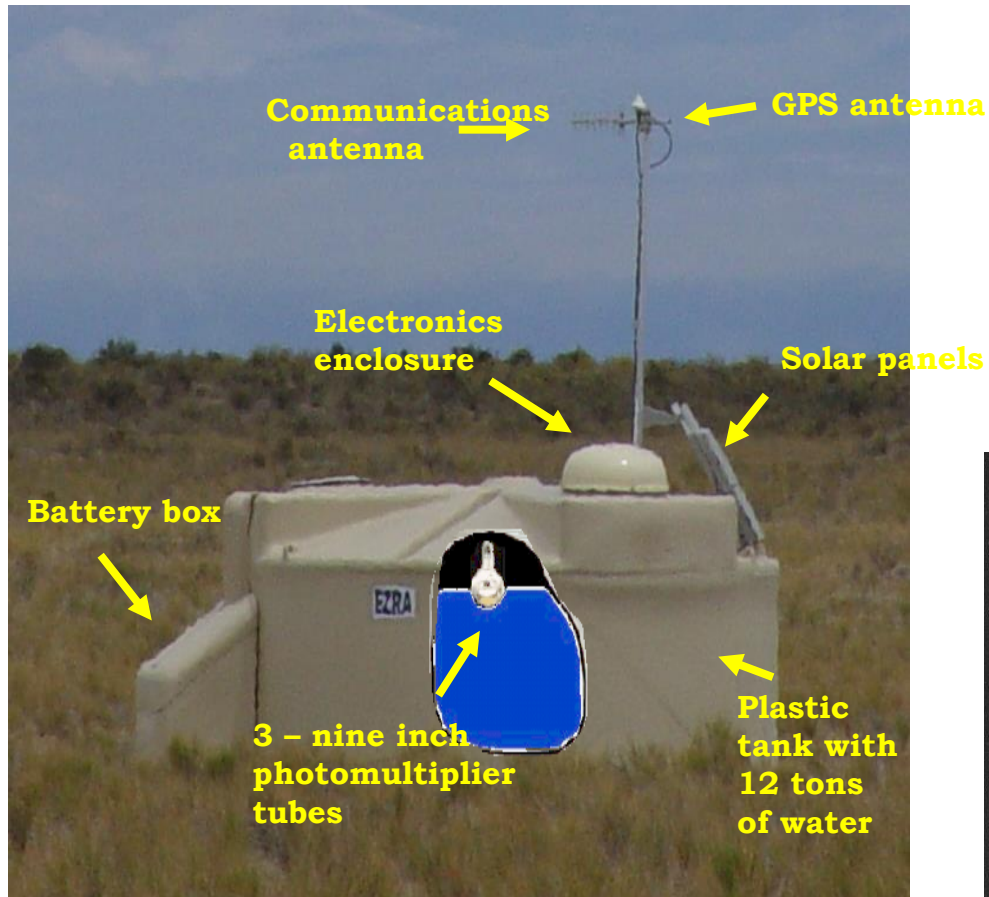


- 1600 surface stations
1.5 km spacing
over 3000 square kilometers
- Fluorescence Detectors:
4 Telescope enclosures,
each with 6 telescopes.

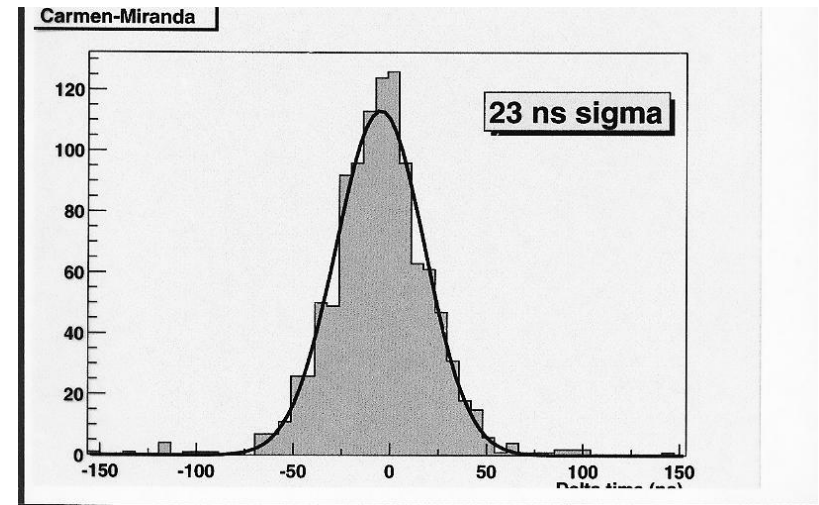


PIERRE
AUGER
OBSERVATORY

AUGER Project: Water Cherenkov Detector

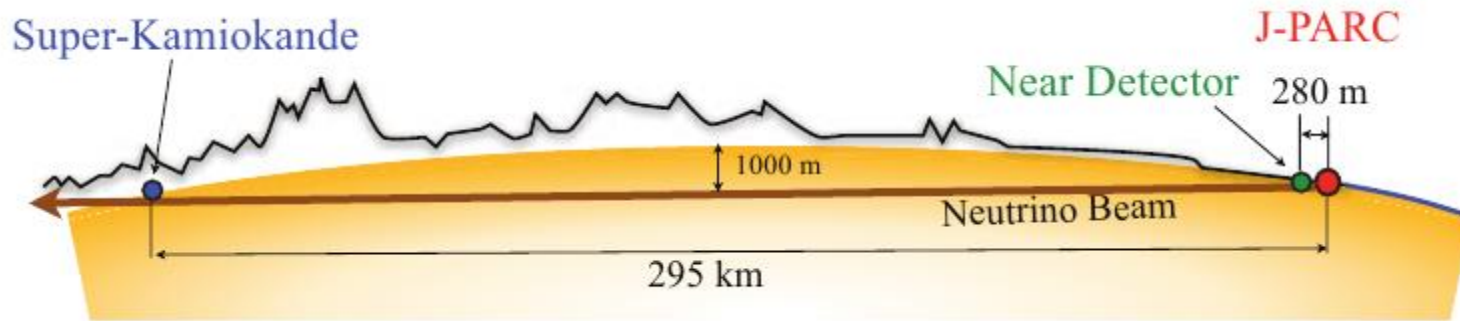


Time difference between
test signals from nearby detectors
(Carmen-Miranda)



- Installation of the Cherenkov detectors are continuing and data taking started.
- First set of results are published

Long Base Line Experiments: T2K

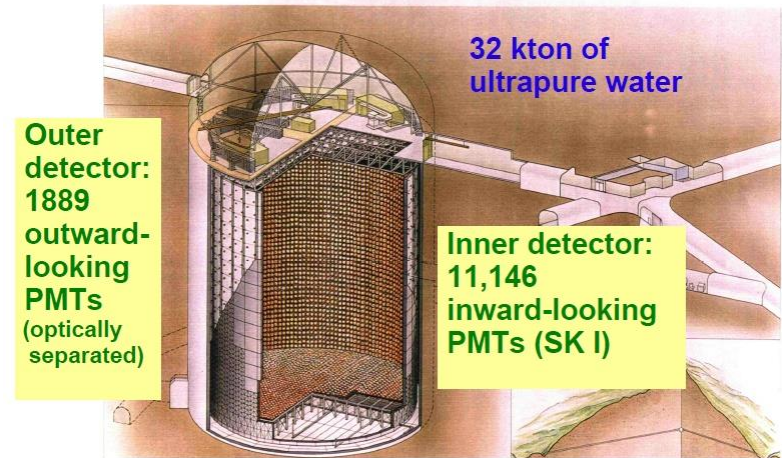
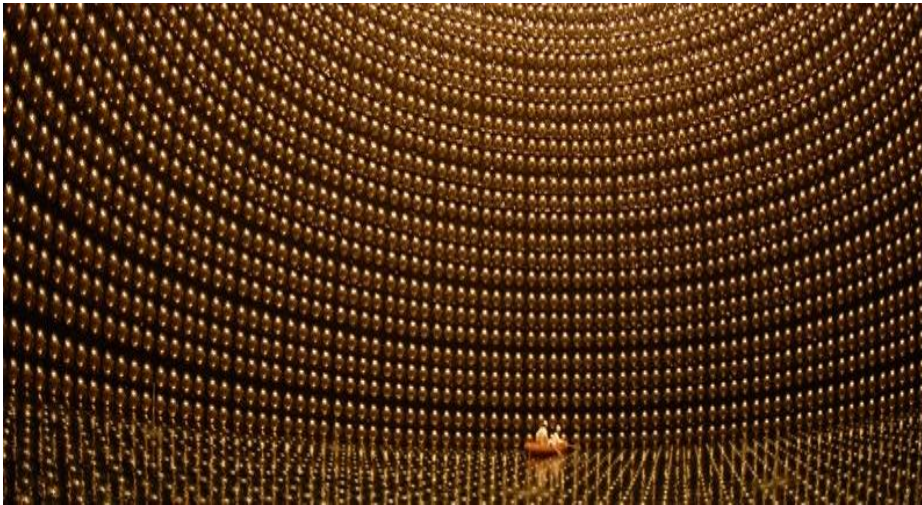


Neutrino production: Protons incident on graphite target to create pions, which decay into μ and ν_{μ} . The muons and any remaining protons and pions are stopped by a second layer of graphite; but the ν_{μ} pass through towards SuperK.

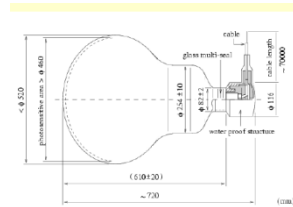
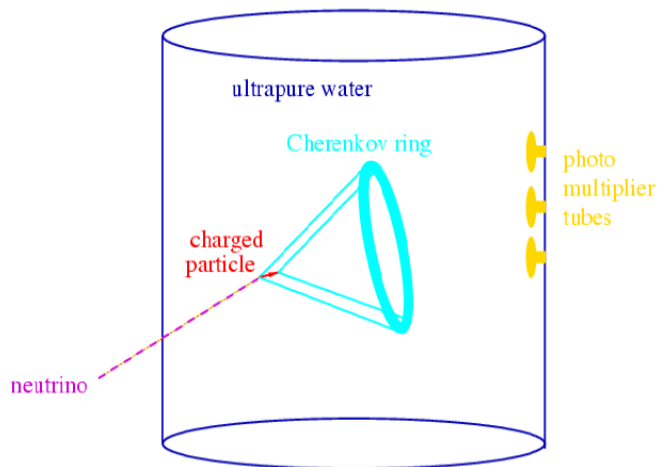
Beam energy: Centered around 600 MeV (to maximize the oscillation probability into ν_{ε}).

Far-detector: underground to reduce cosmic rays.

Super-K water cherenkov detector



40 m high, 17 m radius.



PMT-schematic

Super-K Cherenkov signals

- ▶ ν_e/ν_μ strike nuclei in H₂O, produce e^-/μ^- via weak charged-current (CC) interactions.

The leptons create Cherenkov light in the water.

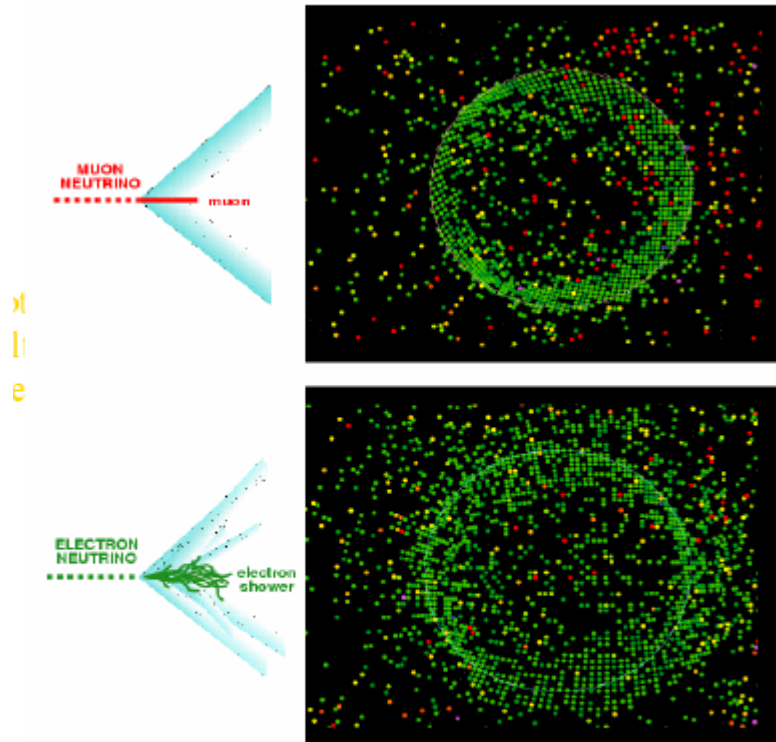
Energy threshold
$$E_{\text{th}} = \frac{m}{(1 - 1/n^2)^{1/2}}$$

- e ; $p > 0.6 \text{ MeV}/c$
 - μ ; $p > 120 \text{ MeV}/c$ (muon) (in water)
 - π ; $p > 160 \text{ MeV}/c$
 - K ; $p > 563 \text{ MeV}/c$
 - p ; $p > 1,070 \text{ MeV}/c$
- + ~50MeV to identify a Cherenkov ring.

$\theta_c = 42^\circ$ for relativistic particle in water

Warwick week 2020 - A Papanestis $\beta \sim 1$

Super-K signals



**Each dot represents
a PMT hit by light**

Measure the charge and time of each pulse. From this estimate :

(a) energy of the charged particle.
(Charge \propto number photons
 \propto energy loss)

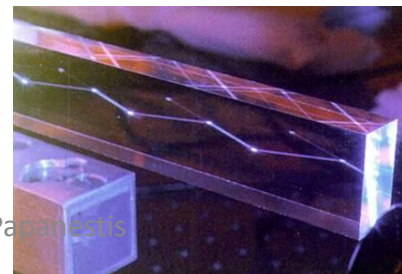
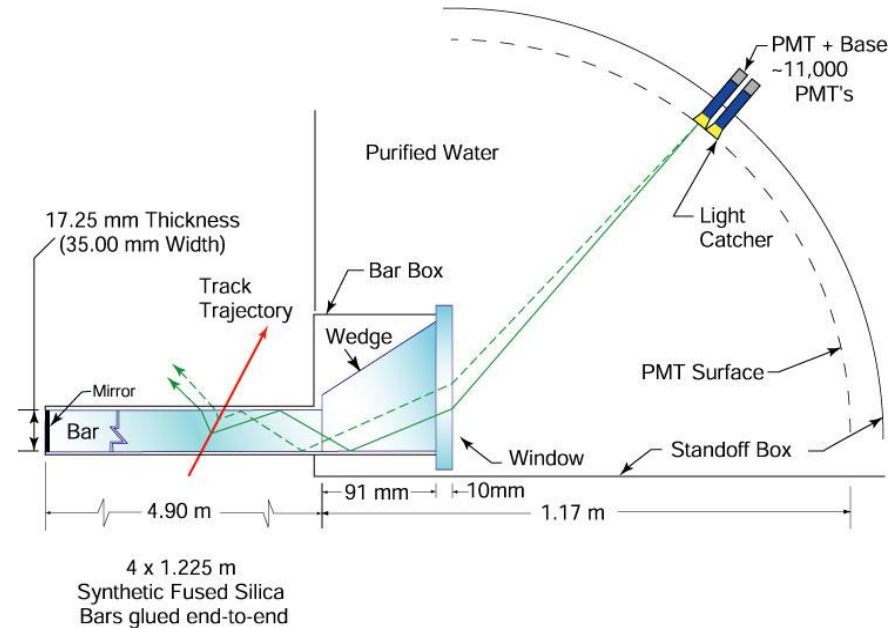
(b) position (vertex) of the interaction.

(c) direction of the charged particle.

Muons create sharp rings,
Electrons scatter and shower and hence create 'fuzzy' rings.

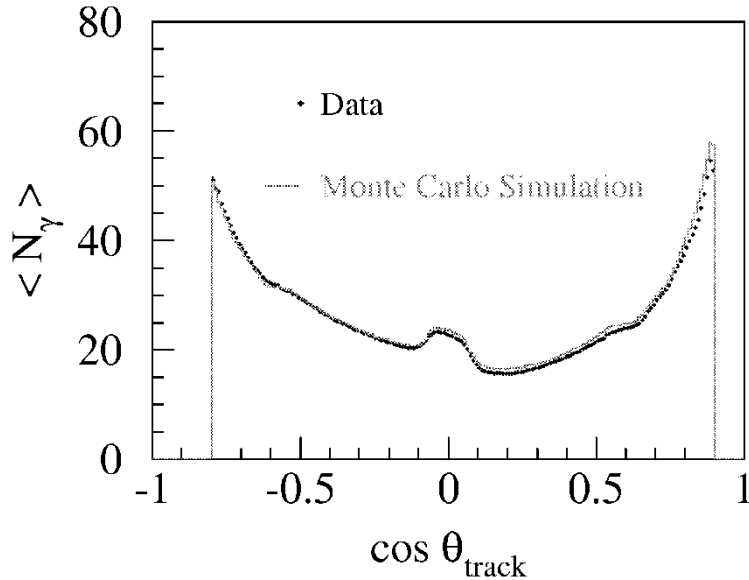
DIRC PRINCIPLE

- If $n > \sqrt{2}$ some photons are always **totally internally reflected** for $\beta \approx 1$ tracks.
- **Radiator and light guide**: Long, rectangular **Synthetic Fused Silica** (“Quartz”) bars (*Spectrosil*: average $\langle n(\lambda) \rangle \approx 1.473$, radiation hard, homogenous, **low chromatic dispersion**)
- Photons exit via wedge into **expansion region** (filled with 6m^3 pure, de-ionized water).
- Pinhole imaging on **PMT array** (bar dimension small compared to standoff distance). (10,752 **traditional PMTs ETL 9125**, immersed in water, surrounded by hexagonal “light-catcher”, transit time spread $\sim 1.5\text{nsec}$, $\sim 30\text{mm}$ diameter)
- **DIRC is a 3-D device**, measuring: x , y and **time** of Cherenkov photons, defining θ_c , ϕ_c , $t_{\text{propagation}}$ of photon.



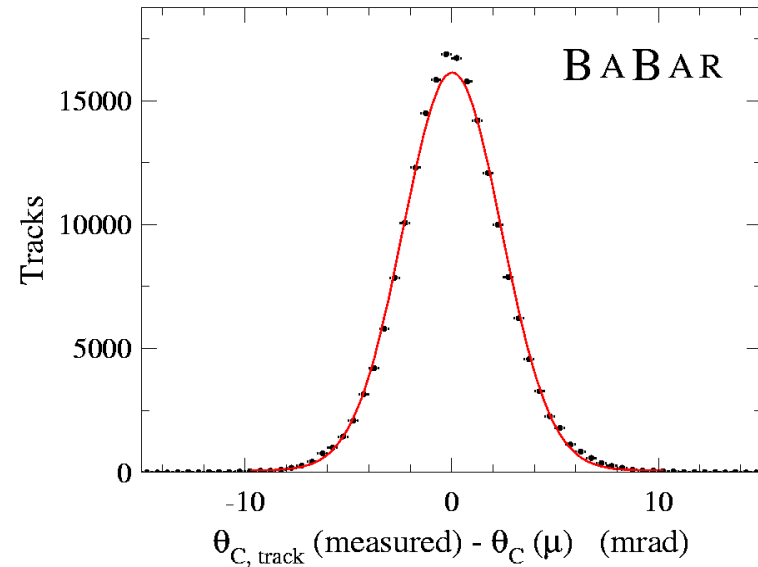
DIRC PERFORMANCE

Number of Cherenkov photons
per track (di-muons) vs. polar angle:



Between 20 and 60 signal photons per track.

Resolution of Cherenkov angle fit
per track (di-muons):

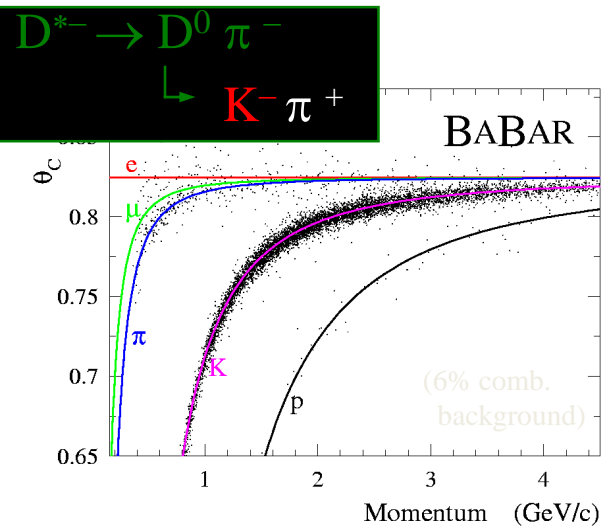


$$\sigma(\Delta\theta_c) = 2.4 \text{ mrad}$$

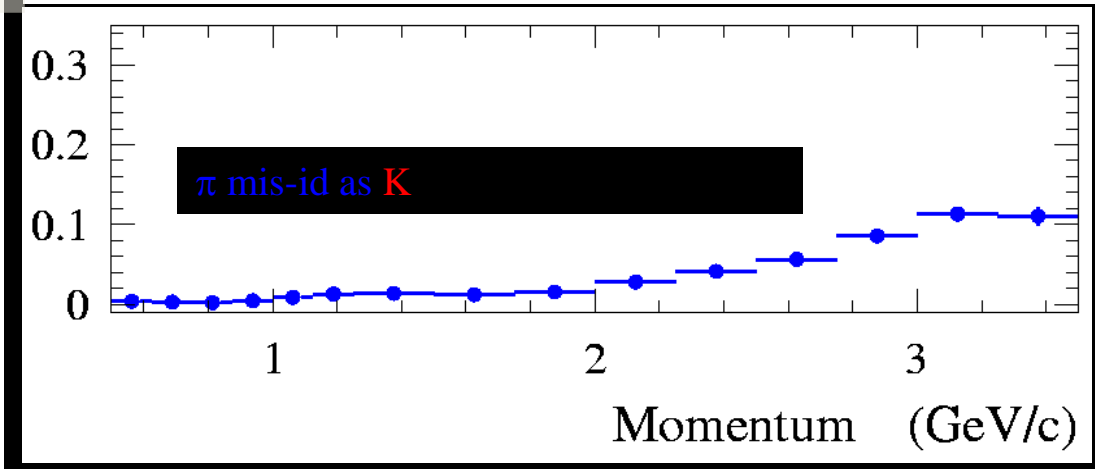
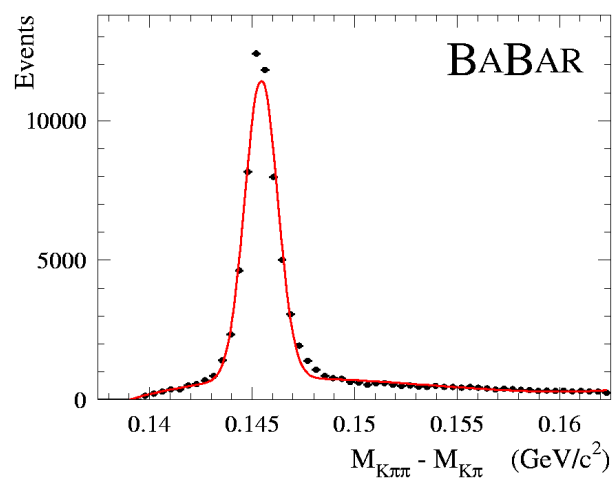
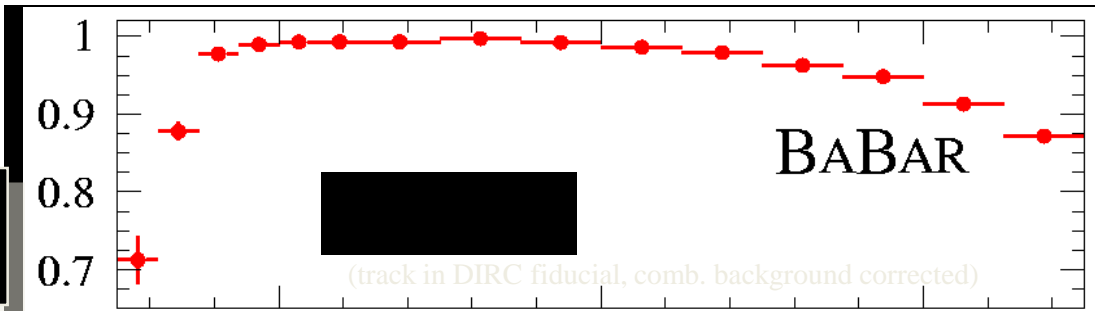
Track Cherenkov angle resolution is
within $\sim 10\%$ of design

DIRC PERFORMANCE

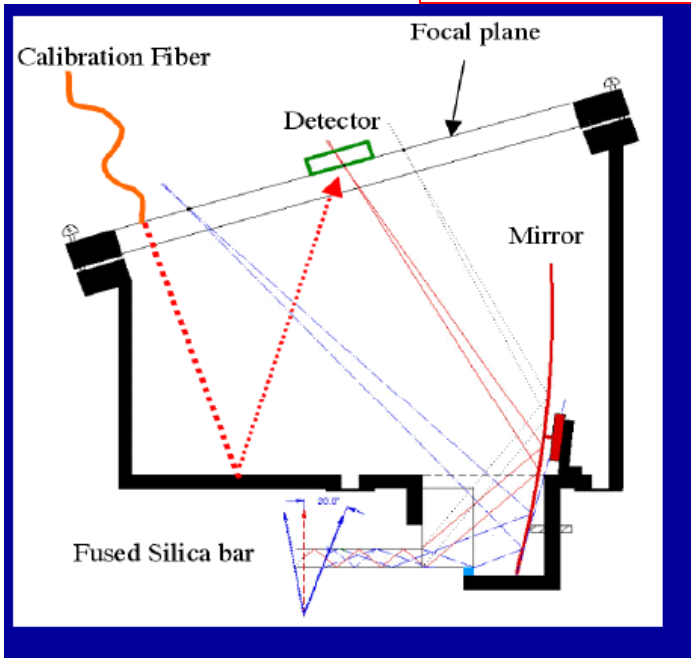
Kaon selection efficiency typically above 95% with mis-ID of 2-10% between 0.8-3 GeV/c.



Kaon selection efficiency for $\mathcal{L}^K > \mathcal{L}^\pi$



New Development: Focussing DIRC



$$v_{\text{group}}(\text{red}) > v_{\text{group}}(\text{blue})$$

- Red photons arrive before blue photons
- Time of Propagation = PathLength / v_{group}
- Correct for Chromatic error from the measurement of time of propagation.

→ Future DIRC needs to be smaller and faster:

Focusing and smaller pixels can **reduce the expansion volume by a factor of 7-10**

Faster PMTs reduce sensitivity to background.

Additional benefit of the faster photon detectors:

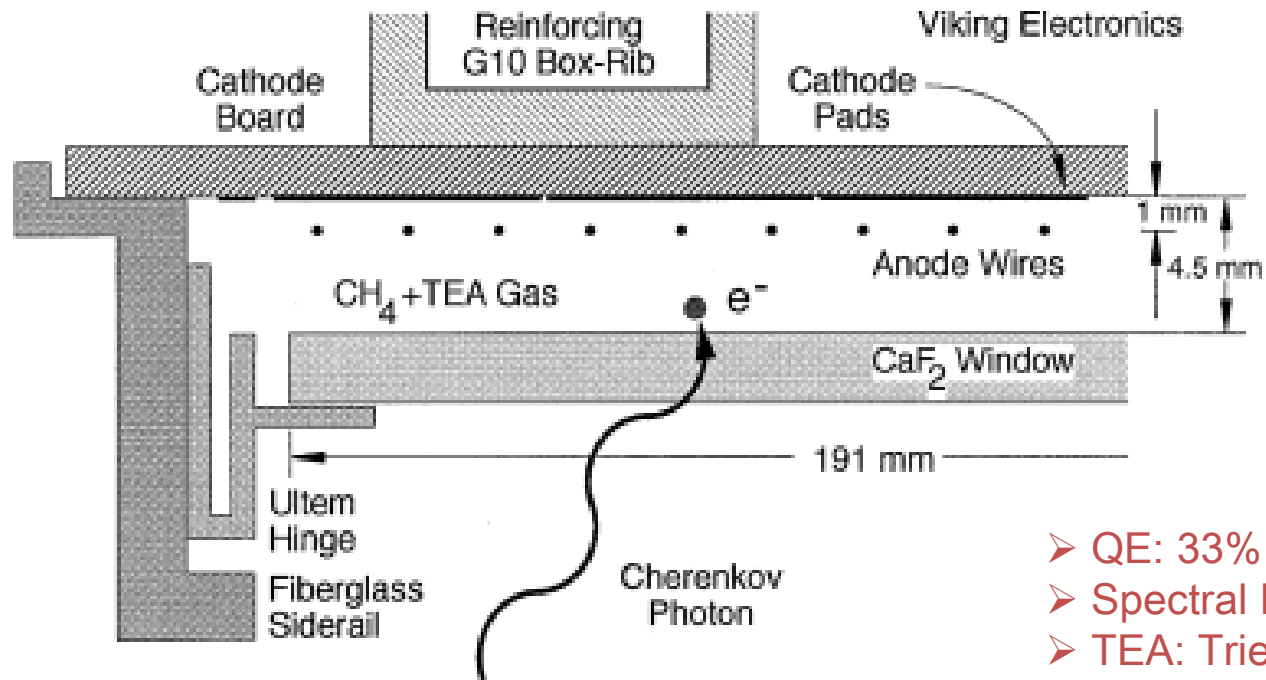
- Timing resolution improvement: $\sigma \sim 1.7\text{ns}$ (BABAR DIRC) $\rightarrow \sigma \leq 150\text{ps}$ ($\sim 10\text{x}$ better) which allows measurement of photon color to correct the chromatic error of θ_c (contributes $\sigma \sim 5.4$ mrad in BABAR DIRC)

Focusing mirror effect:

- Focusing eliminates effect of the bar thickness (contributes $\sigma \sim 4$ mrad in BABAR DIRC)
- However, the spherical mirror introduces an aberration, so its benefit is smaller.

Ref: NIMA 595(2008)104-107

Gas Based Photon Detectors

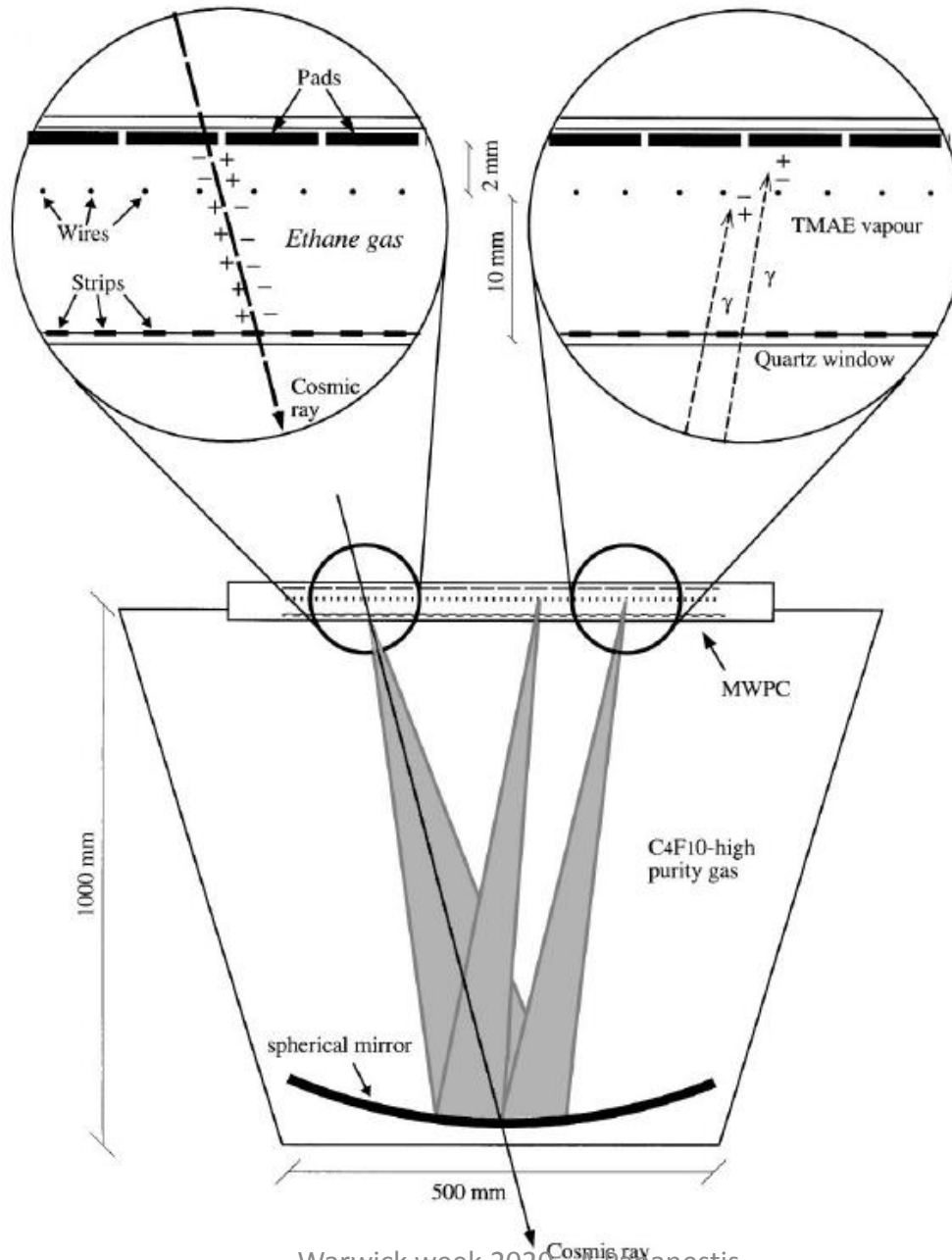


Photon Detector of the CLEO-III Cherenkov detector

- photon passes through the CaF_2 and converts to photoelectron by ionizing a TEA molecule.
- The photoelectron drifts towards and avalanches near the anode wires, thereby inducing a charge signal on the cathode pads.

Balloon Experiment: RICH detector

CAPRICE Experiment



TMAE:
(tetrakis(dimethylamino)
ethylene)

Components of a Cherenkov Detector

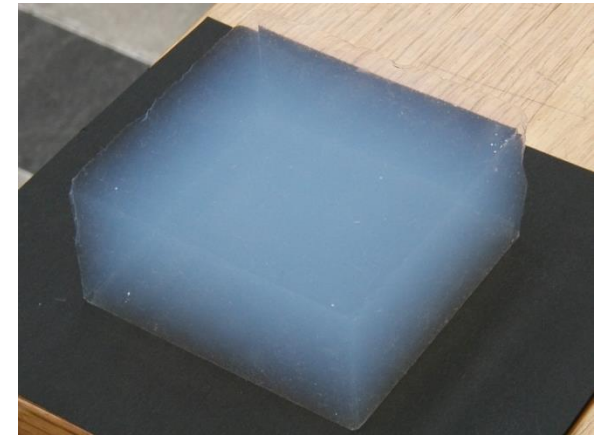
- Main Components:
 - Radiator : To produce photons
 - Mirror/lens etc. : To help with the transport of photons
 - Photodetector : To detect the photons

➤ Radiator: Any medium with a Refractive Index.

Example of radiators

Medium	n-1	γ_{th}	Photons/m
He (STP)	$3.5 \cdot 10^{-5}$	120	3
CO ₂ (STP)	$4.1 \cdot 10^{-4}$	35	40
Silica aerogel	0.025-0.075	4.6-2.7	2400-6600
water	0.33	1.52	21300
Glass	0.46-0.75	1.37-1.22	26100-33100

Aerogel: network of SiO₂ nano-crystals



$$\gamma = 1/\sqrt{1-\beta^2}$$

➤ The atmosphere, ocean are the radiators in some Astro Particle Cherenkov Detectors

LHCb-RICH Design

RICH1: Aerogel L=5cm p:2→10 GeV/c
n=1.03 (nominal at 540 nm)
C₄F₁₀ L=85 cm p: < 70 GeV/c
n=1.0014 (nominal at 400 nm)

Upstream of LHCb Magnet

Acceptance: 25→250 mrad (vertical)
300 mrad (horizontal)

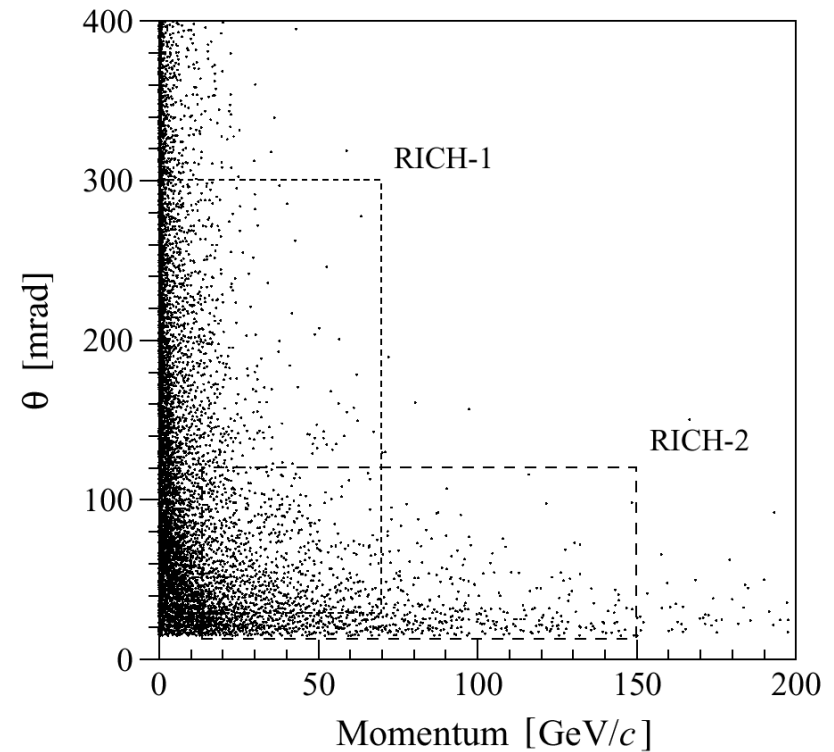
Gas vessel: 2 X 3 X 1 m³

RICH2: CF₄ L=196 cm p: < 100 GeV/c
n =1.0005 (nominal at 400 nm)

Downstream of LHCb Magnet

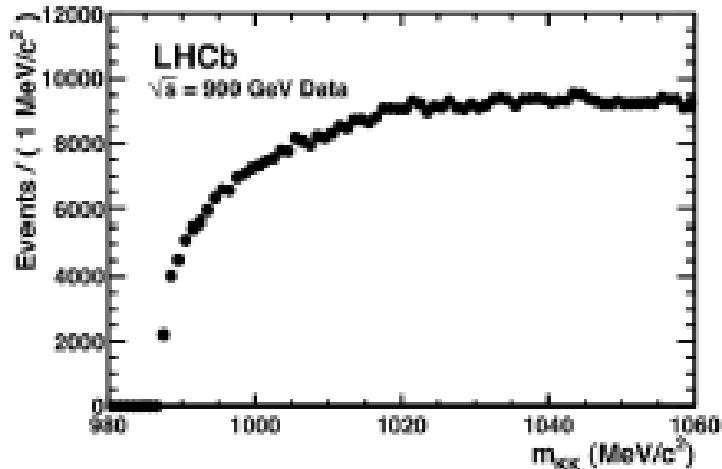
Acceptance: 15→100 mrad (vertical)
120 mrad (horizontal)

Gas vessel : 100 m³

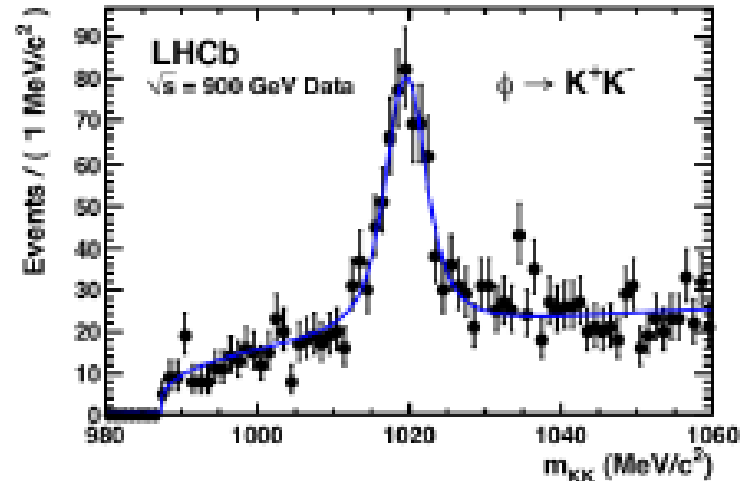


LHCb RICH Data in Physics Analysis

Without RICH data

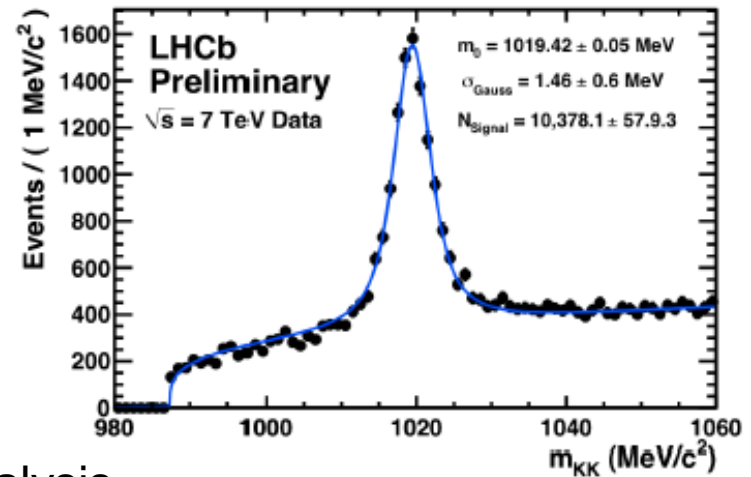


With RICH data



$$\phi \rightarrow K^+K^-$$

Status in 2011
 using RICH data



RICH data has been used in Physics analysis

Example of LHCb-RICH PERFORMANCE

- Performance as seen in Simulated Data in 2010
- **Yield: Mean Number of hits per isolated saturated track ($\beta \sim 1$).**

Aerogel	C4F10	CF4
4.6	34.0	24

Single Photon Cherenkov Angle Resolutions in mrad.

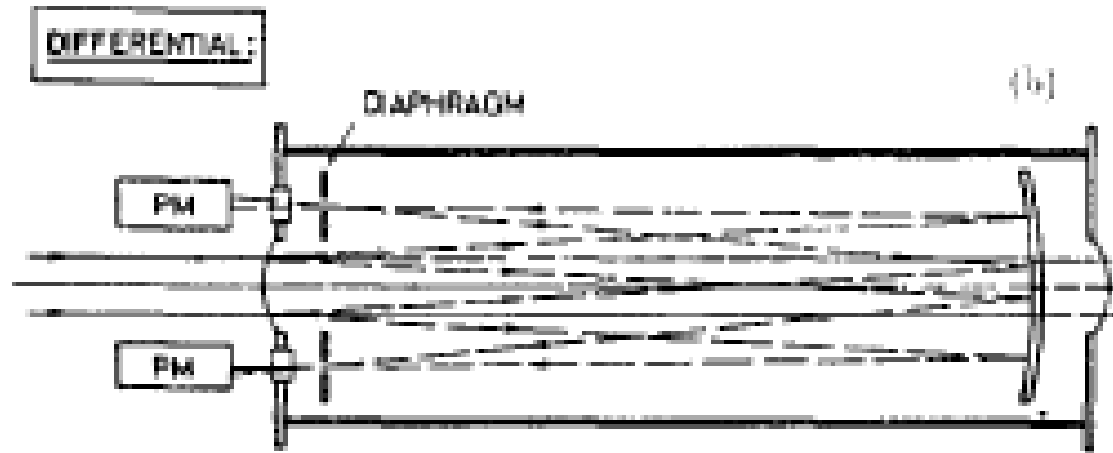
Components and Overall (mrad)	Aerogel	C₄F₁₀	CF₄
Chromatic	2.65	0.84	0.48
Emission Point	0.34	0.61	0.27
Pixel Size	0.59	0.6	0.19
PSF	0.78	0.79	0.29
Overall RICH	2.84	1.45	0.65
Overall RICH+Tracks	2.86	1.50	0.76

- **Chromatic:** From the variation in refractive index.
- **Emission Point:** Essentially from the tilt of the mirrors.
- **Pixel Size:** From the granularity of the Silicon detector pixels in HPD
- **PSF (Point Spread Function):**
From the spread of the Photoelectron direction as it travels inside the HPD,
(from the cross focussing in the electron optics)

Differential Cherenkov Detectors

- Very small acceptance in β and direction of the charged particle. (Narrow range in velocity and direction intervals).
- From the Cherenkov angle (θ) determine β .
- Mostly used for identifying particles in the beam lines.
- Resolution that can be achieved = $\Delta \beta / \beta = (m_1^2 - m_2^2) / 2 p^2 = \tan \theta \Delta \theta$
 m_1, m_2 (particle masses) $\ll p$ (momentum)
- At high momentum, to get better resolution, use gas radiators which have smaller refractive index than solid radiators. Have long enough radiators to get sufficient signal photons in the detector.
- To compensate for Chromatic dispersion ($n(E_{ph})$), lens used in the path of the photons. (DISC: Differential Isochronous self-collimating Cherenkov Counter).
- $\Delta \beta / \beta$ from 0.011 to $4 \cdot 10^{-6}$ achieved.

Differential Cherenkov Detectors



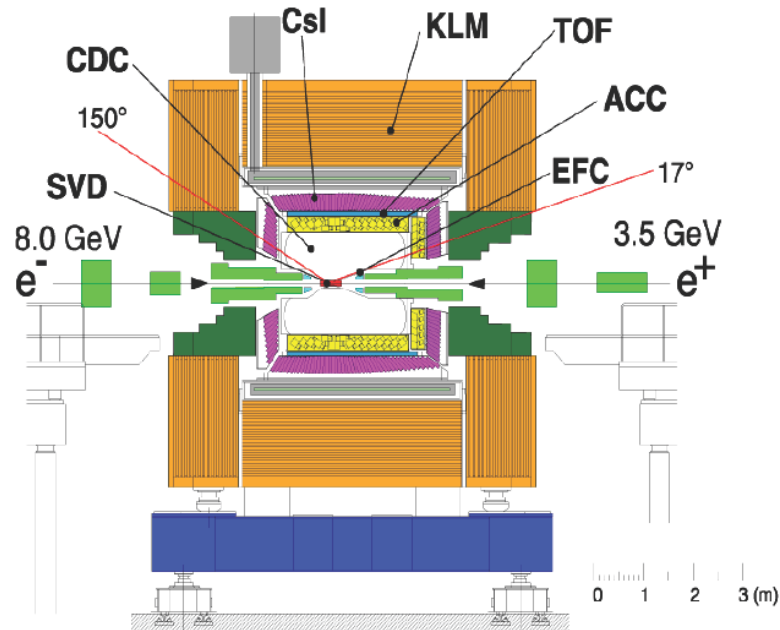
With a Gas radiator

Table 2
Some differential Cherenkov counters

Type	Year	Length [m]	Angle [mrad]	Gas	Range for ($\pi-K$) [GeV/c]	Remarks	Ref.
IHEP [1]	1968	5	23	He, N ₂	< 100	no optical correction	[3]
[2]		10	12		< 200		
DISC	1964	2	44	CO ₂	< 100	corrected	[4]
FNAL DISC	1973	5.5	25	He	< 500	Id.	[2]
					(< 100 for $\pi-\mu-e$)		
CEDAR W	1976	3.25	31	N ₂	< 150	Id	[5]
N		3.90	26	He	< 340		
HYPERON DISC	1972	0.3	120	SF ₆	< 40	Id.	[2]
					(< 100 for $\Sigma-p$)		
For comparison: LDISC	1976	0.05	640	FC88 liquid	< 5	corrected high aperture	[6]

Threshold Cherenkov Detectors

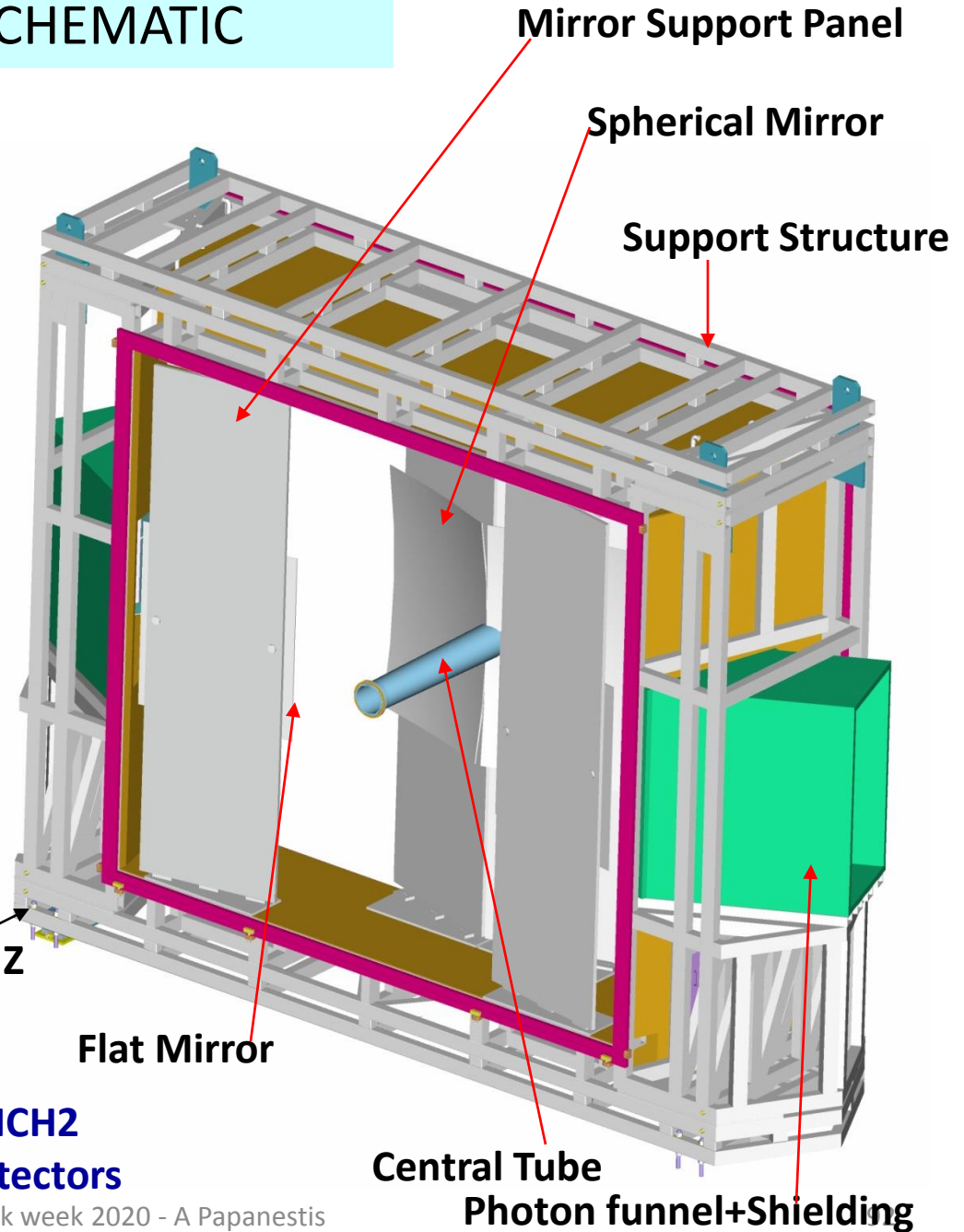
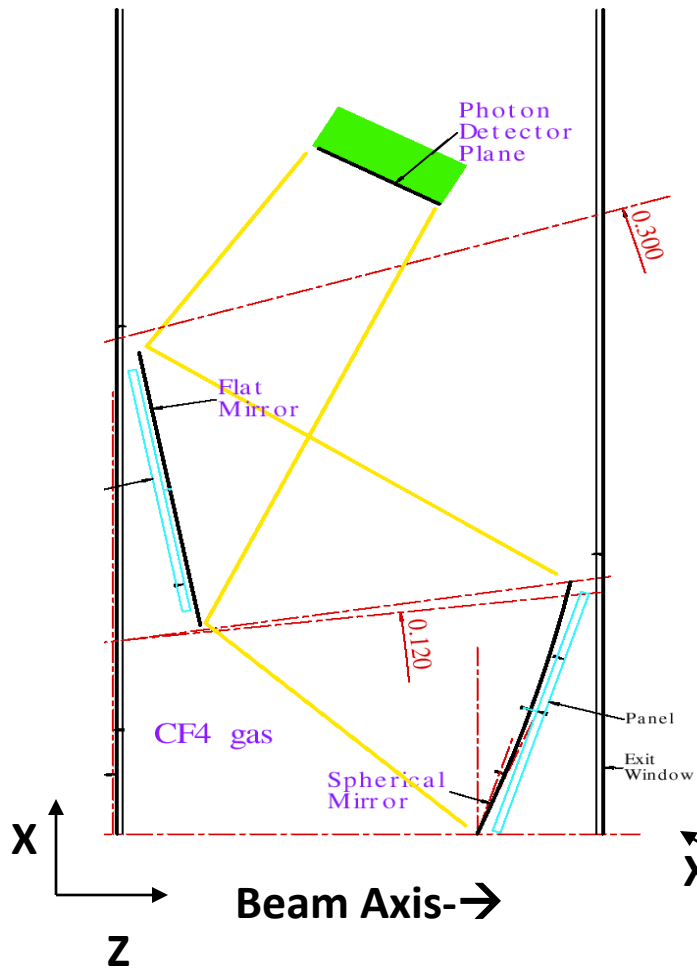
- Can be used over a large area, for Example : For secondary particles in a fixed target or Collider experiment.
- E691 at Fermilab: To study decays of charm particles in the 1980's
 $\Delta\beta/\beta = 2.3 * 10^{-5}$ using gas radiator.
- BELLE Experiment: To observe CP violation in B-meson decays at an electron-positron collider.



- BELLE: Continues to take Data.

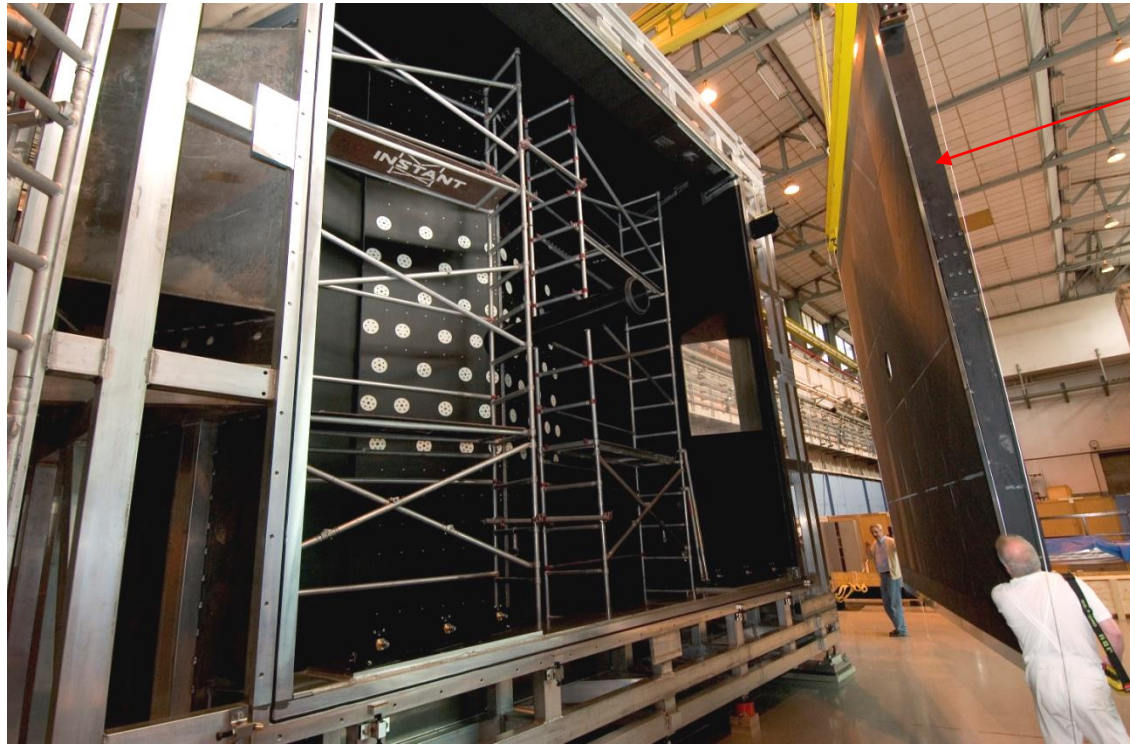
LHCb-RICH2 SCHEMATIC

RICH2 Optics Top View



- Plane Mirrors to reduce the length of RICH2
- Spherical mirror tilted to keep photodetectors outside acceptance. (tilt=0.39 rad)

LHCb- RICH2 STRUCTURE



**Entrance Window
(PMI foam between two
carbon fibre epoxy Skins)**

RICH2



RICH detectors

➤ $\Delta \beta / \beta = \tan(\theta) * \Delta \theta_c = K$ where $\Delta \theta_c = \langle \Delta \theta \rangle / \sqrt{N_{ph}} + C$

where $\langle \Delta \theta \rangle$ is the mean resolution per single photon in a ring and C is the error contribution from the tracking, alignment etc.

➤ For example, for 1.4 m long CF_4 gas radiator at STP and a detector with $N_0 = 75 \text{ cm}^{-1}$
 $K = 1.6 * 10^{-6}$. ($E=6.5 \text{ eV}$, $\Delta E = 1 \text{ eV}$)

➤ This is better than similar Threshold counters by a factor 125.
 This is also better than similar Differential counters by a factor 2.

Reason: RICH measures both θ and N_{ph} directly.
 ➤ RICH detectors have better resolution than equivalent Differential and Threshold counters.

➤ Let $u = \sin^2(\theta) = 1 - (1/n^2) - (m/p*n)^2$

Number of standard deviations to discriminate between mass m_1 and m_2
 $= N_\sigma = (u_2 - u_1) / (\sigma_u * \sqrt{N})$ where σ_u : $\Delta \theta$ converted into the parameter u.
 ($\Delta \theta$ = error in single photon θ measurement)

➤ At momentum p ($=\beta E$), $p = \sqrt{((m_2^2 - m_1^2) / (2 * K * N_\sigma))}$, for $\beta \sim 1$

This equation can be used in the design of the RICH detectors.

➤ One the first large size RICH detector: in DELPHI at LEP.